

Supplementary Information

Discovery of megapolipeptins by genome mining of a Burkholderiales bacteria collection

Bruno S. Paulo^{a,b*}, Michael J. J. Recchia^{c*}, Sanghoon Lee^c, Claire Fergusson^c, Sean B. Romanowski^{a,b}, Antonio Hernandez^a, Nyssa Krull^a, Dennis Liu^c, Hannah Cavanagh^c, Allyson Bos^d, Christopher Gray^d, Brian T. Murphy^{a,b}, Roger G. Linington^c, Alessandra S. Eustaquio^{a,b}

^aDepartment of Pharmaceutical Sciences, College of Pharmacy, University of Illinois at Chicago, Chicago, IL, 60607, USA

^bCenter for Biomolecular Sciences, College of Pharmacy, University of Illinois at Chicago, Chicago, IL, 60607, USA

^cDepartment of Chemistry, Simon Fraser University, Burnaby, BC V5H 1S6, Canada

^dDepartment of Biological Sciences, University of New Brunswick, Saint John, NB, E2L 4L5, Canada

To whom correspondence should be addressed: rliningt@sfu.ca; ase@uic.edu

Table of Contents

METHODS	6
CHEMICALS AND GENERAL EXPERIMENTAL PROCEDURES.	6
DNA PREPARATION FOR ILLUMINA SEQUENCING AND NANOPORE SEQUENCING.	6
POLYMERASE CHAIN REACTION.	6
SAMPLE PREPARATION FOR IDBAC ANALYSIS.	7
IDBAC MALDI-TOF MS DATA ACQUISITION.	7
CLONING OF THE <i>MGP</i> BGC TO YIELD PBS001 AND GENERATION OF THE EMPTY VECTOR CONTROL PBS003.	8
CONJUGATION PROCEDURE TO TRANSFER PBS001 AND PBS003 INTO <i>BURKHOLDERIA</i> SP. FERM BP-3421.	8
COMPARATIVE METABOLITE ANALYSIS VIA LC-MS/MS.	9
MOLECULAR NETWORK ANALYSES.	9
GENERAL EQUIPMENT.	10
PRODUCTION OF MEGAPOLYPEPTINS.	10
ISOLATION OF MEGAPOLYPEPTINS A (1) AND B (2).	11
STRUCTURE ELUCIDATION DETAILS FOR MEGAPOLYPEPTIN A (1).	11
STRUCTURE ELUCIDATION DETAILS FOR MEGAPOLYPEPTIN B (2).	12
DETERMINATION OF THE ABSOLUTE CONFIGURATION OF THE AMINO ACIDS.	13
PARTIAL HYDROLYSIS OF MEGAPOLYPEPTIN B.	13
MEGAPOLYPEPTIN A (1).	14
MEGAPOLYPEPTIN B (2).	14
ANTIMICROBIAL SCREENING.	14
ANTIFUNGAL SCREENING.	15
TABLES	17
TABLE S1. WHOLE-GENOME SHOTGUN PROJECT DATA DEPOSITED ON NCBI GENBANK DATABASE UNDER ACCESSION CODES LISTED ALONG WITH ASSEMBLY METRICS.	17
TABLE S2. SEQUENCING TECHNOLOGY AND ASSEMBLY DETAILS FOR THE 115 <i>BURKHOLDERIALES</i> STRAINS.	24

TABLE S3. COLLECTION DATE, ENVIRONMENTAL CONTEXT, AND GEOGRAPHIC SAMPLE LOCATION FOR THE SEQUENCED STRAINS.....	28
TABLE S4. CONTIG SUMMARY FOR HYBRID ASSEMBLIES (ILLUMINA AND NANOPORE).....	34
TABLE S5. NUMBER OF BGCs, GENOME SIZE, AND RATIO OF NUMBER OF BGCs TO GENOME SIZE PER STRAIN AND PHYLOGENETIC CLADE.	35
TABLE S6. CLUSTER OF ORTHOLOGOUS GENES FAMILIES USED TO GENERATE PHYLOGENOMIC TREE. ..	37
TABLE S7. BLASTp RESULTS (AS OF APR. 2023) OF ENCODED PROTEINS IN REGION 2.11 THAT CONTAINS THE <i>MGP</i> BGC.....	39
TABLE S8. ¹ H (600 MHz) AND ¹³ C NMR (150 MHz) DATA FOR MEGAPOLYPEPTIN A (1) IN DMSO- <i>D</i> ₆ ^d	40
TABLE S9. ¹ H (600 MHz) AND ¹³ C NMR (150 MHz) DATA FOR MEGAPOLYPEPTIN B (2) IN DMSO- <i>D</i> ₆ ^d . ..	42
TABLE S10. BACTERIAL TARGET PANEL STRAINS AND CULTURE CONDITIONS.	44
TABLE S11. ANTIMICROBIAL ACTIVITIES OF MEGAPOLYPEPTINS A (1) AND B (2).....	44
TABLE S12. FUNGAL TARGET PANEL STRAINS AND CULTURE CONDITIONS.	45
TABLE S13. ADENYLATION DOMAIN SIGNATURE ON MEGAPOLYPEPTIN BGC.....	45
TABLE S14. NATURAL PRODUCT FAMILIES WITH STRUCTURAL SIMILARITY TO MEGAPOLYPEPTINS.	46
TABLE S15. DETAILED MALDI-TOF MS PARAMETERS FOR IDBAC ANALYSIS.	47
FIGURES.....	48
FIGURE S1. EXAMPLE OF IDBAC STRAIN PRIORITIZATION.	48
FIGURE S2. BIOSYNTHETIC GENE CLUSTER NUMBERS AND BIOSYNTHETIC CLASS BY STRAIN.	49
FIGURE S3. PIE CHARTS SHOWING SUBDIVISIONS OF ‘OTHER’ BIOSYNTHETIC GENE CLUSTERS.	50
FIGURE S4. PHYLOGENOMIC TREE OF BURKHOLDERIALES LIBRARY.....	51
FIGURE S5. PHYLOGENOMIC TREE OF BURKHOLDERIALES LIBRARY.....	52
FIGURE S6. BIG-SCAPE BIOSYNTHETIC GENE CLUSTER SEQUENCE SIMILARITY NETWORK WITHIN THE 115 BURKHOLDERIALES GENOMES.	53
FIGURE S7. NRPS NETWORKS AND SINGLETONS.	54
FIGURE S8. RiPP NETWORKS AND SINGLETONS.	55
FIGURE S9. PKS NETWORKS AND SINGLETONS. (A) TYPE I PKS, (B) TYPE III.....	56
FIGURE S10. HYBRID PKS-NRPS NETWORKS AND SINGLETONS.	57
FIGURE S11. pBS001 SCREENING IN <i>BURKHOLDERIA</i> SP. FERM BP-3421.	58
FIGURE S12. MOLECULAR NETWORK FOR <i>BURKHOLDERIA</i> SP. FERM BP-3421/pBS001.	59

FIGURE S13. MS ANALYSIS OF NETWORK #1.	60
FIGURE S14. MS ANALYSIS OF NETWORK #2 (MEGAPOLYPEPTINS NETWORK).	61
FIGURE S15. MS ANALYSIS OF NETWORK #3.	62
FIGURE S16. MS ANALYSIS OF NETWORK #4.	63
FIGURE S17. HR-ESI-MS DATA FOR MEGAPOLYPEPTIN A (1).	64
FIGURE S18. MS/MS DATA FOR MEGAPOLYPEPTIN A (1).	64
FIGURE S19. ¹ H NMR SPECTRUM OF MEGAPOLYPEPTIN A (1) ACQUIRED IN DMSO- <i>D</i> ₆ AT 600 MHZ.	65
FIGURE S20. ¹³ C NMR SPECTRUM OF MEGAPOLYPEPTIN A (1) ACQUIRED IN DMSO- <i>D</i> ₆ AT 150 MHZ.	66
FIGURE S21. HSQC SPECTRUM OF MEGAPOLYPEPTIN A (1) ACQUIRED IN DMSO- <i>D</i> ₆ AT 600 MHZ.	67
FIGURE S22. ¹ H- ¹ H COSY SPECTRUM OF MEGAPOLYPEPTIN A (1) ACQUIRED IN DMSO- <i>D</i> ₆ AT 600 MHZ.	68
FIGURE S23. HMBC SPECTRUM OF MEGAPOLYPEPTIN A (1) ACQUIRED IN DMSO- <i>D</i> ₆ AT 600 MHZ.	69
FIGURE S24. NOESY SPECTRUM OF MEGAPOLYPEPTIN A (1) ACQUIRED IN DMSO- <i>D</i> ₆ AT 600 MHZ.	70
FIGURE S25. ROESY SPECTRUM OF MEGAPOLYPEPTIN A (1) ACQUIRED IN DMSO- <i>D</i> ₆ AT 600 MHZ.	71
FIGURE S26. KEY COSY (BOLD LINES) AND HMBC (ARROWS) CORRELATIONS FOR THE PLANAR STRUCTURES OF MEGAPOLYPEPTIN A (1) AND MEGAPOLYPEPTIN B (2).	72
FIGURE S27. COMPARATIVE EXTRACTED ION CHROMATOGRAMS OF MEGAPOLYPEPTIN A (1) AND METHYL ESTER DERIVATIVES.	73
FIGURE S28. COMPARATIVE MS SPECTRA OF MEGAPOLYPEPTIN A (1) AND METHYL ESTER DERIVATIVES.	73
FIGURE S29. PLANAR STRUCTURES OF THE MEGAPOLYPEPTIN A (1) METHYL ESTER DERIVATIVES (3 AND 4).	74
FIGURE S30. KEY COSY AND HMBC CORRELATIONS OF THE METHYLATED PLANAR STRUCTURES OF MEGAPOLYPEPTIN A (1) METHYL ESTER (3) AND B METHYL ESTER (4).	74
FIGURE S31. HR-ESI-MS DATA FOR MEGAPOLYPEPTIN B (2).	75
FIGURE S32. MS/MS DATA FOR MEGAPOLYPEPTIN B (2).	75
FIGURE S33. ¹ H NMR SPECTRUM OF MEGAPOLYPEPTIN B (2) ACQUIRED IN DMSO- <i>D</i> ₆ AT 600 MHZ.	76
FIGURE S34. ¹³ C NMR SPECTRUM OF MEGAPOLYPEPTIN B (2) ACQUIRED IN DMSO- <i>D</i> ₆ AT 150 MHZ.	77
FIGURE S35. HSQC SPECTRUM OF MEGAPOLYPEPTIN B (2) ACQUIRED IN DMSO- <i>D</i> ₆ AT 600 MHZ.	78
FIGURE S36. ¹ H- ¹ H COSY SPECTRUM OF MEGAPOLYPEPTIN B (2) ACQUIRED IN DMSO- <i>D</i> ₆ AT 600 MHZ.	79

FIGURE S37. HMBC SPECTRUM OF MEGAPOLYPEPTIN B (2) ACQUIRED IN DMSO- <i>D</i> ₆ AT 600 MHZ.	80
FIGURE S38. NOESY SPECTRUM OF MEGAPOLYPEPTIN B (2) ACQUIRED IN DMSO- <i>D</i> ₆ AT 600 MHZ.....	81
FIGURE S39. EXTRACTED ION CHROMATOGRAMS OF MEGAPOLYPEPTIN B (2) AND METHYL ESTER DERIVATIVES.	82
FIGURE S40. COMPARATIVE MS SPECTRA OF MEGAPOLYPEPTIN B (2) AND METHYL ESTER DERIVATIVES.	82
FIGURE S41. MARFEY’S ANALYSIS OF MEGAPOLYPEPTIN A (1) AND MEGAPOLYPEPTIN B (2).	83
FIGURE S42. PARTIAL HYDROLYSIS OF MEGAPOLYPEPTIN B (2).	84
FIGURE S43. MULTIPLE SEQUENCE ALIGNMENT OF KR DOMAINS FROM THE MEGAPOLYPEPTIN BGC. ...	85
FIGURE S44. MULTIPLE SEQUENCE ALIGNMENT OF A DOMAINS FROM THE MEGAPOLYPEPTIN BGC.....	85
FIGURE S45. MULTIPLE SEQUENCE ALIGNMENT OF C DOMAINS FROM THE MEGAPOLYPEPTIN BGC.	86
FIGURE S46. NEIGHBOR-JOINING PHYLOGENETIC TREE OF 189 NRPS C DOMAINS.....	87
FIGURE S47. MULTIPLE SEQUENCE ALIGNMENT OF DH DOMAINS FROM THE MEGAPOLYPEPTIN BGC AND LAGRIAMIDE B BGC.	89
FIGURE S48. MULTIPLE SEQUENCE ALIGNMENT OF KS DOMAINS FROM THE MEGAPOLYPEPTIN BGC. ...	90
REFERENCES.....	91

METHODS

Chemicals and general experimental procedures.

Chemicals were purchased from Fischer Scientific and Sigma Aldrich, restriction endonucleases, ligases and Hi-Fi DNA assembler were purchased from New England Biolabs (NEB). Plasmid DNA was isolated using ZR plasmid Miniprep - Classic (Zymo Research, catalog No. D4016) following the manufacturer's protocol. Polymerase chain reaction (PCR) for plasmid construction was carried out using Q5 High fidelity polymerase from NEB, whereas DreamTaq PCR Master mix (2×) (Thermo Scientific, K1072) was used for mutant identification purposes. Oligonucleotides were purchased from Sigma Aldrich. See Supplementary Methods for further PCR details. Vector and primer design was performed using Geneious Prime 2023.1.1. Genomic DNA was isolated using GenElute (Sigma Aldrich, SLCH6584) following the manufacturer's protocol.

DNA preparation for Illumina sequencing and Nanopore sequencing.

A 20 µL cryopreserved sample of each Burkholderiales strain was transferred into 5 ml of either LB (most strains) or BYP liquid media (10.0 g.L⁻¹ starch, 4.0 g.L⁻¹ yeast extract, 2.0 g.L⁻¹ peptone, 3.0 g.L⁻¹, used for *P. megapolitana* and *P. acidicola* strains) and incubated in an orbital shaker at 220 rpm and 30°C for 24-48 h. DNA isolation was performed by using the GenElute Bacterial Genomic DNA Kits (Sigma Aldrich) according to the manufacturer's instruction. Prior to sample submission, the integrity of DNA was analyzed by agarose gel electrophoresis and concentration and purity determined using a Nanodrop.

Polymerase Chain Reaction.

For amplification of pBS003 the PCR was performed in 50 µL consisted of 50 ng of pBS001 as template, 200 mM of dNTPs, 0.5 mM Forward/Reverse primer solution, 10 µL of 5× Q5 High GC Enhancer Buffer, and 0.02 U/mL of Q5 High Fidelity DNA Polymerase. The thermal cycling conditions were according to the NEB Q5 (High Fidelity) manufacturer's protocol which involves: 1 cycle of initial denaturation (98°C, 30 s), 30 cycles of denaturation (98°C, 10 s) annealing (60°C, 30 s), extension (72°C, 30 s/kbp), and 1 cycle of final extension (72°C, 2 min). For pBS001 screening purposes, the PCR was performed using DreamTaq master mix (2×; Thermo Scientific) in 25 µL volume containing 50 ng of template, 0.5 mM Forward/Reverse primer solution, DMSO (3%), and 0.02 U/mL of DreamTaq DNA Polymerase (Thermo Scientific). The thermal cycling conditions were according to Thermo Scientific manufacturer's protocol,

which involves: 1 cycle of initial denaturation (95°C, 60 s), 30 cycles of denaturation (98°C, 10 s) annealing (60°C, 30 s), extension (72°C, 60 s/kbp), and 1 cycle of final extension (72°C, 10 min).

Sample preparation for IDBac analysis.

Burkholderiales bacteria were cultivated on agar medium (LB for most or BYP for slower growing *P. megapolitana* and *P. acidicola* strains) for approximately 3 days at 30°C. Three biological replicates (different colonies) of each bacterium were smeared onto a MALDI 384-well ground steel plate using a sterile wooden toothpick. After the bacterial colonies were smeared onto the target plate, 1 µL of 70% (7:3 Optima, Fisher Chemical: Optima LC-MS Grade Water Fisher Chemical) formic acid was pipetted onto each target with a bacterial smear. After the formic acid dried, 1 µL of 10 mg/mL α -cyano-4-hydroxycinnamic acid matrix was applied to each target with bacterial smears and dried. The matrix was prepared using α -cyano-4-hydroxycinnamic acid (powder, 98% pure, Sigma-Aldrich, part-C2020), 50% acetonitrile, 47.5% water, and 2.5% trifluoroacetic acid. All solvents used were LC-MS grade.

IDBac MALDI-TOF MS data acquisition.

MALDI-TOF MS data acquisition was performed using an Autoflex Speed LRF mass spectrometer (Bruker Daltonics) equipped with a smartbeamTM-II laser (355 nm). Automated data acquisition was accomplished using flexControl software version 3.4.135.0 (Bruker Daltonics) and flexAnalysis software version 3.4. Spectra were collected over three dates (2020-12-08, 2020-12-09, 2021-01-08, year-month-day). Protein spectra were recorded in positive linear mode (1000 shots; RepRate: 2000 Hz; delay: 29918 ns; ion source 1 voltage: 19.5 kV; ion source 2 voltage: 18.25 kV; lens voltage: 7 kV; mass range: 1.9 kDa to 2.1 kDa; matrix suppression cutoff: 1.9 kDa). Protein spectra were corrected with external Bruker Daltonics bacterial test standard (BTS). Specialized metabolite spectra were recorded in positive reflectron mode (1000 shots; RepRate: 2000 Hz; delay: 9316 ns; ion source 1 voltage: 19 kV; ion source 2 voltage: 16.8 kV; reflectron voltage 1: 21 kV; reflectron voltage 2: 9.7 kV; lens voltage: 8.5 kV; mass range: 0.05 kDa to 2.7 kDa; matrix suppression cutoff: 50 Da). Specialized metabolite spectra were corrected with external Bruker Daltonics peptide calibration standard and α -CHCA [2M+H]⁺ (379.0930 Da). Automated data acquisitions were performed using flexControl software version 3.4.135.0 (Bruker Daltonics) and flexAnalysis software version 3.4. Spectra were automatically evaluated during acquisition to determine whether a spectrum was of high enough quality to retain and add to the sum of the sample acquisition.

Cloning of the *mgp* BGC to yield pBS001 and generation of the empty vector control pBS003.

Cloning of the *mgp* BGC from *Paraburkholderia megapolitana* RL18-039-BIC-B (genome #76) was performed by Terra Bioforge (Wisconsin, USA). First, pSK021b containing *attP* and *int* from ϕ CTX1¹, and a pUC replicon was modified into a BAC vector. The high-copy pUC replicon was replaced with a 5.2-kbp *oriV-ori2-repE-incC-sopA-sopB-sopC* cassette to convert the plasmid into a low-copy BAC vector named pSK021b-BAC. The entire *mgp* BGC (located on chromosome #2, coordinates 2,357,111-2,410,193) was selectively excised from the genomic DNA using a CRISPR-Cas9 strategy², followed by isothermal DNA assembly with the linearized vector prepared by PCR^{3,4}. DNA assembly of Cas9-restricted genomic preparations was performed to linearized pSK021b-BAC vector containing overlap regions specific to the target *mgp* fragment. The DNA assembly reaction was transformed into *E. coli* BacOpt2.0 from which colonies were recovered. Transformants were assayed by colony PCR to generate amplicons for both the left and right cloning junctions. Plasmid DNA was restriction digested separately by EcoRI and BamHI and compared to a simulated digest, confirming a match (**SI Figure S11**). The junction PCRs for these clones were purified and Sanger sequenced to confirm the DNA assembly as designed. The BAC vector containing the *mgp* BGC was named pBS001.

To be used as a negative control, pBS003 was generated by amplifying the backbone of pBS001 using primer pair T7_pBS003_Fwd (5' GAATTCAAGCTTCTCGAGCCTATAGTGAGTCGTATTAC 3' – homology arm underlined) and pBAD_pBS003_Rev (5' CTCGAGAAGCTTGAATTCATGGAGAAACAGTAGAGAGT 3' – homology arm underlined) and ligating the PCR product using isothermal assembly methodology, at 50°C for 1 h.

Conjugation procedure to transfer pBS001 and pBS003 into *Burkholderia* sp. FERM BP-3421.

FERM BP-3421 and *E. coli* S17-1/pACYC184_MBurI_MBurII containing either pBS001 or pBS003 were cultivated in 10 mL of LB medium at 30°C, 200 rpm, in an orbital shaker, for ~18 h. The *E. coli* culture was supplemented with kanamycin at 50 $\mu\text{g}\cdot\text{mL}^{-1}$ and tetracycline at 10 $\mu\text{g}\cdot\text{mL}^{-1}$. The overnight cultures were subcultured in 10 mL fresh LB (200 μL of the *E. coli* S17-1 and 400 μL of FERM BP-3421 were used, respectively). Kanamycin and tetracycline as above were used for the *E. coli* cultures. *E. coli* and FERM BP-3421 were cultured at 30°C, 200 rpm, until an OD₆₀₀ range of 0.4 – 0.6. Cells were harvested at 4000 \times g for 5 min at room temperature, and gently washed twice with fresh LB (10 mL) each time followed by centrifugation as above. After the second wash, each cell pellet was resuspended in 1 mL fresh LB. For each given plasmid, 0.5 mL of *E. coli* S17-1/pACYC184_MBurI_MBurII were

combined with 0.5 mL of FERM BP-3421 and plated onto LB agar plates with no kanamycin. Negative control plates were generated by plating only *E. coli* S17-1/pACYC184_MBurI_MBurII (0.25 mL) or only FERM BP-3421 (0.25 mL) in separated LB agar plates. All plates were incubated at 30 °C overnight (~18 h). Cells were collected from the conjugation (and negative control) plates using a loop and streaked for single colonies onto fresh LB agar plates supplemented with kanamycin (500 µg.mL⁻¹ for plasmid selection) and gentamycin (10 µg.mL⁻¹ to prevent *E. coli* grow). Plates were incubated at 30°C for 2 – 3 days until exconjugants were observed. Obtained single colonies were re-streaked onto fresh selection plates. Purified clones were verified via PCR using oligonucleotides pBS001_scpT7_Fwd (5' ATCGAACATGCGTACGAGCC 3') and pBS001_scpT7_Rev (5' GGCCGATTCATTAATGCAGC 3') yielding an amplicon of 460 bp. pBS001 plasmid was used as positive control, and FERM BP-3421 gDNA was used as negative control (SI Figure S11).

Comparative metabolite analysis via LC-MS/MS.

For LC-MS/MS of *Burkholderia* sp. containing either pBS001 or pBS003, crude extract samples at 1 mg.mL⁻¹ were filtered using 4 mm PTFE syringe filters with 0.20 µm pore size (Thermo Scientific). The analyses were made using Ultra Performance Liquid Chromatography (Bruker Daltonics Corporation, Germany) coupled to mass spectrometry (COMPACT ESIQTOF). The chromatography analyses were temperature controlled at 40°C using an InfinityLab Poroshell 120 C-18 column with 2.1 × 50 mm (Agilent, USA), 1.9 mm particle size joined to a guard column InfinityLab Poroshell 120 C18 with 2.1 × 5 mm (Agilent, USA), 1.9 mm particle size, and a flow rate of 0.500 mL.min⁻¹. The mobile phase was composed of water + 0.1% formic acid (A) and acetonitrile + 0.1% formic acid (B) purchased from Thermo Scientific (Optima LC-MS). Analyses were performed using a quadrupole time-of-flight (QToF) using sodium formate (5mM) as internal calibrant. The collision energy applied was ramp-dependent ranging from 10 to 45 eV with end plate offset potential – 500V. The mass window (*m/z*) scanned was between 100 and 1800 with an acquisition rate of 5 Hz for MS and 7 Hz for MS/MS in positive mode [M+H]⁺. The five most intense ions were automated fragmented (auto MS/MS) in a data dependent acquisition mode (DDA). Spectra were processed using DataAnalysis 5.4 software.

Molecular Network analyses.

The MS data was exported to mzXML using DataAnalysis 4.2 software. Molecular networks for crude extracts were created using the mzXML files following the online workflow available at the Global

Natural Products Social Molecular Network (GNPS) platform (<http://gnps.ucsd.edu>)⁵. Consensus spectra with less than two spectra accumulation were not considered in this analysis. Molecular Network parameters were used as follow, ‘Precursor ion mass tolerance (PIMT) = 0.02’; ‘Fragment ion Mass Tolerance (FIMT) = 0.02’ and other settings we kept as default, which includes ‘Min Pairs Cos = 0.7’; ‘Minimum matched fragment ions = 6’; ‘Node TopK = 10’; ‘Minimum Cluster Size = 2’. ‘Library Search Min Matched Peaks = 6’; ‘Score Threshold = 0.7’. The resulting data were subtracted from a blank analysis and then processed as a network of edges and nodes on cytoscape Version (3.9.1)⁶.

General Equipment.

Optical rotations were measured on a Model 341 (Perkin Elmer) polarimeter. Ultraviolet absorption spectra were recorded on a Shimadzu UV-3600 Plus UV–VIS spectrophotometer. HR-ESI-MS and MS/MS experiments were recorded on a Select Series MRT (Waters), a SYNAPT G2-Si UPLC-ESI-qTOF (Waters), and a COMPACT ESI qTOF (Bruker). NMR spectra were measured on an AVANCE III-HD 600 MHz spectrometer equipped with a 5 mm QCI cryoprobe and referenced to residual solvent proton and carbon signals δ_{H} 2.50 and δ_{C} 39.5 for DMSO-*d*₆. MPLC (CombiFlash, Teledyne ISCO) was performed on a RediSep Rf solid load cartridge (5g, Teledyne ISCO). HPLC separations were performed on an Agilent 1200 series HPLC equipped with a binary pump and a diode array detector using a Synergi-RP FUSION (250 × 10 mm, 10 μm) and Kinetex XB-C18 (250 × 4.6 mm, 5 μm) Phenomenex columns. Solvents used for HPLC chromatography were Optima grade and were used without further purification.

Production of megapolipeptins.

For megapolipeptin A (**1**) and B (**2**) production, *Burkholderia* sp. FERM BP-3421 $\Delta fr9A/pBS001$ was cultured in 6 × Erlenmeyer flasks each containing 50 mL of seed medium at 25°C, 200 rpm for one day. 13 × 2.8 L Fernbach flasks each containing 1 L 2S4G production media and L-arabinose at 100 mM were inoculated with 20 ml of a seed culture and cultured at 25°C, 220 rpm for 5 days. The culture broth was collected by centrifugation at 8000 × *g* for 10 min. XAD-16N resin (Amberlite – Sigma) was added (10% w/v) to the supernatant and shaken at 200 rpm overnight (~16 h). The resin was collected by filtration and washed twice with MeOH 1:10 (weight of resin per volume of methanol) using an orbital shaker for 4h at 200 rpm. The resin was then removed by filtration and the MeOH phase was dried under reduced pressure to yield 45.25 g of crude extract. Half of the extract, corresponding to 6.5 L, was used for the isolation of megapolipeptins as described below.

Isolation of megapolipeptins A (1) and B (2).

The dried extract (FERM-BP-XAD-3421-fr9A::pBS001) was suspended in MeOH, and Celite (15 g/L) was added. The dried Celite was then loaded into a cartridge before separation on a C₁₈ (5 g) column using a CombiFlash system using a stepwise elution gradient of MeOH/H₂O (10% aq. MeOH (discarded), 20% aq. MeOH, 40% aq. MeOH, 60% aq. MeOH, 80% aq. MeOH, 100% MeOH, and 100% EtOAc) to afford six fractionated samples (FERM-BP-XAD-A → F).

MS analysis of the fractionated samples showed the presence of both megapolipeptin A (1) and B (2) in FERM-BP-XAD-C (60% aq. MeOH). The fraction was subjected to reversed-phase HPLC (Phenomenex Synergy FUSION RP-80A, 250 × 10 mm, 10 μm, 4 mL.min⁻¹) using a gradient solvent condition of 10% aq. ACN to 80% aq. ACN with 0.02% formic acid over 30 min. Two fractions were collected: FERM-BP-XAD-C-1 (*m/z* 958, 19.3 min) and FERM-BP-XAD-C-2 (*m/z* 984, 20.5 min). FERM-BP-XAD-C-1 was purified on an RP-HPLC column (Phenomenex Kinetex XB-C₁₈, 250 × 4.6 mm, 5 μm, 1.2 mL.min⁻¹) using a gradient of 10% aq. ACN to 40% aq. ACN with 0.02% formic acid over 10 minutes to afford **1** (3.7 mg, *t_R* 5.20 min). FERM-BP-XAD-C-2 containing **2** was purified by isocratic elution using a Phenomenex Kinetex XB-C₁₈ analytical column (250 × 4.6 mm, 5 μm, 1.2 mL.min⁻¹) to yield **2** (9.8 mg; *t_R* 9.46 min).

Structure elucidation details for megapolipeptin A (1).

Megapolipeptin A (1) was isolated as an amorphous, white solid. The molecular formula of C₄₅H₇₅N₅O₁₇ was deduced from HRMS measurements of the protonated cluster ion at [M+H]⁺ *m/z* 958.52350 (calc'd *m/z* 958.52307, 0.449 ppm, **Figure S13**). MS/MS data is presented in **Figure S14**. The planar structure of **1** was obtained using data from a comprehensive set of 1D (¹H and ¹³C) and 2D NMR (COSY, TOCSY, ROESY, phase sensitive HSQC, HMBC) experiments recorded in DMSO-*d*₆ (**Figures S15 – 21**). The 1D NMR spectra suggested the presence of six amide protons (δ_{H} 8.49, 7.93, 7.86, 7.58, 7.19, 6.76), seven carboxylic carbons (δ_{C} 174.0, 173.6, 173.4, 170.5, 169.9, 169.8, 159.8), two ketone carbons (δ_{C} 206.2, 202.4), and two α -protons (δ_{H} 4.32, 4.21) indicating the inclusion of two amino acid residues (**Table S8**). The 2D NMR spectra indicated the molecule was comprised of six isolated spin systems.

Observed gHMBC correlations from two NH protons (δ_{H} 7.19, 6.76) to a carbonyl carbon at δ_{C} 173.6 and a methylene carbon (δ_{C} 39.9) indicated the presence of a terminal amide group. Analysis of gCOSY and gHMBC spectra suggested a terminal 4-amino-3,5-dihydroxypentanamide (Ahp_a) moiety as the first

complete spin system. Two additional spin systems were established based on gCOSY and gHMBC correlations revealing threonine amino acid residues (¹Thr and ²Thr). The ¹H-NMR spectra showed the presence of four vinylic protons (δ_{H} 5.36 – 5.35) with gCOSY correlations to four allylic methylenes (δ_{H} 1.99 – 1.90). Continued gCOSY and gHMBC correlations revealed a 3-amido-5,19-dihydroxyicosan-10,14-dienamide (Adhda) moiety as the fourth completed spin system. From a ketone carbon at δ_{C} 206.2, gHMBC and gCOSY correlations were used to assign a fifth spin system as a 2-hydroxy-4-oxoheptanedioic acid (Hoha) functionality. The sixth spin system was completed based on gHMBC and gCOSY correlations from an additional downfield ketone carbon at δ_{C} 202.4 to give a 2-methyl-propan-1-one (Mpo) moiety. The arrangement of the various spin systems was assigned on the basis of gHMBC correlations between the amide carbon of ¹Thr-1 and A α pa-NH, ¹Thr-NH and ²Thr-1, ²Thr-NH and Adhda-1, Adhda-19 and Hoha-2 (**Figure S22**). The complete planar structure could not be determined due to unobserved gHMBC correlations from Mpo-1 to the main structure.

For unambiguous assignment of carboxylic acids in **1**, the molecule was treated with trimethylsilyl (TMS) diazomethane. Surprisingly, MS analysis of the methylated product showed two peaks, each with an increase in mass of 42 Da ($[\text{M}+\text{H}]^+$ m/z 1000.5632 (calc'd m/z 1000.5670) C₄₈H₈₂N₅O₁₇) suggesting the methylation of three carboxylic acids (**Figure S23** and **S24**). Both derivatized products (**3** and **4**) were separated by HPLC and analyzed by 1D and 2D NMR experiments. The ¹H-NMR spectrum showed two methoxy signals, which were assigned to the acid moieties of Hoha-1 and Hoha-7. Closer inspection of the ¹³C-NMR spectrum revealed the carbonyl carbon Mpo-1 was no longer present. Instead, gCOSY correlations showed this moiety was now a 2-isopropylloxirane (Ipo) due to a Büchner-Curtius-Schlotterbeck reaction between the carbonyl group and TMS diazomethane to generate an epoxide. The complete planar structures of **3** and **4** were determined through 1D and 2D NMR experiments and compared with **1** (**Figure S25** and **S26**). gHMBC correlations from Ipo-2 (δ_{H} 2.27) and Ipo-5 (δ_{H} 2.87, 2.60) to Adhda-21 (δ_{C} 168.4) in both derivatized products established the connection of the Ipo moiety with the rest of the molecule (**Figure S26**). From these data it was determined that the Mpo moiety was attached to Adhda-21, completing the planar structure of **1**. Sequential losses of A α pa [m/z 149.09352], ¹Thr [m/z 250.13945] and ²Thr [m/z 351.19006] in the MS/MS fragmentation data corroborated the positional assignments of these moieties (**Figure S27**).

Structure elucidation details for megapolipeptin B (**2**).

Megapolipeptin B (**2**) was also isolated as an amorphous, white solid. The mass spectrum of **2** displayed a molecular ion $[\text{M}+\text{H}]^+$ m/z 984.53821 (calc'd m/z 984.53872, -0.518 ppm) corresponding to a molecular

formula of $C_{47}H_{77}N_5O_{17}$ by HRMS (**Figure S27**). The mass difference of 26 mass units compared to **1** suggested that **2** contained two additional vinylic methines along the hydrocarbon chain. The NMR data of **2** were comparable to **1** showing six isolated spin systems (**Figures S29 – S34**). Downfield analysis of the 1H -NMR spectrum containing the vinylic signals (δ_H 5.37) integrated for six protons which agreed with the addition of 26 mass units. Comprehensive analysis of the 1D and 2D NMR spectra, when compared with **1**, revealed Ahpa, 1Thr , 2Thr , Hoha, and Mpo moieties. A set of gCOSY and gHMBC experiments established the final spin system of the hydrocarbon chain as 3-amino-5,21-dihydroxydocosa-8,12,16-trienamide (Adhta) (**Table S9, Figure S22**).

The assignment of the Mpa moiety was determined in similar fashion to compound **1**. Compound **2** was treated with TMS diazomethane to generate the epoxide derivative ($[M+H]^+$ 1026.5837 (calc'd 1026.5862). The complete planar structure of the derivatized product was established through gCOSY and gHMBC correlations. Finally, the positions of the Ahpa [m/z 149.09352], 1Thr [m/z 250.13945], and 2Thr [m/z 351.19006] moieties were confirmed by MS/MS.

Determination of the absolute configuration of the amino acids.

Megapolipeptin A (**1**) and B (**2**) (300 μ L each) were hydrolyzed (100 μ L 6 N HCl at 110°C for 18 hours) in a 500 μ L sealed reaction vessel. After the reaction, the excess HCl was removed under a stream of N_2 gas, and the residue was re-suspended in 100 μ L 50% aq. acetone. 100 μ L of FDVA solution (1-fluoro-2,4-dinitrophenyl-5-L-valineamide) in acetone (10 mg/mL) and 40 μ L of 1M $NaHCO_3$ were added to the reaction vessel and heated at 40°C for 1 hour. The reaction was then quenched with 40 μ L 1 N HCl and dried under a stream of N_2 gas. The dried residue was dissolved in 500 μ L MeOH and compared with standard FDVA-amino acids by RP-UHPLC-MS (Waters ACQUITY HSS T3 1.8 μ m, 0.650 mL.min $^{-1}$) using a gradient of 5% aq. ACN to 95% aq. ACN with 0.02% formic acid over 11 minutes. The absolute configuration of each amino acid was determined by comparing retention times of FDVA-amino acid derivatives in **1** and **2** with standard D,L FDVA-amino acids (**Figure S37**).

Partial hydrolysis of megapolipeptin B.

Megapolipeptin B (**2**, 0.5 mg) underwent partial hydrolysis to isolate a fragment containing one threonine residue. Compound **2** was hydrolyzed using 1N HCl at 110°C in a sealed 500 μ L reaction vessel. The reaction was monitored by UPLC-MS to optimize the yield of the desired product. After 30 minutes, the reaction was quenched with 1 M $NaHCO_3$ and dried under a stream of N_2 (g). The resulting hydrolysate

was purified using HPLC on an Agilent 1200 series system equipped with a Kinetex XB-C18 Phenomenex column (250 × 4.6 mm, 5 μm). An elution gradient from 5% to 95% aqueous MeCN over 40 min was employed, with a flow rate of 1.25 mL/min. The desired compound eluted at 25.1 min (0.1 mg) and was monitored by UV/Vis at 254 nm.

Megapolipeptin A (1).

$[\alpha]_D^{20} +5.0$ (c 0.23, MeOH); UV (MeOH) λ_{\max} (log ϵ) = 248 (1.41) nm. See **Table S8** for NMR shifts. See **Figures S14 – S20** for NMR spectra. HR-ESI-MS $[M+H]^+$ m/z 958.52350 (calcd for C₄₅H₇₅N₅O₁₇, 958.52307, 0.449 ppm).

Megapolipeptin B (2).

$[\alpha]_D^{20} +4.0$ (c 0.52, MeOH); UV (MeOH) λ_{\max} (log ϵ) = 248 (2.04) nm. See **Table S9** for NMR shifts. See **Figures S28 – S33** for NMR spectra. HR-ESI-MS $[M+H]^+$ m/z 984.53821 (calcd for C₄₇H₇₇N₅O₁₇, 984.53872, -0.518 ppm).

Antimicrobial screening.

Antimicrobial susceptibility tests against the bacterial target panel were performed using a miniaturized high throughput assay adapted from the broth microdilution methods outlined by the Clinical and Laboratory Standards Institute (CLSI) as described in previous studies^{7–14}. Bacterial test strains were individually grown on fresh nutrient agar (ATCC Medium 3), tryptic soy agar (ATCC Medium 18) or brain heart infusion agar (ATCC Medium 44), respectively (**Table S10**), as recommended by the American Type Culture Collection (ATCC) cultivation protocol. Individual colonies were used to inoculate 3 mL of sterile nutrient broth (NB), tryptic soy broth (TSB) or brain heart infusion broth (BHI) and grown overnight with shaking at 200 rpm, 37°C. *Listeria ivanovii* (ATCC BAA-139) was incubated overnight but not shaken (37°C; 5% CO₂). Saturated overnight cultures were diluted in their respective media according to turbidity to achieve approximately 5 × 10⁵ CFU/mL of final inoculum density and dispensed into sterile clear polystyrene 384-well microplates (Thermo Scientific™ 265202) with a final screening volume of 30 μL. *L. ivanovii* was diluted with and grown in Haemophilus test medium (HTM; ATCC Medium 2167). DMSO solutions of test compounds and antibiotic controls were prepared as 1:1 dilution series and pinned into each assay plate (200 nL) using a high throughput pinning robot (Tecan Freedom EVO 100) to achieve final screening concentrations ranging from 128 μM to 3.91 nM per

compound. In each 384-well plate; lane 1 was reserved for DMSO vehicle and culture medium; lane 2 reserved for DMSO vehicle, culture medium, and target bacteria; lanes 23 and 24 reserved for antibiotic controls, DMSO vehicle, culture medium, and target bacteria. After compound pinning, assay plates were read as t_0 at OD₆₀₀ using an automated plate reader (BioTek Synergy Neo2), sealed with a lid, and placed in a humidity-controlled incubator at 37°C for 18-20 hours before optical density was obtained for t_{20} . *L. ivanovii* was incubated in a separate incubator (37°C; 5% CO₂). Resulting growth curves for each dilution series were used to determine the MIC values for all test compounds following standard procedures.

Antifungal screening.

Antifungal activity against *C. albicans* (ATCC 14053) and *S. cerevisiae* (ATCC 9763) was evaluated using a microbroth dilution antibiotic susceptibility assay modified from McCulloch *et al.* (**Table S11**).¹⁵ Immediately prior to use, stock solutions of test compounds were prepared at the desired concentration in sterile-filtered dimethyl sulfoxide (DMSO, 40 μ L) and diluted with either Sabouraud dextrose broth (SDB, 960 μ L for *C. albicans*; BD Difco, Becton Dickinson, Mississauga, Ontario) or yeast mold broth (YMB; , 960 μ L for *S. cerevisiae*; BD Difco). The resulting test solutions (100 μ L; 4% DMSO) were transferred to the non-peripheral wells of a clear, non-tissue culture treated 96-well microtiter plate in triplicate (BD Falcon, Becton Dickinson, Mississauga, Ontario). Wells were then inoculated with suspensions of either *C. albicans* or *S. cerevisiae* (100 μ L; 1×10^6 CFU/mL), to obtain a cell density of 5×10^5 CFU/mL. Sterile water (200 μ L) was added to all perimeter wells to reduce evaporation from experimental wells. Each plate contained 3 negative control wells (4% DMSO in appropriate broth [100 μ L] inoculated with appropriate fungi [100 μ L; 1×10^6 CFU/mL]) and 3 untreated blank wells (2% DMSO in appropriate broth [200 μ L]). Initial and final optical densities (OD) were determined for each well by recording absorbance at 600 nm immediately before and after incubation for 24 hours at 37°C using a Molecular Devices Emax microplate reader (Molecular Devices; Sunnyvale, CA, USA). Initial OD readings were subtracted from the final readings for each well to obtain the change in OD (Δ OD). Δ OD values were corrected for background absorbance of the culture broth by subtracting the mean Δ OD readings of the blanks from the mean Δ OD readings of the control and test wells. The percentage inhibition of fungal growth is defined as: $[1 - (\text{mean test } \Delta\text{OD}/\text{mean negative control } \Delta\text{OD})] \times 100$, with the lowest concentration that inhibited growth by more than a mean value of 90% being considered the MIC¹⁶.

Antifungal activity against *A. niger* (DSM 737) and *P. lilacinum* (DSM 846) was assessed using the same microbroth dilution procedure with MICs being assessed by direct observation of fungal growth.

Fungal strains were inoculated onto fresh potato dextrose agar (BD Difco) and incubated at 22°C for 3-5 days. Colonies were then immersed in 0.1% Tween 80 in sterile, double distilled water (5 mL) and carefully rubbed with a sterile inoculating loop. The resulting suspension was transferred by pipet to a sterile centrifuge tube, spores were counted using an Improved Neubauer haemocytometer, and the density of the suspension adjusted to 2.5×10^5 CFU/mL with sterile 0.1% aqueous Tween 80. Samples were prepared in 96-well plates as described above using potato dextrose broth (PDB; BD Difco) prepared at twice the recommended concentration (48 g/L) and wells being inoculated with the aqueous suspensions of either *A. niger* or *P. lilacinum*. Following a 24 hour incubation at 22°C, wells were examined using a stereo microscope (320× magnification) with the lowest concentration that showed no discernable fungal growth and no difference in turbidity to the blanks in all three replicate wells being considered the MIC.

TABLES

Table S1. Whole-genome shotgun project data deposited on NCBI GenBank database under accession codes listed along with assembly metrics.

No.	Sample Name	Organism	Strain code	SUBID	BioProject	BioSample	Accession	Genome size (Mbp)	Contig number	G+C content (%)
1	1-A4	<i>Paraburkholderia xenovorans</i>	RL17-329-BIC-A	SUB12338458	PRJNA930029	SAMN32981017	JAQQBV000000000	5.8	140	62.2
2	1-A6	<i>Paraburkholderia nemoris</i>	RL17-333-BIC-B	SUB12338458	PRJNA930029	SAMN32981018	JAQQBW000000000	5.2	151	61.6
3	1-B2	<i>Paraburkholderia sedimicola</i>	RL17-328-BIB-A	SUB12338458	PRJNA930029	SAMN32981019	JAQQBX000000000	8.3	156	62.1
4	1-B5	<i>Paraburkholderia sedimicola</i>	RL17-333-BID-A	SUB12338458	PRJNA930029	SAMN32981020	JAQQBY000000000	7.3	175	61.9
5	1-B9	<i>Paraburkholderia diworthii</i>	RL17-335-BIF-A	SUB12338458	PRJNA930029	SAMN32981021	JAQQBZ000000000	7.9	97	62.4
6	1-C2	<i>Paraburkholderia sedimicola</i>	RL17-337-BIC-A	SUB12338458	PRJNA930029	SAMN32981022	JAQQCA000000000	6.7	200	61.1
7	1-C4	<i>Paraburkholderia xenovorans</i>	RL17-337-BIC-C	SUB12338458	PRJNA930029	SAMN32981023	JAQQCB000000000	8.7	402	62.2
8	1-C8	<i>Paraburkholderia sedimicola</i>	RL17-338-BIB-A	SUB12338458	PRJNA930029	SAMN32981024	JAQQCC000000000	7.5	131	61.4
9	1-C9	<i>Paraburkholderia sedimicola</i>	RL17-333-BIE-B	SUB12338458	PRJNA930029	SAMN32981025	JAQQCD000000000	7.7	344	62.0
10	1-D2	<i>Paraburkholderia sedimicola</i>	RL17-336-BIC-B	SUB12338458	PRJNA930029	SAMN32981026	JAQQCE000000000	7.8	180	61.9
11	1-D4	<i>Paraburkholderia metrosideri</i>	RL17-338-BIC-A	SUB12338458	PRJNA930029	SAMN32981027	JAQQCF000000000	7.3	166	61.5
12	1-D9	<i>Paraburkholderia bryophila</i>	RL17-338-BIF-C	SUB12338458	PRJNA930029	SAMN32981028	JAQQCG000000000	9.3	81	63.5
13	1-E8	<i>Paraburkholderia sedimicola</i>	RL17-340-BIC-B	SUB12338458	PRJNA930029	SAMN32981029	JAQQCH000000000	7.8	75	61.4
14	1-F6	<i>Paraburkholderia strydomiana</i>	RL17-350-BID-A	SUB12338458	PRJNA930029	SAMN32981030	JAQQCI000000000	7.5	85	62.7

15	1-G7	<i>Paraburkholderia strydomiana</i>	RL17-347-BIE-B	SUB12338458	PRJNA930029	SAMN32981031	JAQQCJ000000000	7.5	91	63.6
16	1-G8	<i>Paraburkholderia phytofirmans</i>	RL17-350-BIB-A	SUB12338458	PRJNA930029	SAMN32981032	JAQQCK000000000	7.5	52	62.6
17	1-G9	<i>Paraburkholderia strydomiana</i>	RL17-350-BIC-E	SUB12338458	PRJNA930029	SAMN32981033	JAQQCL000000000	7.9	107	63.1
18	1-H5	<i>Paraburkholderia strydomiana</i>	RL17-350-BIF-D	SUB12338458	PRJNA930029	SAMN32981034	JAQQCM000000000	7.2	56	61.8
19	1-I1	<i>Paraburkholderia strydomiana</i>	RL17-351-BIC-C	SUB12338458	PRJNA930029	SAMN32981035	JAQQCN000000000	7.6	49	61.7
20	1-I2	<i>Paraburkholderia strydomiana</i>	RL17-351-BIC-D	SUB12338458	PRJNA930029	SAMN32981036	JAQQCO000000000	7.4	72	61.8
21	2-B1	<i>Paraburkholderia graminis</i>	RL17-355-BIE-A	SUB12338458	PRJNA930029	SAMN32981037	JAQQCP000000000	7.2	62	62.8
22	2-C4	<i>Paraburkholderia sp.</i>	RL17-368-BIF-A	SUB12338458	PRJNA930029	SAMN32981038	JARESN000000000	7.4	181	64.0
23	2-C5	<i>Paraburkholderia caffeinilytica</i>	RL17-332-BIF-A	SUB12338458	PRJNA930029	SAMN32981039	JAQQCQ000000000	7.3	77	61.2
24	2-C6	<i>Paraburkholderia sedimicola</i>	RL17-333-BIC-A	SUB12338458	PRJNA930029	SAMN32981040	JAQQCR000000000	7.3	362	61.5
25	2-D3	<i>Paraburkholderia graminis</i>	RL17-368-BIF-C	SUB12338458	PRJNA930029	SAMN32981041	JAQQCS000000000	7.4	586	62.7
26	2-D4	<i>Paraburkholderia graminis</i>	RL17-369-BIB-A	SUB12338458	PRJNA930029	SAMN32981042	JAQQCT000000000	7.5	80	63.1
27	2-D9	<i>Paraburkholderia strydomiana</i>	RL17-353-BIB-A	SUB12338458	PRJNA930029	SAMN32981043	JAQQCU000000000	8.1	41	61.9
28	2-E2	<i>Paraburkholderia sedimicola</i>	RL17-357-BIB-A	SUB12338458	PRJNA930029	SAMN32981044	JAQQCV000000000	7.3	217	61.9
29	2-E4	<i>Paraburkholderia caledonica</i>	RL17-369-BIB-B	SUB12338458	PRJNA930029	SAMN32981045	JAQQCW000000000	7.8	138	62.1
30	2-E7	<i>Paraburkholderia caledonica</i>	RL17-371-BIF-A	SUB12338458	PRJNA930029	SAMN32981046	JAQQCX000000000	7.3	124	62.5
31	2-F1	<i>Paraburkholderia strydomiana</i>	RL17-373-BIB-B	SUB12338458	PRJNA930029	SAMN32981047	JAQQCY000000000	7.8	42	61.7

32	2-F2	<i>Paraburkholderia strydomiana</i>	RL17-373-BIB-D	SUB12338458	PRJNA930029	SAMN32981048	JAQQCZ000000000	7.8	38	62.4
33	2-F3	<i>Paraburkholderia sp.</i>	RL17-373-BIF-A	SUB12338458	PRJNA930029	SAMN32981049	JARESO000000000	7.8	594	62.5
34	2-F4	<i>Paraburkholderia strydomiana</i>	RL17-373-BIF-C	SUB12338458	PRJNA930029	SAMN32981050	JAQQDA000000000	7.8	95	62.3
35	2-F8	<i>Caballeronia jiangsuensis</i>	RL17-374-BIF-D	SUB12338458	PRJNA930029	SAMN32981051	JAQQDB000000000	8.5	168	61.5
36	2-F9	<i>Paraburkholderia sedimicola</i>	RL17-376-BIF-A	SUB12338458	PRJNA930029	SAMN32981052	JARESP000000000	8.8	250	63.1
37	2-G2	<i>Paraburkholderia aspalathi</i>	RL17-376-BIF-C	SUB12338458	PRJNA930029	SAMN32981053	JAQQDC000000000	11.4	72	60.8
38	2-G4	<i>Paraburkholderia strydomiana</i>	RL17-378-BIB-A	SUB12338458	PRJNA930029	SAMN32981054	JAQQDD000000000	8.8	166	62.2
39	2-G5	<i>Paraburkholderia strydomiana</i>	RL17-378-BIF-A	SUB12338458	PRJNA930029	SAMN32981055	JAQQDE000000000	8.3	50	62.0
40	2-G6	<i>Paraburkholderia dipogonis</i>	RL17-378-BIF-B	SUB12338458	PRJNA930029	SAMN32981056	JAQQDF000000000	11.4	100	62.3
41	2-G7	<i>Paraburkholderia nemoris</i>	RL17-379-BIB-A	SUB12338458	PRJNA930029	SAMN32981057	JAQQDG000000000	9.7	121	61.5
42	2-G8	<i>Paraburkholderia strydomiana</i>	RL17-379-BIB-C	SUB12338458	PRJNA930029	SAMN32981058	JAQQDH000000000	8.2	70	61.7
43	2-G9	<i>Paraburkholderia aspalathi</i>	RL17-379-BIF-A	SUB12338458	PRJNA930029	SAMN32981059	JAQQDI000000000	9.7	47	61.7
44	2-H1	<i>Paraburkholderia phytofirmans</i>	RL17-379-BIF-B	SUB12338458	PRJNA930029	SAMN32981060	JAQQDJ000000000	8.2	59	62.2
45	2-H2	<i>Paraburkholderia nemoris</i>	RL17-380-BIB-A	SUB12338458	PRJNA930029	SAMN32981061	JAQQDK000000000	7.7	74	62.1
46	2-H3	<i>Paraburkholderia sp.</i>	RL17-380-BIE-A	SUB12338458	PRJNA930029	SAMN32981062	JARESQ000000000	10.9	79	62.6
47	2-H4	<i>Paraburkholderia dipogonis</i>	RL17-381-BIB-A	SUB12338458	PRJNA930029	SAMN32981063	JAQQDL000000000	10.1	240	61.4
48	2-H5	<i>Paraburkholderia aromaticivorans</i>	RL17-381-BIB-B	SUB12338458	PRJNA930029	SAMN32981064	JAQQDM000000000	8.6	79	62.4

49	2-H8	<i>Paraburkholderia</i> <i>sp.</i>	RL17-383-BIF-A	SUB12338458	PRJNA930029	SAMN32981065	JARES000000000	8.6	103	61.7
50	2-H9	<i>Paraburkholderia</i> <i>caledonica</i>	RL17-383-BIF-B	SUB12338458	PRJNA930029	SAMN32981066	JAQQDN000000000	7.9	80	62.4
51	2-I1	<i>Caballeronia</i> <i>grimmiae</i>	RL17-374-BIB-E	SUB12338458	PRJNA930029	SAMN32981067	JAQQDO000000000	8.8	193	64.2
52	2-I2	<i>Paraburkholderia</i> <i>strydomiana</i>	RL17-376-BIB-A	SUB12338458	PRJNA930029	SAMN32981068	JAQQDP000000000	8.0	69	61.7
53	2-I6	<i>Paraburkholderia</i> <i>strydomiana</i>	RL17-379-BIB-D	SUB12338458	PRJNA930029	SAMN32981069	JAQQDQ000000000	10.6	72	61.7
54	2-I8	<i>Paraburkholderia</i> <i>sp.</i>	RL17-347-BIC-D	SUB12338458	PRJNA930029	SAMN32981070	JARESS000000000	7.7	317	62.2
55	2-I9	<i>Paraburkholderia</i> <i>phytofirmans</i>	RL17-351-BIE-A	SUB12338458	PRJNA930029	SAMN32981071	JAQQDR000000000	10.3	44	62.5
56	3-A2	<i>Paraburkholderia</i> <i>strydomiana</i>	RL17-378-BIB-B	SUB12338458	PRJNA930029	SAMN32981072	JAQQDS000000000	9.3	136	62.0
57	3-A6	<i>Paraburkholderia</i> <i>memoris</i>	RL17-376-BIF-D	SUB12338458	PRJNA930029	SAMN32981073	JAQQDT000000000	10.0	56	61.3
58	3-B1	<i>Paraburkholderia</i> <i>sedimicola</i>	RL18-035-BIC-A	SUB12338458	PRJNA930029	SAMN32981074	JAQQDU000000000	10.2	306	62.0
59	3-B2	<i>Paraburkholderia</i> <i>sedimicola</i>	RL18-035-BIE-A	SUB12338458	PRJNA930029	SAMN32981075	JAREST000000000	10.5	211	62.9
60	3-B5	<i>Paraburkholderia</i> <i>sedimicola</i>	RL18-007-BIE-A	SUB12338458	PRJNA930029	SAMN32981076	JAQQDV000000000	8.5	230	62.8
61	3-A9	<i>Paraburkholderia</i> <i>rhynchosiae</i>	RL18-126-BIB-B	SUB12338458	PRJNA930029	SAMN32981077	JAQQDW000000000	8.2	376	64.2
62	3-B6	<i>Paraburkholderia</i> <i>memoris</i>	RL18-009-BIC-B	SUB12338458	PRJNA930029	SAMN32981078	JAQQDX000000000	7.6	124	60.3
63	3-B9	<i>Paraburkholderia</i> <i>sedimicola</i>	RL18-021-BIF-A	SUB12338458	PRJNA930029	SAMN32981079	JAQQDY000000000	9.2	181	61.6
64	3-C2	<i>Paraburkholderia</i> <i>sedimicola</i>	RL18-056-BIE-A	SUB12338458	PRJNA930029	SAMN32981080	JAQQDZ000000000	10.1	171	61.6
65	3-C4	<i>Paraburkholderia</i> <i>memoris</i>	RL18-011-BIC-A	SUB12338458	PRJNA930029	SAMN32981081	JAQQEA000000000	8.6	112	60.5

66	3-C5	<i>Paraburkholderia sediminicola</i>	RL18-012-BIE-A	SUB12338458	PRJNA930029	SAMN32981082	JAQQEB000000000	8.3	222	60.5
67	3-C8	<i>Paraburkholderia sediminicola</i>	RL18-081-BIC-C	SUB12338458	PRJNA930029	SAMN32981083	JAQQEC000000000	10.6	231	62.4
68	3-D3	<i>Paraburkholderia nemoris</i>	RL18-043-BIE-A	SUB12338458	PRJNA930029	SAMN32981084	JAQQED000000000	10.3	78	60.6
69	3-D4	<i>Paraburkholderia sediminicola</i>	RL18-082-BIB-A	SUB12338458	PRJNA930029	SAMN32981085	JAQQEE000000000	8.8	233	62.1
70	3-D5	<i>Paraburkholderia fungorum</i>	RL18-106-BIC-A	SUB12338458	PRJNA930029	SAMN32981086	JAQQEF000000000	7.8	106	61.5
71	3-D6	<i>Paraburkholderia dipogonis</i>	RL18-106-BIC-C	SUB12338458	PRJNA930029	SAMN32981087	JAQQEG000000000	8.3	146	62.6
72	3-D7	<i>Paraburkholderia sediminicola</i>	RL18-106-BID-A	SUB12338458	PRJNA930029	SAMN32981088	JAQQEH000000000	10.2	136	61.9
73	3-E1	<i>Paraburkholderia aspalathi</i>	RL18-012-BIC-A	SUB12338458	PRJNA930029	SAMN32981089	JAQQEI000000000	9.7	114	61.3
74	3-E2	<i>Paraburkholderia sediminicola</i>	RL18-014-BIF-A	SUB12338458	PRJNA930029	SAMN32981090	JAQQEJ000000000	8.4	247	61.8
75	3-E8	<i>Paraburkholderia sediminicola</i>	RL18-017-BIF-B	SUB12338458	PRJNA930029	SAMN32981091	JAQQEK000000000	8.6	174	62.4
76	3-E9	<i>Paraburkholderia megapolitana</i>	RL18-039-BIC-B	SUB12338458	PRJNA930029	SAMN32981092	JAQQEL000000000	8.4	2	62.1
77	3-F3	<i>Paraburkholderia aspalathi</i>	RL18-139-BIC-B	SUB12338458	PRJNA930029	SAMN32981093	JAQQEM000000000	8.3	66	62.4
78	3-F6	<i>Paraburkholderia fungorum</i>	RL18-167-BIC-A	SUB12338458	PRJNA930029	SAMN32981094	JAQQEN000000000	9.7	4	61.9
79	3-F7	<i>Caballeronia glebae</i>	RL18-006-BIC-A	SUB12338458	PRJNA930029	SAMN32981095	JAQQEO000000000	8.6	178	63.7
80	3-F9	<i>Paraburkholderia sediminicola</i>	RL18-106-BIB-A	SUB12338458	PRJNA930029	SAMN32981096	JAQQEP000000000	9.4	154	61.5
81	3-G1	<i>Paraburkholderia sediminicola</i>	RL18-114-BIF-A	SUB12338458	PRJNA930029	SAMN32981097	JAQQEQ000000000	9.9	165	61.8
82	3-G5	<i>Paraburkholderia sp.</i>	RL18-085-BIA-A	SUB12338458	PRJNA930029	SAMN32981098	JARESU000000000	8.7	747	63.6

83	3-G9	<i>Paraburkholderia sp.</i>	RL18-101-BIB-B	SUB12338458	PRJNA930029	SAMN32981099	JARESV000000000	8.8	261	62.7
84	3-H1	<i>Paraburkholderia aspalathi</i>	RL18-101-BIC-A	SUB12338458	PRJNA930029	SAMN32981100	JAQQR000000000	8.9	65	62.3
85	3-H3	<i>Paraburkholderia sedimicola</i>	RL18-154-BIB-A	SUB12338458	PRJNA930029	SAMN32981101	JARESW000000000	9.0	200	60.4
86	3-H5	<i>Paraburkholderia sedimicola</i>	RL18-079-BIE-A	SUB12338458	PRJNA930029	SAMN32981102	JAQQES000000000	9.4	378	61.3
87	3-H6	<i>Paraburkholderia sedimicola</i>	RL18-120-BIB-A	SUB12338458	PRJNA930029	SAMN32981103	JAQQET000000000	9.4	122	61.8
88	3-H8	<i>Paraburkholderia sedimicola</i>	RL18-126-BIB-A	SUB12338458	PRJNA930029	SAMN32981104	JAQQEU000000000	8.6	334	62.5
89	3-I1	<i>Paraburkholderia aspalathi</i>	RL18-045-BIB-A	SUB12338458	PRJNA930029	SAMN32981105	JAQQEV000000000	9.5	287	60.3
90	3-I5	<i>Paraburkholderia sedimicola</i>	RL18-085-BIF-A	SUB12338458	PRJNA930029	SAMN32981106	JAQQEW000000000	8.8	194	61.7
91	1-B6	<i>Paraburkholderia sedimicola</i>	RL17-333-BIE-A	SUB12338458	PRJNA930029	SAMN32981107	JAQQEX000000000	9.6	391	60.8
92	1-F8	<i>Paraburkholderia sedimicola</i>	RL17-342-BIF-A	SUB12338458	PRJNA930029	SAMN32981108	JAQQEY000000000	8.8	3	60.8
93	1-G3	<i>Paraburkholderia dipogonis</i>	RL17-350-BIC-A	SUB12338458	PRJNA930029	SAMN32981109	JAQQEZ000000000	9.9	277	62.8
94	1-H1	<i>Paraburkholderia azotifigens</i>	RL17-350-BID-B	SUB12338458	PRJNA930029	SAMN32981110	JAQQFA000000000	8.3	129	63.4
95	2-E6	<i>Paraburkholderia strydomiana</i>	RL17-368-BIB-B	SUB12338458	PRJNA930029	SAMN32981111	JAQQFB000000000	8.8	112	62.2
96	2-E8	<i>Caballeronia grimmiae</i>	RL17-372-BIF-A	SUB12338458	PRJNA930029	SAMN32981112	JAQQFC000000000	10.2	115	62.0
97	2-E9	<i>Paraburkholderia graminis</i>	RL17-372-BIF-C	SUB12338458	PRJNA930029	SAMN32981113	JAQQFD000000000	9.1	92	62.7
98	2-G3	<i>Paraburkholderia phytofirmans</i>	RL17-377-BIF-A	SUB12338458	PRJNA930029	SAMN32981114	JAQQFE000000000	8.4	121	62.8
99	2-H6	<i>Paraburkholderia sp.</i>	RL17-381-BIF-C	SUB12338458	PRJNA930029	SAMN32981115	JARESX000000000	9.1	290	61.9

100	3-A1	<i>Paraburkholderia graminis</i>	RL17-369-BIF-A	SUB12338458	PRJNA930029	SAMN32981116	JAQQFF000000000	9.1	87	62.7
101	3-D2	<i>Paraburkholderia nemoris</i>	RL18-043-BID-A	SUB12338458	PRJNA930029	SAMN32981117	JAQQFG000000000	8.7	3	61.8
102	1-C1	<i>Paraburkholderia agricolaris</i>	RL17-342-BIF-B	SUB12338458	PRJNA930029	SAMN32981118	JAQQFH000000000	9.1	146	62.3
103	1-D8	<i>Paraburkholderia acidicola</i>	RL17-338-BIF-B	SUB11958114	PRJNA875462	SAMN30619028	JAQALG000000000	9.3	6	61.8
104	3-C1	<i>Paraburkholderia fungorum</i>	RL18-030-BIB-A	SUB12338458	PRJNA930029	SAMN32981119	JAQQFI000000000	10.9	175	62.5
105	3-E3	<i>Paraburkholderia madseniana</i>	RL18-015-BIC-B	SUB12338458	PRJNA930029	SAMN32981120	JAQQFJ000000000	9.0	206	61.8
106	4-F6	<i>Paraburkholderia agricolaris</i>	RL19-001-BIB-A	SUB12338458	PRJNA930029	SAMN32981121	JAQQFK000000000	8.9	167	62.0
107	4-H5	<i>Paraburkholderia fungorum</i>	RL19-015-BID-A	SUB12338458	PRJNA930029	SAMN32981122	JAQQFL000000000	9.0	115	62.5
108	5-A2	<i>Herbaspirillum lusitanum</i>	RL21-008-BIB-A	SUB12338458	PRJNA930029	SAMN32981123	JAQQFM000000000	9.5	46	60.3
109	5-A3	<i>Paraburkholderia agricolaris</i>	RL16-012-BIC-B	SUB12338458	PRJNA930029	SAMN32981124	JAQQFN000000000	9.6	132	62.3
110	5-A5	<i>Paraburkholderia fungorum</i>	RL17-336-BIC-C	SUB12338458	PRJNA930029	SAMN32981125	JAQQFO000000000	8.5	4	61.8
111	5-A6	<i>Paraburkholderia sp.</i>	RL17-337-BIB-A	SUB12338458	PRJNA930029	SAMN32981126	JARESY000000000	8.6	4	61.6
112	5-A7	<i>Paraburkholderia megapolitana</i>	RL17-339-BIF-C	SUB12338458	PRJNA930029	SAMN32981127	JAQQFP000000000	9.0	4	62.2
113	5-A8	<i>Paraburkholderia madseniana</i>	RL17-342-BIB-A	SUB12338458	PRJNA930029	SAMN32981128	JAQQFQ000000000	10.4	234	61.8
114	5-A9	<i>Herbaspirillum rhizosphaerae</i>	RL21-008-BIB-B	SUB12338458	PRJNA930029	SAMN32981129	JAQQFR000000000	10.8	40	57.9
115	5-B2	<i>Paraburkholderia sp.</i>	RL18-103-BIB-C	SUB12338458	PRJNA930029	SAMN32981130	JARESZ000000000	9.6	780	63.4

Table S2. Sequencing technology and assembly details for the 115 Burkholderiales strains.

No.	Sample Name	Organism	Strain code	Assembly Date	Assembly method/Version	Genome Coverage	Sequencing Technology
1	1-A4	<i>Paraburkholderia xenovorans</i>	RL17-329-BIC-A	2021-03-03	Unicycler Mar-2021.	93.2	Illumina
2	1-A6	<i>Paraburkholderia nemoris</i>	RL17-333-BIC-B	2021-03-03	Unicycler Mar-2021.	83.2	Illumina
3	1-B2	<i>Paraburkholderia sediminicola</i>	RL17-328-BIB-A	2021-03-03	Unicycler Mar-2021.	65.7	Illumina
4	1-B5	<i>Paraburkholderia sediminicola</i>	RL17-333-BID-A	2021-03-03	Unicycler Mar-2021.	46.5	Illumina
5	1-B9	<i>Paraburkholderia dilworthii</i>	RL17-335-BIF-A	2021-03-03	Unicycler Mar-2021.	81.6	Illumina
6	1-C2	<i>Paraburkholderia sediminicola</i>	RL17-337-BIC-A	2021-03-03	Unicycler Mar-2021.	88.6	Illumina
7	1-C4	<i>Paraburkholderia xenovorans</i>	RL17-337-BIC-C	2021-03-03	Unicycler Mar-2021.	80.0	Illumina
8	1-C8	<i>Paraburkholderia sediminicola</i>	RL17-338-BIB-A	2021-03-03	Unicycler Mar-2021.	92.5	Illumina
9	1-C9	<i>Paraburkholderia sediminicola</i>	RL17-333-BIE-B	2021-03-03	Unicycler Mar-2021.	56.0	Illumina
10	1-D2	<i>Paraburkholderia sediminicola</i>	RL17-336-BIC-B	2021-03-03	Unicycler Mar-2021.	71.2	Illumina
11	1-D4	<i>Paraburkholderia metrosideri</i>	RL17-338-BIC-A	2021-03-03	Unicycler Mar-2021.	72.3	Illumina
12	1-D9	<i>Paraburkholderia bryophila</i>	RL17-338-BIF-C	2021-03-03	Unicycler Mar-2021.	111.8	Illumina
13	1-E8	<i>Paraburkholderia sediminicola</i>	RL17-340-BIC-B	2021-03-03	Unicycler Mar-2021.	110.6	Illumina
14	1-F6	<i>Paraburkholderia strydomiana</i>	RL17-350-BID-A	2021-03-03	Unicycler Mar-2021.	85.0	Illumina
15	1-G7	<i>Paraburkholderia strydomiana</i>	RL17-347-BIE-B	2021-03-03	Unicycler Mar-2021.	71.7	Illumina
16	1-G8	<i>Paraburkholderia phytofirmans</i>	RL17-350-BIB-A	2021-03-03	Unicycler Mar-2021.	63.1	Illumina
17	1-G9	<i>Paraburkholderia strydomiana</i>	RL17-350-BIC-E	2021-03-03	Unicycler Mar-2021.	70.5	Illumina
18	1-H5	<i>Paraburkholderia strydomiana</i>	RL17-350-BIF-D	2021-03-03	Unicycler Mar-2021.	82.7	Illumina
19	1-I1	<i>Paraburkholderia strydomiana</i>	RL17-351-BIC-C	2021-03-03	Unicycler Mar-2021.	90.0	Illumina
20	1-I2	<i>Paraburkholderia strydomiana</i>	RL17-351-BIC-D	2021-03-03	Unicycler Mar-2021.	82.5	Illumina
21	2-B1	<i>Paraburkholderia graminis</i>	RL17-355-BIE-A	2021-03-03	Unicycler Mar-2021.	81.1	Illumina
22	2-C4	<i>Paraburkholderia sp.</i>	RL17-368-BIF-A	2021-03-03	Unicycler Mar-2021.	46.7	Illumina
23	2-C5	<i>Paraburkholderia caffeinilytica</i>	RL17-332-BIF-A	2021-03-03	Unicycler Mar-2021.	67.9	Illumina

24	2-C6	<i>Paraburkholderia sedimicola</i>	RL17-333-BIC-A	2021-03-03	Unicycler Mar-2021.	58.7	Illumina
25	2-D3	<i>Paraburkholderia graminis</i>	RL17-368-BIF-C	2021-03-03	Unicycler Mar-2021.	95.7	Illumina
26	2-D4	<i>Paraburkholderia graminis</i>	RL17-369-BIB-A	2021-03-03	Unicycler Mar-2021.	90.9	Illumina
27	2-D9	<i>Paraburkholderia strydomiana</i>	RL17-353-BIB-A	2021-03-03	Unicycler Mar-2021.	60.9	Illumina
28	2-E2	<i>Paraburkholderia sedimicola</i>	RL17-357-BIB-A	2021-03-03	Unicycler Mar-2021.	33.6	Illumina
29	2-E4	<i>Paraburkholderia caledonica</i>	RL17-369-BIB-B	2021-03-03	Unicycler Mar-2021.	65.8	Illumina
30	2-E7	<i>Paraburkholderia caledonica</i>	RL17-371-BIF-A	2021-03-03	Unicycler Mar-2021.	70.6	Illumina
31	2-F1	<i>Paraburkholderia strydomiana</i>	RL17-373-BIB-B	2021-03-03	Unicycler Mar-2021.	79.4	Illumina
32	2-F2	<i>Paraburkholderia strydomiana</i>	RL17-373-BIB-D	2021-03-03	Unicycler Mar-2021.	73.8	Illumina
33	2-F3	<i>Paraburkholderia sp.</i>	RL17-373-BIF-A	2021-03-03	Unicycler Mar-2021.	56.6	Illumina
34	2-F4	<i>Paraburkholderia strydomiana</i>	RL17-373-BIF-C	2021-03-03	Unicycler Mar-2021.	81.9	Illumina
35	2-F8	<i>Caballeronia jiangsuensis</i>	RL17-374-BIF-D	2021-03-03	Unicycler Mar-2021.	61.5	Illumina
36	2-F9	<i>Paraburkholderia sedimicola</i>	RL17-376-BIF-A	2021-03-03	Unicycler Mar-2021.	47.1	Illumina
37	2-G2	<i>Paraburkholderia aspalathi</i>	RL17-376-BIF-C	2021-03-03	Unicycler Mar-2021.	89.2	Illumina
38	2-G4	<i>Paraburkholderia strydomiana</i>	RL17-378-BIB-A	2021-03-03	Unicycler Mar-2021.	91.1	Illumina
39	2-G5	<i>Paraburkholderia strydomiana</i>	RL17-378-BIF-A	2021-03-03	Unicycler Mar-2021.	108.8	Illumina
40	2-G6	<i>Paraburkholderia dipogonis</i>	RL17-378-BIF-B	2021-03-03	Unicycler Mar-2021.	123.7	Illumina
41	2-G7	<i>Paraburkholderia nemoris</i>	RL17-379-BIB-A	2021-03-03	Unicycler Mar-2021.	86.1	Illumina
42	2-G8	<i>Paraburkholderia strydomiana</i>	RL17-379-BIB-C	2021-03-03	Unicycler Mar-2021.	100.6	Illumina
43	2-G9	<i>Paraburkholderia aspalathi</i>	RL17-379-BIF-A	2021-03-03	Unicycler Mar-2021.	81.2	Illumina
44	2-H1	<i>Paraburkholderia phytofirmans</i>	RL17-379-BIF-B	2021-03-03	Unicycler Mar-2021.	110.6	Illumina
45	2-H2	<i>Paraburkholderia nemoris</i>	RL17-380-BIB-A	2021-03-03	Unicycler Mar-2021.	87.6	Illumina
46	2-H3	<i>Paraburkholderia sp.</i>	RL17-380-BIE-A	2021-03-03	Unicycler Mar-2021.	91.9	Illumina
47	2-H4	<i>Paraburkholderia dipogonis</i>	RL17-381-BIB-A	2021-03-03	Unicycler Mar-2021.	80.1	Illumina
48	2-H5	<i>Paraburkholderia aromaticivorans</i>	RL17-381-BIB-B	2021-03-03	Unicycler Mar-2021.	76.9	Illumina
49	2-H8	<i>Paraburkholderia sp.</i>	RL17-383-BIF-A	2021-03-03	Unicycler Mar-2021.	108.8	Illumina

50	2-H9	<i>Paraburkholderia caledonica</i>	RL17-383-BIF-B	2021-03-03	Unicycler Mar-2021.	131.3	Illumina
51	2-I1	<i>Caballeronia grimmiae</i>	RL17-374-BIB-E	2021-03-03	Unicycler Mar-2021.	86.1	Illumina
52	2-I2	<i>Paraburkholderia strydomiana</i>	RL17-376-BIB-A	2021-03-03	Unicycler Mar-2021.	85.1	Illumina
53	2-I6	<i>Paraburkholderia strydomiana</i>	RL17-379-BIB-D	2021-03-03	Unicycler Mar-2021.	93.9	Illumina
54	2-I8	<i>Paraburkholderia sp.</i>	RL17-347-BIC-D	2021-03-03	Unicycler Mar-2021.	84.3	Illumina
55	2-I9	<i>Paraburkholderia phytofirmans</i>	RL17-351-BIE-A	2021-03-03	Unicycler Mar-2021.	110.3	Illumina
56	3-A2	<i>Paraburkholderia strydomiana</i>	RL17-378-BIB-B	2021-03-03	Unicycler Mar-2021.	85.7	Illumina
57	3-A6	<i>Paraburkholderia nemoris</i>	RL17-376-BIF-D	2021-03-03	Unicycler Mar-2021.	79.3	Illumina
58	3-B1	<i>Paraburkholderia sedimicola</i>	RL18-035-BIC-A	2021-03-03	Unicycler Mar-2021.	53.3	Illumina
59	3-B2	<i>Paraburkholderia sedimicola</i>	RL18-035-BIE-A	2021-03-03	Unicycler Mar-2021.	89.8	Illumina
60	3-B5	<i>Paraburkholderia sedimicola</i>	RL18-007-BIE-A	2021-03-03	Unicycler Mar-2021.	64.4	Illumina
61	3-A9	<i>Paraburkholderia rhynchosiae</i>	RL18-126-BIB-B	2021-03-03	Unicycler Mar-2021.	101.6	Illumina
62	3-B6	<i>Paraburkholderia nemoris</i>	RL18-009-BIC-B	2021-03-03	Unicycler Mar-2021.	122.5	Illumina
63	3-B9	<i>Paraburkholderia sedimicola</i>	RL18-021-BIF-A	2021-03-03	Unicycler Mar-2021.	80.1	Illumina
64	3-C2	<i>Paraburkholderia sedimicola</i>	RL18-056-BIE-A	2021-03-03	Unicycler Mar-2021.	70.2	Illumina
65	3-C4	<i>Paraburkholderia nemoris</i>	RL18-011-BIC-A	2021-03-03	Unicycler Mar-2021.	62.5	Illumina
66	3-C5	<i>Paraburkholderia sedimicola</i>	RL18-012-BIE-A	2021-03-03	Unicycler Mar-2021.	69.0	Illumina
67	3-C8	<i>Paraburkholderia sedimicola</i>	RL18-081-BIC-C	2021-03-03	Unicycler Mar-2021.	83.0	Illumina
68	3-D3	<i>Paraburkholderia nemoris</i>	RL18-043-BIE-A	2021-03-03	Unicycler Mar-2021.	76.6	Illumina
69	3-D4	<i>Paraburkholderia sedimicola</i>	RL18-082-BIB-A	2021-03-03	Unicycler Mar-2021.	65.2	Illumina
70	3-D5	<i>Paraburkholderia fungorum</i>	RL18-106-BIC-A	2021-03-03	Unicycler Mar-2021.	78.1	Illumina
71	3-D6	<i>Paraburkholderia dipogonis</i>	RL18-106-BIC-C	2021-03-03	Unicycler Mar-2021.	74.2	Illumina
72	3-D7	<i>Paraburkholderia sedimicola</i>	RL18-106-BID-A	2021-03-03	Unicycler Mar-2021.	135.0	Illumina
73	3-E1	<i>Paraburkholderia aspalathi</i>	RL18-012-BIC-A	2021-03-03	Unicycler Mar-2021.	107.7	Illumina
74	3-E2	<i>Paraburkholderia sedimicola</i>	RL18-014-BIF-A	2021-03-03	Unicycler Mar-2021.	98.8	Illumina
75	3-E8	<i>Paraburkholderia sedimicola</i>	RL18-017-BIF-B	2021-03-30	Unicycler Mar-2021.	97.3	Illumina + Oxford Nanopore

76	3-E9	<i>Paraburkholderia megapolitana</i>	RL18-039-BIC-B	2021-03-03	Unicycler Mar-2021.	190.3	Illumina
77	3-F3	<i>Paraburkholderia aspalathi</i>	RL18-139-BIC-B	2021-03-30	Unicycler Mar-2021.	61.7	Illumina + Oxford Nanopore
78	3-F6	<i>Paraburkholderia fungorum</i>	RL18-167-BIC-A	2021-03-03	Unicycler Mar-2021.	130.0	Illumina
79	3-F7	<i>Caballeronia glebae</i>	RL18-006-BIC-A	2021-03-03	Unicycler Mar-2021.	92.6	Illumina
80	3-F9	<i>Paraburkholderia sediminicola</i>	RL18-106-BIB-A	2021-03-03	Unicycler Mar-2021.	71.1	Illumina
81	3-G1	<i>Paraburkholderia sediminicola</i>	RL18-114-BIF-A	2021-03-03	Unicycler Mar-2021.	69.0	Illumina
82	3-G5	<i>Paraburkholderia sp.</i>	RL18-085-BIA-A	2021-03-03	Unicycler Mar-2021.	49.4	Illumina
83	3-G9	<i>Paraburkholderia sp.</i>	RL18-101-BIB-B	2021-03-03	Unicycler Mar-2021.	76.2	Illumina
84	3-H1	<i>Paraburkholderia aspalathi</i>	RL18-101-BIC-A	2021-03-03	Unicycler Mar-2021.	89.3	Illumina
85	3-H3	<i>Paraburkholderia sediminicola</i>	RL18-154-BIB-A	2021-03-03	Unicycler Mar-2021.	51.4	Illumina
86	3-H5	<i>Paraburkholderia sediminicola</i>	RL18-079-BIE-A	2021-03-03	Unicycler Mar-2021.	121.5	Illumina
87	3-H6	<i>Paraburkholderia sediminicola</i>	RL18-120-BIB-A	2021-03-03	Unicycler Mar-2021.	80.5	Illumina
88	3-H8	<i>Paraburkholderia sediminicola</i>	RL18-126-BIB-A	2021-03-03	Unicycler Mar-2021.	71.8	Illumina
89	3-I1	<i>Paraburkholderia aspalathi</i>	RL18-045-BIB-A	2021-03-03	Unicycler Mar-2021.	67.5	Illumina
90	3-I5	<i>Paraburkholderia sediminicola</i>	RL18-085-BIF-A	2021-03-03	Unicycler Mar-2021.	75.4	Illumina
91	1-B6	<i>Paraburkholderia sediminicola</i>	RL17-333-BIE-A	2021-03-03	Unicycler Mar-2021.	56.8	Illumina + Oxford Nanopore
92	1-F8	<i>Paraburkholderia sediminicola</i>	RL17-342-BIF-A	2021-03-03	Unicycler Mar-2021.	105.7	Illumina
93	1-G3	<i>Paraburkholderia dipogonis</i>	RL17-350-BIC-A	2021-03-03	Unicycler Mar-2021.	69.5	Illumina
94	1-H1	<i>Paraburkholderia azotifigens</i>	RL17-350-BID-B	2021-03-03	Unicycler Mar-2021.	91.1	Illumina
95	2-E6	<i>Paraburkholderia strydomiana</i>	RL17-368-BIB-B	2021-03-03	Unicycler Mar-2021.	65.8	Illumina
96	2-E8	<i>Caballeronia grimmiae</i>	RL17-372-BIF-A	2021-03-03	Unicycler Mar-2021.	72.8	Illumina
97	2-E9	<i>Paraburkholderia graminis</i>	RL17-372-BIF-C	2021-03-03	Unicycler Mar-2021.	58.1	Illumina
98	2-G3	<i>Paraburkholderia phytofirmans</i>	RL17-377-BIF-A	2021-03-03	Unicycler Mar-2021.	74.5	Illumina
99	2-H6	<i>Paraburkholderia sp.</i>	RL17-381-BIF-C	2021-03-03	Unicycler Mar-2021.	61.4	Illumina
100	3-A1	<i>Paraburkholderia graminis</i>	RL17-369-BIF-A	2021-03-03	Unicycler Mar-2021.	87.6	Illumina + Oxford Nanopore
101	3-D2	<i>Paraburkholderia nemoris</i>	RL18-043-BID-A	2021-03-03	Unicycler Mar-2021.	112.9	Illumina

102	1-C1	<i>Paraburkholderia agricolaris</i>	RL17-342-BIF-B	2021-05-28	Unicycler May-2021.	119.0	Illumina
103	1-D8	<i>Paraburkholderia acidicola</i>	RL17-338-BIF-B	2022-03-08	Unicycler Mar-2021.	137.3	Illumina + Oxford Nanopore
104	3-C1	<i>Paraburkholderia fungorum</i>	RL18-030-BIB-A	2021-05-28	Unicycler May-2021.	120.9	Illumina
105	3-E3	<i>Paraburkholderia madseniana</i>	RL18-015-BIC-B	2021-05-28	Unicycler May-2021.	94.2	Illumina
106	4-F6	<i>Paraburkholderia agricolaris</i>	RL19-001-BIB-A	2021-10-21	Unicycler Oct-2021.	64.0	Illumina
107	4-H5	<i>Paraburkholderia fungorum</i>	RL19-015-BID-A	2021-10-21	Unicycler Oct-2021.	83.1	Illumina
108	5-A2	<i>Herbaspirillum lusitanum</i>	RL21-008-BIB-A	2021-10-21	Unicycler Oct-2021.	142.5	Illumina
109	5-A3	<i>Paraburkholderia agricolaris</i>	RL16-012-BIC-B	2021-10-21	Unicycler Oct-2021.	158.3	Illumina
110	5-A5	<i>Paraburkholderia fungorum</i>	RL17-336-BIC-C	2022-03-08	Unicycler Mar-2021.	113.0	Illumina + Oxford Nanopore
111	5-A6	<i>Paraburkholderia sp.</i>	RL17-337-BIB-A	2022-03-08	Unicycler Mar-2021.	67.6	Illumina + Oxford Nanopore
112	5-A7	<i>Paraburkholderia megapolitana</i>	RL17-339-BIF-C	2022-03-08	Unicycler Mar-2021.	118.3	Illumina + Oxford Nanopore
113	5-A8	<i>Paraburkholderia madseniana</i>	RL17-342-BIB-A	2021-10-21	Unicycler Oct-2021.	104.6	Illumina
114	5-A9	<i>Herbaspirillum rhizosphaerae</i>	RL21-008-BIB-B	2021-10-21	Unicycler Oct-2021.	128.9	Illumina
115	5-B2	<i>Paraburkholderia sp.</i>	RL18-103-BIB-C	2021-10-21	Unicycler Oct-2021.	146.9	Illumina

Table S3. Collection date, environmental context, and geographic sample location for the sequenced strains.

No.	Sample Name	Organism	Strain	Collection Date	Broad-Scale Environmental context	Local-Scale Environmental context	Environmental Medium	Geographic location	Latitude and Longitude
1	1-A4	<i>Paraburkholderia xenovorans</i>	RL17-329-BIC-A	2017-02-25	temperate Coniferous Forest [ENVO:01000211]	rhizosphere environment [ENVO:01000999]	plant matter [ENVO:01001121]	Canada: British Columbia	49.62 N 123.19 W
2	1-A6	<i>Paraburkholderia nemoris</i>	RL17-333-BIC-B	2017-02-25	temperate Coniferous Forest [ENVO:01000211]	rhizosphere environment [ENVO:01000999]	plant matter [ENVO:01001121]	Canada: British Columbia	49.42 N 123.49 W
3	1-B2	<i>Paraburkholderia sediminicola</i>	RL17-328-BIB-A	2017-02-25	temperate Coniferous Forest [ENVO:01000211]	rhizosphere environment [ENVO:01000999]	plant matter [ENVO:01001121]	Canada: British Columbia	49.62 N 123.19 W
4	1-B5	<i>Paraburkholderia sediminicola</i>	RL17-333-BID-A	2017-02-25	temperate Coniferous Forest [ENVO:01000211]	rhizosphere environment [ENVO:01000999]	plant matter [ENVO:01001121]	Canada: British Columbia	49.42 N 123.49 W
5	1-B9	<i>Paraburkholderia diworthii</i>	RL17-335-BIF-A	2017-02-25	temperate Coniferous Forest [ENVO:01000211]	rhizosphere environment [ENVO:01000999]	plant matter [ENVO:01001121]	Canada: British Columbia	49.42 N 123.49 W
6	1-C2	<i>Paraburkholderia sediminicola</i>	RL17-337-BIC-A	2017-02-25	temperate Coniferous Forest [ENVO:01000211]	rhizosphere environment [ENVO:01000999]	plant matter [ENVO:01001121]	Canada: British Columbia	49.42 N 123.49 W
7	1-C4	<i>Paraburkholderia xenovorans</i>	RL17-337-BIC-C	2017-02-25	temperate Coniferous Forest [ENVO:01000211]	rhizosphere environment [ENVO:01000999]	plant matter [ENVO:01001121]	Canada: British Columbia	49.42 N 123.49 W
8	1-C8	<i>Paraburkholderia sediminicola</i>	RL17-338-BIB-A	2017-02-25	temperate Coniferous Forest [ENVO:01000211]	rhizosphere environment [ENVO:01000999]	plant matter [ENVO:01001121]	Canada: British Columbia	49.42 N 123.49 W

9	1-C9	<i>Paraburkholderia sediminicola</i>	RL17-333-BIE-B	2017-02-25	temperate Coniferous Forest [ENVO:01000211]	rhizosphere environment [ENVO:01000999]	plant matter [ENVO:01001121]	Canada: British Columbia	49.42 N 123.49 W
10	1-D2	<i>Paraburkholderia sediminicola</i>	RL17-336-BIC-B	2017-02-25	temperate Coniferous Forest [ENVO:01000211]	rhizosphere environment [ENVO:01000999]	plant matter [ENVO:01001121]	Canada: British Columbia	49.42 N 123.49 W
11	1-D4	<i>Paraburkholderia metrosideri</i>	RL17-338-BIC-A	2017-02-25	temperate Coniferous Forest [ENVO:01000211]	rhizosphere environment [ENVO:01000999]	plant matter [ENVO:01001121]	Canada: British Columbia	49.42 N 123.49 W
12	1-D9	<i>Paraburkholderia bryophila</i>	RL17-338-BIF-C	2017-02-25	temperate Coniferous Forest [ENVO:01000211]	rhizosphere environment [ENVO:01000999]	plant matter [ENVO:01001121]	Canada: British Columbia	49.42 N 123.49 W
13	1-E8	<i>Paraburkholderia sediminicola</i>	RL17-340-BIC-B	2017-02-25	temperate Coniferous Forest [ENVO:01000211]	rhizosphere environment [ENVO:01000999]	plant matter [ENVO:01001121]	Canada: British Columbia	49.42 N 123.49 W
14	1-F6	<i>Paraburkholderia strydomiana</i>	RL17-350-BID-A	2017-02-26	temperate Coniferous Forest [ENVO:01000211]	rhizosphere environment [ENVO:01000999]	plant matter [ENVO:01001121]	Canada: British Columbia	49.16 N 123.96 W
15	1-G7	<i>Paraburkholderia strydomiana</i>	RL17-347-BIE-B	2017-02-26	temperate Coniferous Forest [ENVO:01000211]	rhizosphere environment [ENVO:01000999]	plant matter [ENVO:01001121]	Canada: British Columbia	49.17 N 123.96 W
16	1-G8	<i>Paraburkholderia phytofirmans</i>	RL17-350-BIB-A	2017-02-26	temperate Coniferous Forest [ENVO:01000211]	rhizosphere environment [ENVO:01000999]	plant matter [ENVO:01001121]	Canada: British Columbia	49.16 N 123.96 W
17	1-G9	<i>Paraburkholderia strydomiana</i>	RL17-350-BIC-E	2017-02-26	temperate Coniferous Forest [ENVO:01000211]	rhizosphere environment [ENVO:01000999]	plant matter [ENVO:01001121]	Canada: British Columbia	49.16 N 123.96 W
18	1-H5	<i>Paraburkholderia strydomiana</i>	RL17-350-BIF-D	2017-02-26	temperate Coniferous Forest [ENVO:01000211]	rhizosphere environment [ENVO:01000999]	plant matter [ENVO:01001121]	Canada: British Columbia	49.16 N 123.96 W
19	1-I1	<i>Paraburkholderia strydomiana</i>	RL17-351-BIC-C	2017-02-26	temperate Coniferous Forest [ENVO:01000211]	rhizosphere environment [ENVO:01000999]	plant matter [ENVO:01001121]	Canada: British Columbia	49.16 N 123.96 W
20	1-I2	<i>Paraburkholderia strydomiana</i>	RL17-351-BIC-D	2017-02-26	temperate Coniferous Forest [ENVO:01000211]	rhizosphere environment [ENVO:01000999]	plant matter [ENVO:01001121]	Canada: British Columbia	49.16 N 123.96 W
21	2-B1	<i>Paraburkholderia graminis</i>	RL17-355-BIE-A	2017-02-27	temperate Coniferous Forest [ENVO:01000211]	rhizosphere environment [ENVO:01000999]	plant matter [ENVO:01001121]	Canada: British Columbia	48.64 N 123.65 W
22	2-C4	<i>Paraburkholderia sp.</i>	RL17-368-BIF-A	2017-08-06	temperate Coniferous Forest [ENVO:01000211]	rhizosphere environment [ENVO:01000999]	plant matter [ENVO:01001121]	Canada: British Columbia	54.50 N 128.71 W
23	2-C5	<i>Paraburkholderia caffeinilytica</i>	RL17-332-BIF-A	2017-02-25	temperate Coniferous Forest [ENVO:01000211]	rhizosphere environment [ENVO:01000999]	plant matter [ENVO:01001121]	Canada: British Columbia	49.42 N 123.49 W
24	2-C6	<i>Paraburkholderia sediminicola</i>	RL17-333-BIC-A	2017-02-25	temperate Coniferous Forest [ENVO:01000211]	rhizosphere environment [ENVO:01000999]	plant matter [ENVO:01001121]	Canada: British Columbia	49.42 N 123.49 W
25	2-D3	<i>Paraburkholderia graminis</i>	RL17-368-BIF-C	2017-08-06	temperate Coniferous Forest [ENVO:01000211]	rhizosphere environment [ENVO:01000999]	plant matter [ENVO:01001121]	Canada: British Columbia	54.50 N 128.71 W
26	2-D4	<i>Paraburkholderia graminis</i>	RL17-369-BIB-A	2017-08-06	temperate Coniferous Forest [ENVO:01000211]	rhizosphere environment [ENVO:01000999]	plant matter [ENVO:01001121]	Canada: British Columbia	54.50 N 128.71 W
27	2-D9	<i>Paraburkholderia strydomiana</i>	RL17-353-BIB-A	2017-02-26	temperate Coniferous Forest [ENVO:01000211]	rhizosphere environment [ENVO:01000999]	plant matter [ENVO:01001121]	Canada: British Columbia	49.16 N 123.96 W
28	2-E2	<i>Paraburkholderia sediminicola</i>	RL17-357-BIB-A	2017-02-27	temperate Coniferous Forest [ENVO:01000211]	rhizosphere environment [ENVO:01000999]	plant matter [ENVO:01001121]	Canada: British Columbia	48.64 N 123.65 W
29	2-E4	<i>Paraburkholderia caledonica</i>	RL17-369-BIB-B	2017-08-06	temperate Coniferous Forest [ENVO:01000211]	rhizosphere environment [ENVO:01000999]	plant matter [ENVO:01001121]	Canada: British Columbia	54.50 N 128.71 W
30	2-E7	<i>Paraburkholderia caledonica</i>	RL17-371-BIF-A	2017-08-06	temperate Coniferous Forest [ENVO:01000211]	rhizosphere environment [ENVO:01000999]	plant matter [ENVO:01001121]	Canada: British Columbia	54.50 N 128.71 W
31	2-F1	<i>Paraburkholderia strydomiana</i>	RL17-373-BIB-B	2017-08-06	temperate Coniferous Forest [ENVO:01000211]	rhizosphere environment [ENVO:01000999]	plant matter [ENVO:01001121]	Canada: British Columbia	54.50 N 128.71 W
32	2-F2	<i>Paraburkholderia strydomiana</i>	RL17-373-BIB-D	2017-08-06	temperate Coniferous Forest [ENVO:01000211]	rhizosphere environment [ENVO:01000999]	plant matter [ENVO:01001121]	Canada: British Columbia	54.50 N 128.71 W
33	2-F3	<i>Paraburkholderia sp.</i>	RL17-373-BIF-A	2017-08-06	temperate Coniferous Forest [ENVO:01000211]	rhizosphere environment [ENVO:01000999]	plant matter [ENVO:01001121]	Canada: British Columbia	54.50 N 128.71 W
34	2-F4	<i>Paraburkholderia strydomiana</i>	RL17-373-BIF-C	2017-08-06	temperate Coniferous Forest [ENVO:01000211]	rhizosphere environment [ENVO:01000999]	plant matter [ENVO:01001121]	Canada: British Columbia	54.50 N 128.71 W

35	2-F8	<i>Caballeronia jiangsuensis</i>	RL17-374-BIF-D	2017-08-06	temperate Coniferous Forest [ENVO:01000211]	rhizosphere environment [ENVO:01000999]	plant matter [ENVO:01001121]	Canada: British Columbia	54.50 N 128.71 W
36	2-F9	<i>Paraburkholderia sedimicola</i>	RL17-376-BIF-A	2017-07-22	temperate Coniferous Forest [ENVO:01000211]	rhizosphere environment [ENVO:01000999]	plant matter [ENVO:01001121]	Canada: British Columbia	49.38 N 121.93 W
37	2-G2	<i>Paraburkholderia aspalathi</i>	RL17-376-BIF-C	2017-07-22	temperate Coniferous Forest [ENVO:01000211]	rhizosphere environment [ENVO:01000999]	plant matter [ENVO:01001121]	Canada: British Columbia	49.38 N 121.93 W
38	2-G4	<i>Paraburkholderia strydomiana</i>	RL17-378-BIB-A	2017-07-22	temperate Coniferous Forest [ENVO:01000211]	rhizosphere environment [ENVO:01000999]	plant matter [ENVO:01001121]	Canada: British Columbia	49.38 N 121.94 W
39	2-G5	<i>Paraburkholderia strydomiana</i>	RL17-378-BIF-A	2017-07-22	temperate Coniferous Forest [ENVO:01000211]	rhizosphere environment [ENVO:01000999]	plant matter [ENVO:01001121]	Canada: British Columbia	49.38 N 121.94 W
40	2-G6	<i>Paraburkholderia dipogonis</i>	RL17-378-BIF-B	2017-07-22	temperate Coniferous Forest [ENVO:01000211]	rhizosphere environment [ENVO:01000999]	plant matter [ENVO:01001121]	Canada: British Columbia	49.38 N 121.94 W
41	2-G7	<i>Paraburkholderia nemoris</i>	RL17-379-BIB-A	2017-07-22	temperate Coniferous Forest [ENVO:01000211]	rhizosphere environment [ENVO:01000999]	plant matter [ENVO:01001121]	Canada: British Columbia	49.38 N 121.94 W
42	2-G8	<i>Paraburkholderia strydomiana</i>	RL17-379-BIB-C	2017-07-22	temperate Coniferous Forest [ENVO:01000211]	rhizosphere environment [ENVO:01000999]	plant matter [ENVO:01001121]	Canada: British Columbia	49.38 N 121.94 W
43	2-G9	<i>Paraburkholderia aspalathi</i>	RL17-379-BIF-A	2017-07-22	temperate Coniferous Forest [ENVO:01000211]	rhizosphere environment [ENVO:01000999]	plant matter [ENVO:01001121]	Canada: British Columbia	49.38 N 121.94 W
44	2-H1	<i>Paraburkholderia phytofirmans</i>	RL17-379-BIF-B	2017-07-22	temperate Coniferous Forest [ENVO:01000211]	rhizosphere environment [ENVO:01000999]	plant matter [ENVO:01001121]	Canada: British Columbia	49.38 N 121.94 W
45	2-H2	<i>Paraburkholderia nemoris</i>	RL17-380-BIB-A	2017-07-22	temperate Coniferous Forest [ENVO:01000211]	rhizosphere environment [ENVO:01000999]	plant matter [ENVO:01001121]	Canada: British Columbia	49.38 N 121.94 W
46	2-H3	<i>Paraburkholderia sp.</i>	RL17-380-BIE-A	2017-07-22	temperate Coniferous Forest [ENVO:01000211]	rhizosphere environment [ENVO:01000999]	plant matter [ENVO:01001121]	Canada: British Columbia	49.38 N 121.94 W
47	2-H4	<i>Paraburkholderia dipogonis</i>	RL17-381-BIB-A	2017-07-22	temperate Coniferous Forest [ENVO:01000211]	rhizosphere environment [ENVO:01000999]	plant matter [ENVO:01001121]	Canada: British Columbia	49.37 N 121.93 W
48	2-H5	<i>Paraburkholderia aromaticivorans</i>	RL17-381-BIB-B	2017-07-22	temperate Coniferous Forest [ENVO:01000211]	rhizosphere environment [ENVO:01000999]	plant matter [ENVO:01001121]	Canada: British Columbia	49.37 N 121.93 W
49	2-H8	<i>Paraburkholderia sp.</i>	RL17-383-BIF-A	2017-07-22	temperate Coniferous Forest [ENVO:01000211]	rhizosphere environment [ENVO:01000999]	plant matter [ENVO:01001121]	Canada: British Columbia	49.35 N 121.90 W
50	2-H9	<i>Paraburkholderia caledonica</i>	RL17-383-BIF-B	2017-07-22	temperate Coniferous Forest [ENVO:01000211]	rhizosphere environment [ENVO:01000999]	plant matter [ENVO:01001121]	Canada: British Columbia	49.35 N 121.90 W
51	2-I1	<i>Caballeronia grimmiae</i>	RL17-374-BIB-E	2017-08-06	temperate Coniferous Forest [ENVO:01000211]	rhizosphere environment [ENVO:01000999]	plant matter [ENVO:01001121]	Canada: British Columbia	54.50 N 128.71 W
52	2-I2	<i>Paraburkholderia strydomiana</i>	RL17-376-BIB-A	2017-07-22	temperate Coniferous Forest [ENVO:01000211]	rhizosphere environment [ENVO:01000999]	plant matter [ENVO:01001121]	Canada: British Columbia	49.38 N 121.93 W
53	2-I6	<i>Paraburkholderia strydomiana</i>	RL17-379-BIB-D	2017-07-22	temperate Coniferous Forest [ENVO:01000211]	rhizosphere environment [ENVO:01000999]	plant matter [ENVO:01001121]	Canada: British Columbia	49.38 N 121.93 W
54	2-I8	<i>Paraburkholderia sp.</i>	RL17-347-BIC-D	2017-02-26	temperate Coniferous Forest [ENVO:01000211]	rhizosphere environment [ENVO:01000999]	plant matter [ENVO:01001121]	Canada: British Columbia	49.17 N 123.96 W
55	2-I9	<i>Paraburkholderia phytofirmans</i>	RL17-351-BIE-A	2017-02-26	temperate Coniferous Forest [ENVO:01000211]	rhizosphere environment [ENVO:01000999]	plant matter [ENVO:01001121]	Canada: British Columbia	49.16 N 123.96 W
56	3-A2	<i>Paraburkholderia strydomiana</i>	RL17-378-BIB-B	2017-07-22	temperate Coniferous Forest [ENVO:01000211]	rhizosphere environment [ENVO:01000999]	plant matter [ENVO:01001121]	Canada: British Columbia	49.38 N 121.94 W
57	3-A6	<i>Paraburkholderia nemoris</i>	RL17-376-BIF-D	2017-07-22	temperate Coniferous Forest [ENVO:01000211]	rhizosphere environment [ENVO:01000999]	plant matter [ENVO:01001121]	Canada: British Columbia	49.38 N 121.93 W
58	3-B1	<i>Paraburkholderia sedimicola</i>	RL18-035-BIC-A	2018-04-09	temperate Coniferous Forest [ENVO:01000211]	rhizosphere environment [ENVO:01000999]	plant matter [ENVO:01001121]	Canada: British Columbia	49.38 N 121.94 W
59	3-B2	<i>Paraburkholderia sedimicola</i>	RL18-035-BIE-A	2018-04-09	temperate Coniferous Forest [ENVO:01000211]	rhizosphere environment [ENVO:01000999]	plant matter [ENVO:01001121]	Canada: British Columbia	49.38 N 121.94 W
60	3-B5	<i>Paraburkholderia sedimicola</i>	RL18-007-BIE-A	2018-04-09	temperate Coniferous Forest [ENVO:01000211]	rhizosphere environment [ENVO:01000999]	plant matter [ENVO:01001121]	Canada: British Columbia	49.38 N 121.94 W

61	3-A9	<i>Paraburkholderia rhynchosiae</i>	RL18-126-BIB-B	2018-08-15	temperate Coniferous Forest [ENVO:01000211]	rhizosphere environment [ENVO:01000999]	plant matter [ENVO:01001121]	Canada: British Columbia	49.33 N 124.92 W
62	3-B6	<i>Paraburkholderia nemoris</i>	RL18-009-BIC-B	2018-04-09	temperate Coniferous Forest [ENVO:01000211]	rhizosphere environment [ENVO:01000999]	plant matter [ENVO:01001121]	Canada: British Columbia	49.38 N 121.94 W
63	3-B9	<i>Paraburkholderia sediminicola</i>	RL18-021-BIF-A	2018-04-09	temperate Coniferous Forest [ENVO:01000211]	rhizosphere environment [ENVO:01000999]	plant matter [ENVO:01001121]	Canada: British Columbia	49.38 N 121.94 W
64	3-C2	<i>Paraburkholderia sediminicola</i>	RL18-056-BIE-A	2018-08-14	temperate Coniferous Forest [ENVO:01000211]	rhizosphere environment [ENVO:01000999]	plant matter [ENVO:01001121]	Canada: British Columbia	49.25 N 124.79 W
65	3-C4	<i>Paraburkholderia nemoris</i>	RL18-011-BIC-A	2018-04-09	temperate Coniferous Forest [ENVO:01000211]	rhizosphere environment [ENVO:01000999]	plant matter [ENVO:01001121]	Canada: British Columbia	49.38 N 121.94 W
66	3-C5	<i>Paraburkholderia sediminicola</i>	RL18-012-BIE-A	2018-04-09	temperate Coniferous Forest [ENVO:01000211]	rhizosphere environment [ENVO:01000999]	plant matter [ENVO:01001121]	Canada: British Columbia	49.38 N 121.94 W
67	3-C8	<i>Paraburkholderia sediminicola</i>	RL18-081-BIC-C	2018-08-14	temperate Coniferous Forest [ENVO:01000211]	rhizosphere environment [ENVO:01000999]	plant matter [ENVO:01001121]	Canada: British Columbia	49.21 N 124.79 W
68	3-D3	<i>Paraburkholderia nemoris</i>	RL18-043-BIE-A	2018-04-09	temperate Coniferous Forest [ENVO:01000211]	rhizosphere environment [ENVO:01000999]	plant matter [ENVO:01001121]	Canada: British Columbia	49.38 N 121.94 W
69	3-D4	<i>Paraburkholderia sediminicola</i>	RL18-082-BIB-A	2018-08-14	temperate Coniferous Forest [ENVO:01000211]	rhizosphere environment [ENVO:01000999]	plant matter [ENVO:01001121]	Canada: British Columbia	49.25 N 124.86 W
70	3-D5	<i>Paraburkholderia fungorum</i>	RL18-106-BIC-A	2018-08-15	temperate Coniferous Forest [ENVO:01000211]	rhizosphere environment [ENVO:01000999]	plant matter [ENVO:01001121]	Canada: British Columbia	49.29 N 124.91 W
71	3-D6	<i>Paraburkholderia dipogonis</i>	RL18-106-BIC-C	2018-08-15	temperate Coniferous Forest [ENVO:01000211]	rhizosphere environment [ENVO:01000999]	plant matter [ENVO:01001121]	Canada: British Columbia	49.29 N 124.91 W
72	3-D7	<i>Paraburkholderia sediminicola</i>	RL18-106-BID-A	2018-08-15	temperate Coniferous Forest [ENVO:01000211]	rhizosphere environment [ENVO:01000999]	plant matter [ENVO:01001121]	Canada: British Columbia	49.29 N 124.91 W
73	3-E1	<i>Paraburkholderia aspalathi</i>	RL18-012-BIC-A	2018-04-09	temperate Coniferous Forest [ENVO:01000211]	rhizosphere environment [ENVO:01000999]	plant matter [ENVO:01001121]	Canada: British Columbia	49.38 N 121.94 W
74	3-E2	<i>Paraburkholderia sediminicola</i>	RL18-014-BIF-A	2018-04-09	temperate Coniferous Forest [ENVO:01000211]	rhizosphere environment [ENVO:01000999]	plant matter [ENVO:01001121]	Canada: British Columbia	49.38 N 121.94 W
75	3-E8	<i>Paraburkholderia sediminicola</i>	RL18-017-BIF-B	2018-04-09	temperate Coniferous Forest [ENVO:01000211]	rhizosphere environment [ENVO:01000999]	plant matter [ENVO:01001121]	Canada: British Columbia	49.38 N 121.94 W
76	3-E9	<i>Paraburkholderia megapolitana</i>	RL18-039-BIC-B	2018-04-09	temperate Coniferous Forest [ENVO:01000211]	rhizosphere environment [ENVO:01000999]	plant matter [ENVO:01001121]	Canada: British Columbia	49.38 N 121.94 W
77	3-F3	<i>Paraburkholderia aspalathi</i>	RL18-139-BIC-B	2018-08-15	temperate Coniferous Forest [ENVO:01000211]	rhizosphere environment [ENVO:01000999]	plant matter [ENVO:01001121]	Canada: British Columbia	49.24 N 125.36 W
78	3-F6	<i>Paraburkholderia fungorum</i>	RL18-167-BIC-A	2018-08-16	temperate Coniferous Forest [ENVO:01000211]	rhizosphere environment [ENVO:01000999]	plant matter [ENVO:01001121]	Canada: British Columbia	48.94 N 125.56 W
79	3-F7	<i>Caballeronia glebae</i>	RL18-006-BIC-A	2018-04-09	temperate Coniferous Forest [ENVO:01000211]	rhizosphere environment [ENVO:01000999]	plant matter [ENVO:01001121]	Canada: British Columbia	49.38 N 121.94 W
80	3-F9	<i>Paraburkholderia sediminicola</i>	RL18-106-BIB-A	2018-08-15	temperate Coniferous Forest [ENVO:01000211]	rhizosphere environment [ENVO:01000999]	plant matter [ENVO:01001121]	Canada: British Columbia	49.29 N 124.91 W
81	3-G1	<i>Paraburkholderia sediminicola</i>	RL18-114-BIF-A	2018-08-15	temperate Coniferous Forest [ENVO:01000211]	rhizosphere environment [ENVO:01000999]	plant matter [ENVO:01001121]	Canada: British Columbia	49.92 N 124.92 W
82	3-G5	<i>Paraburkholderia sp.</i>	RL18-085-BIA-A	2018-08-14	temperate Coniferous Forest [ENVO:01000211]	rhizosphere environment [ENVO:01000999]	plant matter [ENVO:01001121]	Canada: British Columbia	49.21 N 124.79 W
83	3-G9	<i>Paraburkholderia sp.</i>	RL18-101-BIB-B	2018-08-14	temperate Coniferous Forest [ENVO:01000211]	rhizosphere environment [ENVO:01000999]	plant matter [ENVO:01001121]	Canada: British Columbia	49.24 N 124.94 W
84	3-H1	<i>Paraburkholderia aspalathi</i>	RL18-101-BIC-A	2018-08-14	temperate Coniferous Forest [ENVO:01000211]	rhizosphere environment [ENVO:01000999]	plant matter [ENVO:01001121]	Canada: British Columbia	49.24 N 124.94 W
85	3-H3	<i>Paraburkholderia sediminicola</i>	RL18-154-BIB-A	2018-08-15	temperate Coniferous Forest [ENVO:01000211]	rhizosphere environment [ENVO:01000999]	plant matter [ENVO:01001121]	Canada: British Columbia	49.24 N 125.36 W
86	3-H5	<i>Paraburkholderia sediminicola</i>	RL18-079-BIE-A	2018-08-14	temperate Coniferous Forest [ENVO:01000211]	rhizosphere environment [ENVO:01000999]	plant matter [ENVO:01001121]	Canada: British Columbia	49.26 N 124.73 W

87	3-H6	<i>Paraburkholderia sediminicola</i>	RL18-120-BIB-A	2018-08-15	temperate Coniferous Forest [ENVO:01000211]	rhizosphere environment [ENVO:01000999]	plant matter [ENVO:01001121]	Canada: British Columbia	49.34 N 124.92 W
88	3-H8	<i>Paraburkholderia sediminicola</i>	RL18-126-BIB-A	2018-08-15	temperate Coniferous Forest [ENVO:01000211]	rhizosphere environment [ENVO:01000999]	plant matter [ENVO:01001121]	Canada: British Columbia	49.33 N 124.92 W
89	3-I1	<i>Paraburkholderia aspalathi</i>	RL18-045-BIB-A	2018-04-09	temperate Coniferous Forest [ENVO:01000211]	rhizosphere environment [ENVO:01000999]	plant matter [ENVO:01001121]	Canada: British Columbia	49.38 N 121.94 W
90	3-I5	<i>Paraburkholderia sediminicola</i>	RL18-085-BIF-A	2018-08-14	temperate Coniferous Forest [ENVO:01000211]	rhizosphere environment [ENVO:01000999]	plant matter [ENVO:01001121]	Canada: British Columbia	49.21 N 124.79 W
91	1-B6	<i>Paraburkholderia sediminicola</i>	RL17-333-BIE-A	2017-02-25	temperate Coniferous Forest [ENVO:01000211]	rhizosphere environment [ENVO:01000999]	plant matter [ENVO:01001121]	Canada: British Columbia	49.42 N 123.49 W
92	1-F8	<i>Paraburkholderia sediminicola</i>	RL17-342-BIF-A	2017-02-25	temperate Coniferous Forest [ENVO:01000211]	rhizosphere environment [ENVO:01000999]	plant matter [ENVO:01001121]	Canada: British Columbia	49.42 N 123.49 W
93	1-G3	<i>Paraburkholderia dipogonis</i>	RL17-350-BIC-A	2017-02-26	temperate Coniferous Forest [ENVO:01000211]	rhizosphere environment [ENVO:01000999]	plant matter [ENVO:01001121]	Canada: British Columbia	49.16 N 123.96 W
94	1-H1	<i>Paraburkholderia azotifigens</i>	RL17-350-BID-B	2017-02-26	temperate Coniferous Forest [ENVO:01000211]	rhizosphere environment [ENVO:01000999]	plant matter [ENVO:01001121]	Canada: British Columbia	49.16 N 123.96 W
95	2-E6	<i>Paraburkholderia strydomiana</i>	RL17-368-BIB-B	2017-08-06	temperate Coniferous Forest [ENVO:01000211]	rhizosphere environment [ENVO:01000999]	plant matter [ENVO:01001121]	Canada: British Columbia	54.50 N 128.71 W
96	2-E8	<i>Caballeronia grimmiae</i>	RL17-372-BIF-A	2017-08-06	temperate Coniferous Forest [ENVO:01000211]	rhizosphere environment [ENVO:01000999]	plant matter [ENVO:01001121]	Canada: British Columbia	54.50 N 128.71 W
97	2-E9	<i>Paraburkholderia graminis</i>	RL17-372-BIF-C	2017-08-06	temperate Coniferous Forest [ENVO:01000211]	rhizosphere environment [ENVO:01000999]	plant matter [ENVO:01001121]	Canada: British Columbia	54.50 N 128.71 W
98	2-G3	<i>Paraburkholderia phytofirmans</i>	RL17-377-BIF-A	2017-07-22	temperate Coniferous Forest [ENVO:01000211]	rhizosphere environment [ENVO:01000999]	plant matter [ENVO:01001121]	Canada: British Columbia	49.38 N 121.94 W
99	2-H6	<i>Paraburkholderia sp.</i>	RL17-381-BIF-C	2017-07-22	temperate Coniferous Forest [ENVO:01000211]	rhizosphere environment [ENVO:01000999]	plant matter [ENVO:01001121]	Canada: British Columbia	49.37 N 121.93 W
100	3-A1	<i>Paraburkholderia graminis</i>	RL17-369-BIF-A	2017-08-06	temperate Coniferous Forest [ENVO:01000211]	rhizosphere environment [ENVO:01000999]	plant matter [ENVO:01001121]	Canada: British Columbia	54.50 N 128.71 W
101	3-D2	<i>Paraburkholderia nemoris</i>	RL18-043-BID-A	2018-04-09	temperate Coniferous Forest [ENVO:01000211]	rhizosphere environment [ENVO:01000999]	plant matter [ENVO:01001121]	Canada: British Columbia	49.38 N 121.94 W
102	1-C1	<i>Paraburkholderia agricolaris</i>	RL17-342-BIF-B	2017-02-25	temperate Coniferous Forest [ENVO:01000211]	rhizosphere environment [ENVO:01000999]	plant matter [ENVO:01001121]	Canada: British Columbia	49.42 N 123.49 W
103	1-D8	<i>Paraburkholderia acidicola</i>	RL17-338-BIF-B	2021-03-25	temperate Coniferous Forest [ENVO:01000211]	rhizosphere environment [ENVO:01000999]	plant matter [ENVO:01001121]	Canada: British Columbia	49.42 N 123.49 W
104	3-C1	<i>Paraburkholderia acidicola</i>	RL18-030-BIB-A	2018-04-09	temperate Coniferous Forest [ENVO:01000211]	rhizosphere environment [ENVO:01000999]	plant matter [ENVO:01001121]	Canada: British Columbia	49.38 N 121.94 W
105	3-E3	<i>Paraburkholderia fungorum</i>	RL18-015-BIC-B	2018-04-09	temperate Coniferous Forest [ENVO:01000211]	rhizosphere environment [ENVO:01000999]	plant matter [ENVO:01001121]	Canada: British Columbia	49.38 N 121.94 W
106	4-F6	<i>Paraburkholderia madseniana</i>	RL19-001-BIB-A	2019-03-26	temperate Coniferous Forest [ENVO:01000211]	rhizosphere environment [ENVO:01000999]	plant matter [ENVO:01001121]	Canada: British Columbia	49.30 N 122.71 W
107	4-H5	<i>Paraburkholderia agricolaris</i>	RL19-015-BID-A	2019-03-26	temperate Coniferous Forest [ENVO:01000211]	rhizosphere environment [ENVO:01000999]	plant matter [ENVO:01001121]	Canada: British Columbia	49.30 N 122.70 W
108	5-A2	<i>Paraburkholderia fungorum</i>	RL21-008-BIB-A	2021-03-25	temperate Coniferous Forest [ENVO:01000211]	rhizosphere environment [ENVO:01000999]	plant matter [ENVO:01001121]	Canada: British Columbia	49.36 N 123.26 W
109	5-A3	<i>Herbaspirillum lusitanum</i>	RL16-012-BIC-B	2016-08-24	temperate Coniferous Forest [ENVO:01000211]	rhizosphere environment [ENVO:01000999]	plant matter [ENVO:01001121]	Canada: British Columbia	49.26 N 122.95 W
110	5-A5	<i>Paraburkholderia agricolaris</i>	RL17-336-BIC-C	2017-02-25	temperate Coniferous Forest [ENVO:01000211]	rhizosphere environment [ENVO:01000999]	plant matter [ENVO:01001121]	Canada: British Columbia	49.42 N 123.49 W
111	5-A6	<i>Paraburkholderia fungorum</i>	RL17-337-BIB-A	2017-02-25	temperate Coniferous Forest [ENVO:01000211]	rhizosphere environment [ENVO:01000999]	plant matter [ENVO:01001121]	Canada: British Columbia	49.42 N 123.49 W
112	5-A7	<i>Paraburkholderia sp.</i>	RL17-339-BIF-C	2017-02-25	temperate Coniferous Forest [ENVO:01000211]	rhizosphere environment [ENVO:01000999]	plant matter [ENVO:01001121]	Canada: British Columbia	49.42 N 123.49 W

113	5-A8	<i>Paraburkholderia megapolitana</i>	RL17-342-BIB-A	2017-02-25	temperate Coniferous Forest [ENVO:01000211]	rhizosphere environment [ENVO:01000999]	plant matter [ENVO:01001121]	Canada: British Columbia	49.42 N 123.49 W
114	5-A9	<i>Paraburkholderia madseniana</i>	RL21-008-BIB-B	2021-03-25	temperate Coniferous Forest [ENVO:01000211]	rhizosphere environment [ENVO:01000999]	plant matter [ENVO:01001121]	Canada: British Columbia	49.36 N 123.26 W
115	5-B2	<i>Herbaspirillum rhizosphaerae</i>	RL18-103-BIB-C	2018-08-14	temperate Coniferous Forest [ENVO:01000211]	rhizosphere environment [ENVO:01000999]	plant matter [ENVO:01001121]	Canada: British Columbia	49.21 N 124.79 W

Table S4. Contig summary for hybrid assemblies (Illumina and Nanopore).

<i>Paraburkholderia acidicola</i> RL17-338-BIF-B		
Contig Number	Length (bp)	Notes
1	4521181	
2	2989334	circular
3	216655	
4	5238	
5	5179	
6	2905	
7	192	
8	191	
9	173	
10	142	
11	128	
<i>Paraburkholderia fungorum</i> RL18-167-BIC-A		
Contig Number	Length (bp)	Notes
1	4603259	circular
2	3440274	
3	739317	
4	26249	circular
<i>Paraburkholderia megapolitana</i> RL18-039-BIC-B		
Contig Number	Length (bp)	Notes
1	4513754	circular
2	2988503	circular
<i>Paraburkholderia nemoris</i> RL18-043-BID-A		
Contig Number	Length (bp)	Notes
1	4572990	circular
2	3886260	circular
3	493061	circular
<i>Paraburkholderia</i> sp. RL17-337-BIB-A		
Contig Number	Length (bp)	Notes
1	4719104	
2	3808221	circular
3	1454917	circular
4	859067	circular

Table S5. Number of BGCs, genome size, and ratio of number of BGCs to genome size per strain and phylogenetic clade.

Genome	Strain ID	Species	Clade*	Total # of BGCs	Genome Size (Mbp)	Ratio (# of BGCs per Mbp)	Ratio per Clade
108	5-A2	<i>Herbaspirillum lusitanum</i> RL21-008-BIB-A	A	5	5.79	0.9	0.75
114	5-A9	<i>Herbaspirillum rhizosphaerae</i> RL21-008-BIB-B	A	3	5.16	0.6	
35	2-F8	<i>Caballeronia jiangsuensis</i> RL17-374-BIF-D	B	15	8.3	1.8	1.3
51	2-I1	<i>Caballeronia grimmiae</i> RL17-374-BIB-E	B	6	7.29	0.8	
79	3-F7	<i>Caballeronia glebae</i> RL18-006-BIC-A	B	11	7.94	1.4	
96	2-E8	<i>Caballeronia grimmiae</i> RL17-372-BIF-A	B	6	6.74	0.9	
94	1-H1	<i>Paraburkholderia azotifigens</i> RL17-350-BID-B	C	14	8.71	1.6	1.6
76	3-E9	<i>Paraburkholderia megapolitana</i> RL18-039-BIC-B	D	16	7.5	2.1	2.1
103	1-D8	<i>Paraburkholderia acidicola</i> RL17-338-BIF-B	D	16	7.74	2.1	
112	5-A7	<i>Paraburkholderia megapolitana</i> RL17-339-BIF-C	D	17	7.81	2.2	
21	2-B1	<i>Paraburkholderia graminis</i> RL17-355-BIE-A	E	11	7.32	1.5	1.4
22	2-C4	<i>Paraburkholderia graminis</i> RL17-368-BIF-A	E	10	9.3	1.1	
25	2-D3	<i>Paraburkholderia graminis</i> RL17-368-BIF-C	E	12	7.84	1.5	
26	2-D4	<i>Paraburkholderia graminis</i> RL17-369-BIB-A	E	11	7.51	1.5	
97	2-E9	<i>Paraburkholderia graminis</i> RL17-372-BIF-C	E	11	7.48	1.5	
100	3-A1	<i>Paraburkholderia graminis</i> RL17-369-BIF-A	E	11	7.52	1.5	
14	1-F6	<i>Paraburkholderia strydomiana</i> RL17-350-BID-A	F	14	7.89	1.8	1.3
18	1-H5	<i>Paraburkholderia strydomiana</i> RL17-350-BIF-D	F	10	7.16	1.4	
19	1-I1	<i>Paraburkholderia strydomiana</i> RL17-351-BIC-C	F	11	7.64	1.4	
20	1-I2	<i>Paraburkholderia strydomiana</i> RL17-351-BIC-D	F	11	7.37	1.5	
27	2-D9	<i>Paraburkholderia strydomiana</i> RL17-353-BIB-A	F	11	7.17	1.5	
29	2-E4	<i>Paraburkholderia caledonica</i> RL17-369-BIB-B	F	10	7.4	1.4	
30	2-E7	<i>Paraburkholderia caledonica</i> RL17-371-BIF-A	F	10	7.28	1.4	
31	2-F1	<i>Paraburkholderia strydomiana</i> RL17-373-BIB-B	F	9	7.34	1.2	
32	2-F2	<i>Paraburkholderia strydomiana</i> RL17-373-BIB-D	F	9	7.39	1.2	
34	2-F4	<i>Paraburkholderia strydomiana</i> RL17-373-BIF-C	F	10	7.5	1.3	
38	2-G4	<i>Paraburkholderia strydomiana</i> RL17-378-BIB-A	F	9	8.07	1.1	
39	2-G5	<i>Paraburkholderia strydomiana</i> RL17-378-BIF-A	F	11	7.29	1.5	
42	2-G8	<i>Paraburkholderia strydomiana</i> RL17-379-BIB-C	F	9	7.8	1.2	
50	2-H9	<i>Paraburkholderia caledonica</i> RL17-383-BIF-B	F	10	7.27	1.4	
52	2-I2	<i>Paraburkholderia strydomiana</i> RL17-376-BIB-A	F	9	7.8	1.2	
53	2-I6	<i>Paraburkholderia strydomiana</i> RL17-379-BIB-D	F	9	7.8	1.2	
56	3-A2	<i>Paraburkholderia strydomiana</i> RL17-378-BIB-B	F	9	7.77	1.2	
15	1-G7	<i>Paraburkholderia strydomiana</i> RL17-347-BIE-B	G	10	7.77	1.3	
17	1-G9	<i>Paraburkholderia strydomiana</i> RL17-350-BIC-E	G	10	8.46	1.2	
61	3-A9	<i>Paraburkholderia rhynchosiae</i> RL18-126-BIB-B	G	11	8.79	1.3	
82	3-G5	<i>Paraburkholderia</i> sp. RL18-085-BIA-A	G	14	11.4	1.2	
88	3-H8	<i>Paraburkholderia sedimicola</i> RL18-126-BIB-A	G	9	8.76	1.0	
95	2-E6	<i>Paraburkholderia strydomiana</i> RL17-368-BIB-B	G	11	8.3	1.3	
115	5-B2	<i>Paraburkholderia</i> sp. RL18-103-BIB-C	G	13	11.45	1.1	
3	1-B2	<i>Paraburkholderia sedimicola</i> RL17-328-BIB-A	H	10	9.73	1.0	1.2
5	1-B9	<i>Paraburkholderia dilworthii</i> RL17-335-BIF-A	H	14	8.21	1.7	
7	1-C4	<i>Paraburkholderia xenovorans</i> RL17-337-BIC-C	H	10	9.72	1.0	
12	1-D9	<i>Paraburkholderia bryophila</i> RL17-338-BIF-C	H	14	8.23	1.7	
16	1-G8	<i>Paraburkholderia phytofirmans</i> RL17-350-BIB-A	H	10	7.7	1.3	
33	2-F3	<i>Paraburkholderia phytofirmans</i> RL17-373-BIF-A	H	10	10.93	0.9	
36	2-F9	<i>Paraburkholderia phytofirmans</i> RL17-376-BIF-A	H	11	10.12	1.1	
40	2-G6	<i>Paraburkholderia dipogonis</i> RL17-378-BIF-B	H	14	8.65	1.6	
44	2-H1	<i>Paraburkholderia phytofirmans</i> RL17-379-BIF-B	H	12	8.59	1.4	
46	2-H3	<i>Paraburkholderia</i> sp. RL17-380-BIE-A	H	12	7.93	1.5	
48	2-H5	<i>Paraburkholderia aromaticivorans</i> RL17-381-BIB-B	H	14	8.81	1.6	
49	2-H8	<i>Paraburkholderia</i> sp. RL17-383-BIF-A	H	12	8.05	1.5	
54	2-I8	<i>Paraburkholderia</i> sp. RL17-347-BIC-D	H	8	10.6	0.8	
55	2-I9	<i>Paraburkholderia phytofirmans</i> RL17-351-BIE-A	H	10	7.72	1.3	
60	3-B5	<i>Paraburkholderia sedimicola</i> RL18-007-BIE-A	H	12	10.28	1.2	
71	3-D6	<i>Paraburkholderia dipogonis</i> RL18-106-BIC-C	H	11	9.32	1.2	
75	3-E8	<i>Paraburkholderia sedimicola</i> RL18-017-BIF-B	H	10	10.01	1.0	
83	3-G9	<i>Paraburkholderia</i> sp. RL18-101-BIB-B	H	8	10.2	0.8	
93	1-G3	<i>Paraburkholderia dipogonis</i> RL17-350-BIC-A	H	11	10.5	1.0	
98	2-G3	<i>Paraburkholderia phytofirmans</i> RL17-377-BIF-A	H	11	8.52	1.3	
99	2-H6	<i>Paraburkholderia</i> sp. RL17-381-BIF-C	H	13	8.19	1.6	
1	1-A4	<i>Paraburkholderia xenovorans</i> RL17-329-BIC-A	I	11	7.64	1.4	1.5
2	1-A6	<i>Paraburkholderia nemoris</i> RL17-333-BIC-B	I	17	9.23	1.8	

4	1-B5	<i>Paraburkholderia sediminicola</i> RL17-333-BID-A	I	12	10.15	1.2
6	1-C2	<i>Paraburkholderia sediminicola</i> RL17-337-BIC-A	I	13	8.57	1.5
8	1-C8	<i>Paraburkholderia sediminicola</i> RL17-338-BIB-A	I	13	8.26	1.6
9	1-C9	<i>Paraburkholderia sediminicola</i> RL17-333-BIE-B	I	13	10.62	1.2
10	1-D2	<i>Paraburkholderia sediminicola</i> RL17-336-BIC-B	I	12	10.27	1.2
11	1-D4	<i>Paraburkholderia metrosideri</i> RL17-338-BIC-A	I	14	8.78	1.6
13	1-E8	<i>Paraburkholderia sediminicola</i> RL17-340-BIC-B	I	9	7.77	1.2
23	2-C5	<i>Paraburkholderia caffeinolytica</i> RL17-332-BIF-A	I	12	8.29	1.4
24	2-C6	<i>Paraburkholderia sediminicola</i> RL17-333-BIC-A	I	13	10.24	1.3
28	2-E2	<i>Paraburkholderia sediminicola</i> RL17-357-BIB-A	I	18	9.68	1.9
37	2-G2	<i>Paraburkholderia aspalathi</i> RL17-376-BIF-C	I	13	8.41	1.5
41	2-G7	<i>Paraburkholderia nemoris</i> RL17-379-BIF-A	I	15	8.59	1.7
43	2-G9	<i>Paraburkholderia aspalathi</i> RL17-379-BIF-A	I	11	8.4	1.3
45	2-H2	<i>Paraburkholderia nemoris</i> RL17-380-BIB-A	I	15	8.35	1.8
47	2-H4	<i>Paraburkholderia dipogonis</i> RL17-381-BIB-A	I	15	9.69	1.5
57	3-A6	<i>Paraburkholderia nemoris</i> RL17-376-BIF-D	I	17	8.57	2.0
58	3-B1	<i>Paraburkholderia sediminicola</i> RL18-035-BIC-A	I	12	9.38	1.3
59	3-B2	<i>Paraburkholderia sediminicola</i> RL18-035-BIE-A	I	13	9.89	1.3
62	3-B6	<i>Paraburkholderia nemoris</i> RL18-009-BIC-B	I	15	8.66	1.7
63	3-B9	<i>Paraburkholderia sediminicola</i> RL18-021-BIF-A	I	12	8.82	1.4
64	3-C2	<i>Paraburkholderia sediminicola</i> RL18-056-BIE-A	I	13	8.89	1.5
65	3-C4	<i>Paraburkholderia nemoris</i> RL18-011-BIC-A	I	16	8.99	1.8
66	3-C5	<i>Paraburkholderia sediminicola</i> RL18-012-BIE-A	I	17	9.37	1.8
67	3-C8	<i>Paraburkholderia sediminicola</i> RL18-081-BIC-C	I	14	9.39	1.5
68	3-D3	<i>Paraburkholderia nemoris</i> RL18-043-BIE-A	I	15	8.65	1.7
69	3-D4	<i>Paraburkholderia sediminicola</i> RL18-082-BIB-A	I	15	9.51	1.6
70	3-D5	<i>Paraburkholderia fungorum</i> RL18-106-BIC-A	I	13	8.79	1.5
72	3-D7	<i>Paraburkholderia sediminicola</i> RL18-106-BID-A	I	11	9.58	1.1
73	3-E1	<i>Paraburkholderia aspalathi</i> RL18-012-BIC-A	I	14	8.76	1.6
74	3-E2	<i>Paraburkholderia sediminicola</i> RL18-014-BIF-A	I	18	9.89	1.8
77	3-F3	<i>Paraburkholderia aspalathi</i> RL18-139-BIC-B	I	11	8.33	1.3
78	3-F6	<i>Paraburkholderia fungorum</i> RL18-167-BIC-A	I	13	8.81	1.5
80	3-F9	<i>Paraburkholderia sediminicola</i> RL18-106-BIB-A	I	11	10.16	1.1
81	3-G1	<i>Paraburkholderia sediminicola</i> RL18-114-BIF-A	I	16	9.06	1.8
84	3-H1	<i>Paraburkholderia aspalathi</i> RL18-101-BIC-A	I	13	8.41	1.5
85	3-H3	<i>Paraburkholderia sediminicola</i> RL18-154-BIB-A	I	14	9.15	1.5
86	3-H5	<i>Paraburkholderia sediminicola</i> RL18-079-BIE-A	I	14	9.15	1.5
87	3-H6	<i>Paraburkholderia sediminicola</i> RL18-120-BIB-A	I	14	8.74	1.6
89	3-I1	<i>Paraburkholderia aspalathi</i> RL18-045-BIB-A	I	14	9.13	1.5
90	3-I5	<i>Paraburkholderia sediminicola</i> RL18-085-BIF-A	I	15	9.33	1.6
91	1-B6	<i>Paraburkholderia sediminicola</i> RL17-333-BIE-A	I	13	10.89	1.2
92	1-F8	<i>Paraburkholderia sediminicola</i> RL17-342-BIF-A	I	14	8.98	1.6
101	3-D2	<i>Paraburkholderia nemoris</i> RL18-043-BID-A	I	12	8.95	1.3
102	1-C1	<i>Paraburkholderia agricolaris</i> RL17-342-BIF-B	I	10	8.96	1.1
104	3-C1	<i>Paraburkholderia fungorum</i> RL18-030-BIB-A	I	14	9.5	1.5
105	3-E3	<i>Paraburkholderia madseniana</i> RL18-015-BIC-B	I	12	9.57	1.3
106	4-F6	<i>Paraburkholderia agricolaris</i> RL19-001-BIB-A	I	10	8.47	1.2
107	4-H5	<i>Paraburkholderia fungorum</i> RL19-015-BID-A	I	12	8.61	1.4
109	5-A3	<i>Paraburkholderia agricolaris</i> RL16-012-BIC-B	I	11	8.97	1.2
110	5-A5	<i>Paraburkholderia fungorum</i> RL17-336-BIC-C	I	15	10.41	1.4
111	5-A6	<i>Paraburkholderia sp.</i> RL17-337-BIB-A	I	16	10.84	1.5
113	5-A8	<i>Paraburkholderia madseniana</i> RL17-342-BIB-A	I	12	9.56	1.3

*Clades are color-coded according to the phylogenetic tree in Figure 3. A, *Herbaspirillum* spp.; B, *Caballeronia* spp.; C, *P. azotifingens*; D, *P. megapolitana/acidicola*; E, *P. graminis*; F, *P. strydomiana* A; G, *P. strydomiana* B; H, *P. phytofirmans*; I, *P. sediminicola/fungorum*.

Table S6. Cluster of Orthologous Genes families used to generate phylogenomic tree.

COG Code	Gene	Function
COG0012	COG0012	Predicted GTPase, probable translation factor [Translation, ribosomal structure and biogenesis].
COG0013	AlaS	Alanyl-tRNA synthetase [Translation, ribosomal structure and biogenesis].
COG0016	PheS	Phenylalanyl-tRNA synthetase alpha subunit [Translation, ribosomal structure and biogenesis].
COG0018	ArgS	Arginyl-tRNA synthetase [Translation, ribosomal structure and biogenesis].
COG0030	KsgA	Dimethyladenosine transferase (rRNA methylation) [Translation, ribosomal structure and biogenesis].
COG0041	PurE	Phosphoribosylcarboxyaminoimidazole (NCAIR) mutase [Nucleotide transport and metabolism].
COG0046	PurL	Phosphoribosylformylglycinamide (FGAM) synthase, synthetase domain [Nucleotide transport and metabolism].
COG0048	RpsL	Ribosomal protein S12 [Translation, ribosomal structure and biogenesis].
COG0049	RpsG	Ribosomal protein S7 [Translation, ribosomal structure and biogenesis].
COG0051	RpsJ	Ribosomal protein S10 [Translation, ribosomal structure and biogenesis].
COG0052	RpsB	Ribosomal protein S2 [Translation, ribosomal structure and biogenesis].
COG0072	PheT	Phenylalanyl-tRNA synthetase beta subunit [Translation, ribosomal structure and biogenesis].
COG0080	RplK	Ribosomal protein L11 [Translation, ribosomal structure and biogenesis].
COG0081	RplA	Ribosomal protein L1 [Translation, ribosomal structure and biogenesis].
COG0082	AroC	Chorismate synthase [Amino acid transport and metabolism].
COG0086	RpoC	DNA-directed RNA polymerase, beta' subunit/160 kD subunit [Transcription].
COG0087	RplC	Ribosomal protein L3 [Translation, ribosomal structure and biogenesis].
COG0088	RplD	Ribosomal protein L4 [Translation, ribosomal structure and biogenesis].
COG0089	RplW	Ribosomal protein L23 [Translation, ribosomal structure and biogenesis].
COG0090	RplB	Ribosomal protein L2 [Translation, ribosomal structure and biogenesis].
COG0091	RplV	Ribosomal protein L22 [Translation, ribosomal structure and biogenesis].
COG0092	RpsC	Ribosomal protein S3 [Translation, ribosomal structure and biogenesis].
COG0093	RplN	Ribosomal protein L14 [Translation, ribosomal structure and biogenesis].
COG0094	RplE	Ribosomal protein L5 [Translation, ribosomal structure and biogenesis].
COG0096	RpsH	Ribosomal protein S8 [Translation, ribosomal structure and biogenesis].
COG0097	RplF	Ribosomal protein L6P/L9E [Translation, ribosomal structure and biogenesis].
COG0098	RpsE	Ribosomal protein S5 [Translation, ribosomal structure and biogenesis].
COG0099	RpsM	Ribosomal protein S13 [Translation, ribosomal structure and biogenesis].
COG0100	RpsK	Ribosomal protein S11 [Translation, ribosomal structure and biogenesis].
COG0102	RplM	Ribosomal protein L13 [Translation, ribosomal structure and biogenesis].
COG0103	RpsI	Ribosomal protein S9 [Translation, ribosomal structure and biogenesis].

COG0105	Ndk	Nucleoside diphosphate kinase [Nucleotide transport and metabolism].
COG0126	Pgk	3-phosphoglycerate kinase [Carbohydrate transport and metabolism].
COG0127	COG0127	Xanthosine triphosphate pyrophosphatase [Nucleotide transport and metabolism].
COG0130	TruB	Pseudouridine synthase [Translation, ribosomal structure and biogenesis].
COG0150	PurM	Phosphoribosylaminoimidazole (AIR) synthetase [Nucleotide transport and metabolism].
COG0151	PurD	Phosphoribosylamine-glycine ligase [Nucleotide transport and metabolism].
COG0164	RnhB	Ribonuclease HII [DNA replication, recombination, and repair].
COG0172	SerS	Seryl-tRNA synthetase [Translation, ribosomal structure and biogenesis].
COG0185	RpsS	Ribosomal protein S19 [Translation, ribosomal structure and biogenesis].
COG0186	RpsQ	Ribosomal protein S17 [Translation, ribosomal structure and biogenesis].
COG0215	CysS	Cysteinyl-tRNA synthetase [Translation, ribosomal structure and biogenesis].
COG0244	RplJ	Ribosomal protein L10 [Translation, ribosomal structure and biogenesis].
COG0256	RplR	Ribosomal protein L18 [Translation, ribosomal structure and biogenesis].
COG0343	Tgt	Queuine/archaeosine tRNA-ribosyltransferase [Translation, ribosomal structure and biogenesis].
COG0504	PyrG	CTP synthase (UTP-ammonia lyase) [Nucleotide transport and metabolism].
COG0519	GuaA	GMP synthase, PP-ATPase domain/subunit [Nucleotide transport and metabolism].
COG0532	InfB	Translation initiation factor 2 (IF-2; GTPase) [Translation, ribosomal structure and biogenesis].
COG0533	QRI7	Metal-dependent proteases with possible chaperone activity [Posttranslational modification, protein turnover, chaperones].

Table S7. BLASTp results (as of Apr. 2023) of encoded proteins in region 2.11 that contains the *mgp* BGC.

Name	Size (aa)	Top Blast hit	Species, % identity, accession code
MgpA	1281	Polyketide synthase (PKS)	<i>Paraburkholderia megapolitana</i> , 97.81%, WP_266253531.1
MgpB	2664	Polyketide synthase - non-ribosomal peptide synthetase hybrid (PKS-NRPS)	<i>Paraburkholderia megapolitana</i> , 99.44%, WP_091015046.1
MgpC	3743	Non-ribosomal peptide synthetase (NRPS)	<i>Paraburkholderia megapolitana</i> , 99.12%, WP_091015044.1
MgpD	2369	Polyketide synthase - non-ribosomal peptide synthetase (PKS-NRPS)	<i>Paraburkholderia megapolitana</i> , 97.98%, WP_091015042.1
MgpE	2332	Polyketide synthase (PKS)	<i>Paraburkholderia megapolitana</i> , 98.46%, WP_091015040.1
MgpF	1892	Polyketide synthase (PKS)	<i>Paraburkholderia megapolitana</i> , 100%, WP_170275684.1
MgpG	312	Cupin-like domain protein	<i>Paraburkholderia megapolitana</i> , 98.94%, WP_091015038.2
MgpH	569	PP-Binding domain	<i>Paraburkholderia megapolitana</i> , 98.95%, WP_266253524.1
MgpI	271	Thioesterase (TE)	<i>Paraburkholderia megapolitana</i> , 98.63%, WP_266253523.1
MgpJ	240	4'-phosphopantetheinyl transferase	<i>Paraburkholderia megapolitana</i> , 100%, WP_091015031.2
MgpK	483	polysaccharide pyruvyl transferase family protein	<i>Paraburkholderia megapolitana</i> , 99.49%, WP_091015023.1
MgpL	587	2-succinyl-5-enolpyruvyl-6-hydroxy-3-cyclohexene-1-carboxylate synthase (thiamine pyrophosphate dependent lyase)	<i>Paraburkholderia megapolitana</i> , 99.79%, WP_170275682.2
MgpM	254	metallophosphoesterase	<i>Paraburkholderia megapolitana</i> , 100%, WP_266253521.1
MgpN	550	AMP-binding	<i>Paraburkholderia megapolitana</i> , 99.82%, WP_091015017.1

Table S8. ¹H (600 MHz) and ¹³C NMR (150 MHz) data for megapolipeptin A (1) in DMSO-*d*₆^a.

	position	δ _H (J in Hz)	δ _C , mult
A _{hpa}	1		173.4, qC
	2a	2.26, dd (14.6, 2.8)	39.9, CH ₂
	2b	2.08, dd (14.6, 9.8)	
	3	3.85, m	67.5, CH
	4	3.64, m	55.1, CH
	5a	3.49, m	60.4, CH ₂
	5b	3.49, m	
	4-NH	7.58, d (9.0)	
	1-NH ₂	7.19, s	
		6.76, s	
¹ Thr	1		169.8, qC
	2	4.21, m	58.6, CH
	3	3.84, m	67.1, CH
	4	1.04, d (6.4)	19.6, CH ₃
	2-NH	7.86, brd (7.6)	
	² Thr	1	
2		4.32, dd (8.4)	57.6, CH
3		3.93, m	66.8, CH
4		0.96, d (6.3)	19.2, CH ₃
2-NH		7.93, brs	
A _{dhda}		1	
	2a	2.56, m	39.3, CH ₂
	2b	2.36, m	
	3	4.21, m	44.4, CH
	4a	1.51, m	41.8, CH ₂
	4b	1.51, m	
	5	3.39, m	66.6, CH
	6a	1.37, m	36.8, CH ₂
	6b	1.23, m	
	7a	1.25, m	29.2, CH ₂
	7b	1.25, m	
	8a	1.33, m	24.3, CH ₂
	8b	1.23, m	
	9a	1.91, m	32.0, CH ₂
	9b	1.91, m	
	10	5.36, m	130.3, CH
	11	5.35, m	129.6, CH
	12a	1.99, brs	32.1, CH ₂

	12b	1.99, brs	
	13a	1.99, brs	32.1, CH ₂
	13b	1.99, brs	
	14	5.35, m	129.4, CH
	15	5.36, m	130.2, CH
	16a	1.90, m	32, CH ₂
	16b	1.90, m	
	17a	1.23, m	24.7, CH ₂
	17b	1.23, m	
	18a	1.42, m	34.8, CH ₂
	18b	1.26, m	
	19	3.45, m	75.1, CH
	20	1.04, d (6.4)	20.3, CH ₃
	21		159.8, qC
	3-NH	8.49, d (9.0)	
Hoha	1		174.0, qC
	2	4.16, m	72.9, CH
	3a	2.72, m	45.3, CH ₂
	3b	2.72, m	
	4		206.2, qC
	5a	2.71, m	37.4, CH ₂
	5b	2.66, m	
	6a	2.38, m	27.7, CH ₂
	6b	2.38, m	
	7		173.6, qC
Mpo	1		202.4, qC
	2	3.39, m	33.9, CH
	3	1.01, d (7.2)	17.5, CH ₃
	4	1.01, d (7.2)	17.3, CH ₃

^a All data was acquired on a 600 MHz NMR spectrometer equipped with a 5mm QCI cryoprobe.

Table S9. ¹H (600 MHz) and ¹³C NMR (150 MHz) data for megapolipeptin B (2) in DMSO-*d*₆^a.

	position	δ _H (J in Hz)	δ _C , mult	
A _{hpa}	1		173.4, qC	
	2a	2.26, m	39.9, CH ₂	
	2b	2.08, dd (14.8, 9.5)		
	3	3.85, m	67.5, CH	
	4	3.64, m	55.1, CH	
	5a	3.48, m	60.4, CH ₂	
	5b	3.48, m		
	4-NH	7.62, d (8.7)		
	1-NH ₂		7.20, s	
			6.75, s	
¹ Thr	1		169.8, qC	
	2	4.21, m	58.6, CH	
	3	3.84, m	67.1, CH	
	4	1.05, m	19.6, CH ₃	
	2-NH	7.95, brs		
	² Thr	1		169.9, qC
2		4.31, m	57.8, CH	
3		3.93, m	66.8, CH	
4		0.95, d (6.0)	19.2, CH ₃	
2-NH		8.04, brs		
A _{dhta}		1		170.5, qC
	2a	2.56, m	39.3, CH ₂	
	2b	2.36, m		
	3	4.21, m	44.4, CH	
	4a	1.52, m	41.8, CH ₂	
	4b	1.52, m		
	5	3.39, m	66.5, CH	
	6a	1.42, m	36.8, CH ₂	
	6b	1.30, m		
	7a	2.03, m	28.2, CH ₂	
	7b	1.92, m		
	8	5.36, m	130.3, CH	
	9	5.36, m	129.8, CH	
	10a	1.99, m	32.1, CH ₂	
	10b	1.99, m		
	11a	1.99, m	32.1, CH ₂	
	11b	1.99, m		
	12	5.36, m	129.5, CH	

	13	5.36, m	129.1, CH
	14a	1.99, m	32.1, CH ₂
	14b	1.99, m	
	15a	1.99, m	32.1, CH ₂
	15b	1.99, m	
	16	5.36, m	129.7, CH
	17	5.36, m	130.2, CH
	18a	1.91, m	32.0, CH ₂
	18b	1.91, m	
	19a	1.23, m	24.6, CH ₂
	19b	1.23, m	
	20a	1.42, m	34.8, CH ₂
	20b	1.25, m	
	21	3.46, m	75.1, CH
	22	1.04, m	20.3, CH ₃
	23		159.8, qC
	3-NH	8.49, d (8.7)	
Hoha	1		174.5, qC
	2	4.13, m	73.5, CH
	3a	2.72, m	45.3, CH ₂
	3b	2.72, m	
	4		206.3, qC
	5a	2.71, m	37.4, CH ₂
	5b	2.66, m	
	6a	2.37, m	27.6, CH ₂
	6b	2.37, m	
	7		173.8, qC
Mpo	1		202.3, qC
	2	3.39, m	33.9, CH
	3	1.01, d (7.3)	17.5, CH ₃
	4	1.01, d (7.3)	17.3, CH ₃

^a All data was acquired on a 600 MHz NMR spectrometer equipped with a 5mm QCI cryoprobe.

Table S10. Bacterial target panel strains and culture conditions.

Strain Name	Strain Designation	BSL	Growth Medium	Growth Condition
Gram-Positive				
<i>Bacillus subtilis</i>	ATCC 6051	1	TSB	37°C
<i>Enterococcus faecalis</i>	ATCC 29212	2	BHI	37°C
<i>Enterococcus faecium</i>	ATCC 6569	2	BHI	37°C
<i>Listeria ivanovii</i>	BAA-139	1	BHI-A; HTM	37°C; 5% CO ₂
<i>Staphylococcus aureus</i> (Methicillin-Resistant)	BAA-44	2	TSB	37°C
<i>Staphylococcus aureus</i> (Methicillin-Sensitive)	ATCC 29213	2	TSB	37°C
<i>Staphylococcus epidermidis</i>	ATCC 14990	1	TSB	37°C
Gram-Negative				
<i>Escherichia coli</i>	K-12 MG1655	1	NB	37°C
<i>Klebsiella aerogenes</i>	ATCC 35029	1	NB	37°C
<i>Klebsiella pneumoniae</i>	ATCC 700603	2	NB	37°C
<i>Ochrobactrum anthropi</i>	ATCC 49687	1	TSB	37°C
<i>Providencia alcalifaciens</i>	ATCC 9886	1	TSB	37°C
<i>Pseudomonas aeruginosa</i>	ATCC 27853	2	TSB	37°C
<i>Salmonella enterica</i>	ATCC 13311	2	NB	37°C
<i>Shigella sonnei</i>	ATCC 25931	2	NB	37°C
<i>Vibrio cholerae</i>	A1552 El Tor	2	TSB	37°C
<i>Yersinia pseudotuberculosis</i>	ATCC 6904	2	BHI	37°C

Table S11. Antimicrobial activities of megapolipectins A (1) and B (2).

Strain Name	Megapolipectin A (1)	Megapolipectin B (2)
Gram-Positive Bacteria		
<i>Bacillus subtilis</i>	>128 µM	>128 µM
<i>Enterococcus faecalis</i>	>128 µM	>128 µM
<i>Enterococcus faecium</i>	>128 µM	>128 µM
<i>Listeria ivanovii</i>	>128 µM	>128 µM
<i>Staphylococcus aureus</i> (Methicillin-Resistant)	>128 µM	>128 µM
<i>Staphylococcus aureus</i> (Methicillin-Sensitive)	>128 µM	>128 µM
<i>Staphylococcus epidermidis</i>	>128 µM	>128 µM
Gram-Negative Bacteria		
<i>Escherichia coli</i>	>128 µM	>128 µM
<i>Klebsiella aerogenes</i>	>128 µM	>128 µM
<i>Klebsiella pneumoniae</i>	>128 µM	>128 µM
<i>Ochrobactrum anthropi</i>	>128 µM	>128 µM
<i>Providencia alcalifaciens</i>	>128 µM	>128 µM
<i>Pseudomonas aeruginosa</i>	>128 µM	>128 µM
<i>Salmonella enterica</i>	>128 µM	>128 µM
<i>Shigella sonnei</i>	>128 µM	>128 µM
<i>Vibrio cholerae</i>	>128 µM	>128 µM
<i>Yersinia pseudotuberculosis</i>	>128 µM	>128 µM
Fungi		
<i>Aspergillus niger</i>	>100 µM	>100 µM
<i>Candida albicans</i>	>100 µM	>100 µM
<i>Purpureocillium lilacinum</i>	>100 µM	>100 µM
<i>Saccharomyces cerevisiae</i>	>100 µM	>100 µM

Table S12. Fungal target panel strains and culture conditions.

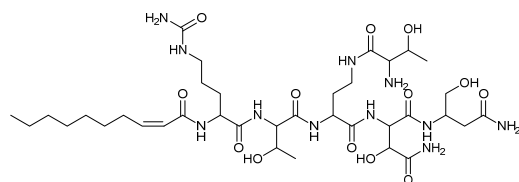
Strain Name	Strain Designation	BSL	Growth Medium	Growth Condition
<i>Aspergillus niger</i>	DSM 737	1	PDB	22°C
<i>Candida albicans</i>	ATCC 14053	2	SDB	37°C
<i>Purpureocillium lilacinum</i>	DSM 846	2	PDB	22°C
<i>Saccharomyces cerevisiae</i>	ATCC 9763	1	YMB	37°C

Table S13. Adenylation domain signature on megapolipeptin BGC. Comparative analysis of adenylation domains encoded in the megapolipeptin BGC and their respective amino acid candidate codes. First row is adenylation domain signatures found in the megapolipeptin BGC followed by the predicted code according to Stachelhaus *et al.*¹⁷. For MgpB_A1, the α -keto acid code¹⁸ is also shown. Red letters indicate amino acids that can vary, yellow letters, amino acids mutated from the expected code, and brown letters, amino acids mutated but where variations can occur according to the code.

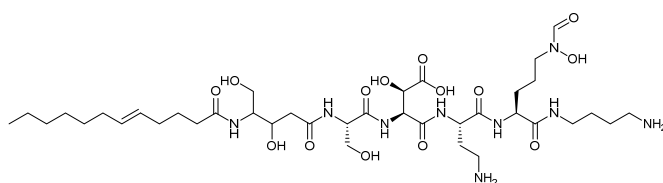
Domain	235	236	239	278	299	301	322	330	331	517	amino acid predicted
MgpB_A1	D	V	L	F	L	G	A	I	L	K	?
Pro	D	V	Q	L	I	A	H	V	V	K	Pro code
α -keto group	I	G	M	I	G	A	M	S	A	K	α -keto acid code
Domain	235	236	239	278	299	301	322	330	331	517	amino acid predicted
MgpC_A1	D	F	W	N	V	G	M	V	H	K	Thr
Thr/Dht	D	F	W	N	I	G	M	V	H	K	Thr/Dht code
Domain	235	236	239	278	299	301	322	330	331	517	amino acid predicted
MgpC_A2	D	V	W	H	F	S	L	V	D	K	Ser
Ser	D	V	W	H	L	S	L	I	D	K	Ser code
Domain	235	236	239	278	299	301	322	330	331	517	amino acid predicted
MgpD_A1	D	A	M	W	I	G	G	V	L	K	Val (1)
Val (1)	D	A	F	W	I	G	G	T	F	K	Val (1) code
Val (2)	D	F	E	S	T	A	A	V	Y	K	Val (2) code
Val (3)	D	A	W	M	F	A	A	V	L	K	Val (3) code

Table S14. Natural product families with structural similarity to megapolipeptins. Top 10 NP Atlas natural product family hits and bolagladin. Only one congener for each natural product family is shown. For example, rotihibin A, B, and C appear in the top10 for compounds but only rotihibin C is listed as the family member. Compounds in bold are mentioned in the main text.

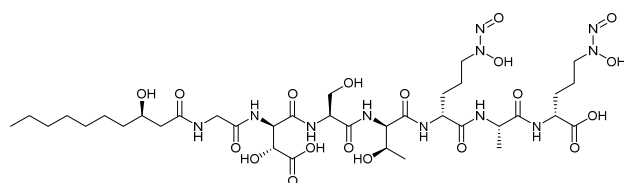
NPA ID	Compound name	Compound molecular formula	Compound accurate mass	Bacterium	Original reference PMID	Similarity score	Reported activity
NPA033310	Rotihibin C	C36H65N11O13	859.4763	<i>Streptomyces scabies</i>	34346752	0.58	herbicidal (mTOR inhibitor)
NPA024388	Crochelin C	C38H69N9O14	875.4964	Unknown-bacterium	29134779	0.57	siderophore
NPA021543	Linear surfactins	C52H93N7O14	1039.6781	<i>Micromonospora</i> sp. CPCC 202787	27301660	0.56	biosurfactant
NPA025683	Megapolibactin A	C36H63N11O19	953.4302	<i>Paraburkholderia megapolitana</i>	31276269	0.56	siderophore
NPA024966	Gramibactin B	C32H56N10O17	852.3825	<i>Trinickia caryophylli</i>	31605027	0.55	siderophore
NPA031566	Pseudodesmin C	C54H98N10O16	1142.7162	<i>Pseudomonas tolaasii</i>	32868430	0.55	moderate antibacterial
NPA032808	Syringafactin D	C56H103N9O13	1109.7675	<i>Pseudomonas syringae</i> pv. tomato DC3000	17601782	0.55	biosurfactant
NPA033288	Thanafactin A	C43H75N9O13	925.5484	<i>Pseudomonas fluorescens</i> DSM 11579	33382250	0.55	weak protease inhibitory activity and swarming motility modulator
NPA009608	Gageostatin A	C52H93N7O14	1039.6781	<i>Bacillus</i> sp. SNA-60-367	24492520	0.54	antifungal, antibacterial, cytotoxic
NPA010214	Cupriachelin	C33H57N7O16	807.3862	<i>Cupriavidus necator</i> H16	22381697	0.54	siderophore
NPA033055	Bolagladin A	C39H61N5O14	823.4215	<i>Burkholderia gladioli</i> BCC0238		0.39	moderate antibacterial



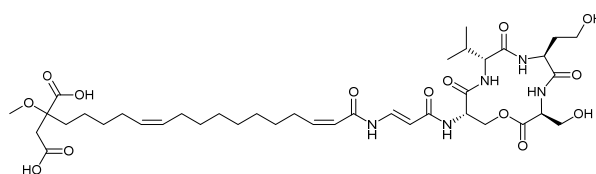
Rotihibin C



Crochelin C



Megapolibactin A



Bolagladin A

Table S15. Detailed MALDI-TOF MS parameters for IDBac analysis.

Parameter	Protein Spectra	Specialized Metabolite Spectra
Instrument type	autoflex	autoflex
flexControl version	flexControl 3.4.135.0	flexControl 3.4.135.0
Digitizer type	LeCroy LSA2000	LeCroy LSA2000
Number of shots	1000	1000
Retention time for Warp-LC	0 s	0 s
Digitizer bit depth	8	8
AIDA version number	AIDA4.7.373.7	AIDA4.7.373.7
Target type	280784	280784
Spectrum delay	29918 ns	9316 ns
SampleRate reciprocal	1.6 ns	0.2 ns
Spectrum Size	41642 pts	253781 pts
Himass turbo mode	FALSE	FALSE
Laser repetition rate	2000 Hz	2000 Hz
Linear detector voltage	3.072 – 3.107 kV	3.072 kV
Reflector detector voltage	2.166 – 2.317 kV	2.166 – 2.232 kV
Voltage of high mass detector	0 kV	0 kV
Realtime smooth	high	off
AutoXecute method	IDBac_Protein_AutoX	IDBac_Small-Molecule_autoX
flexAnalysis method	IDBac Protein CalibrantCalibration	IDBac Small Molecule Calibrant Calibration
A flat line is created if the acceptance criteria of AutoXecute are not met	FALSE	FALSE
Flag indicating in source decay measurement	FALSE	FALSE
Flag indicating HPC usage	FALSE	FALSE
Calibration mass control list	MBT_Standard	IDBac small molecule calibration
Sensitivity of digitizer	100 mV/fullscale	100 mV/fullscale
Analog Offset	1.4 mV	1.6 mV
Deflection pulser cal	0	0
PIE decay	330 ns	200 ns
Positive voltage polarity	POS	POS
Reflector voltage 1	0 kV	21 kV
Reflector voltage 2	0 kV	9.7 kV
Ion source voltage 1	19.5 kV	19 kV
Ion source voltage 2	18.25 kV	16.8 kV
Lens voltage	7 kV	8.5 kV
Matrix suppression mode	deflection	deflection
Matric suppression cut off mass	1900	50

FIGURES

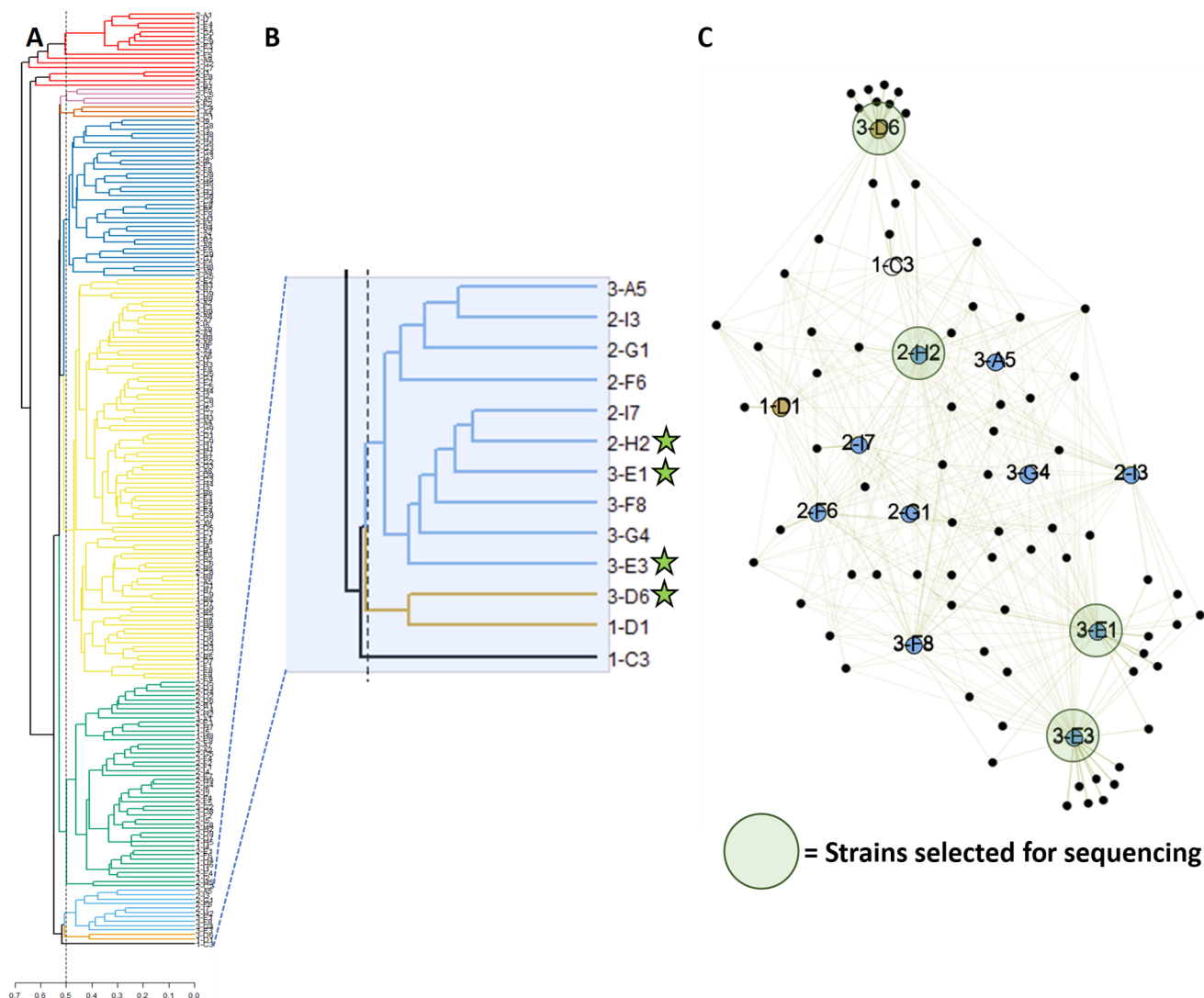


Figure S1. Example of IDBac strain prioritization. (A) An IDBac dendrogram showing MALDI-TOF MS protein spectrum similarity (2,000-15,000 Da) of 230 isolates from cycle 1. (B) Zoom-in of a grouping that contains 13 isolates. (C) Metabolite association network (200-2,000 Da) of the 13 isolates from panel B. Large nodes represent isolates color-coded according to panel B. Small black nodes represent m/z features. Association of a m/z feature with an isolate is represented with a yellow line. To prioritize isolates, the first step was to eliminate those lacking any unique m/z features (e.g., 2-I3). Next, isolates were prioritized by the total number of unique m/z features, selecting the minimum number of isolates that would maximize chemical space coverage. Isolates highlighted with a large green circle were selected for genome sequencing.

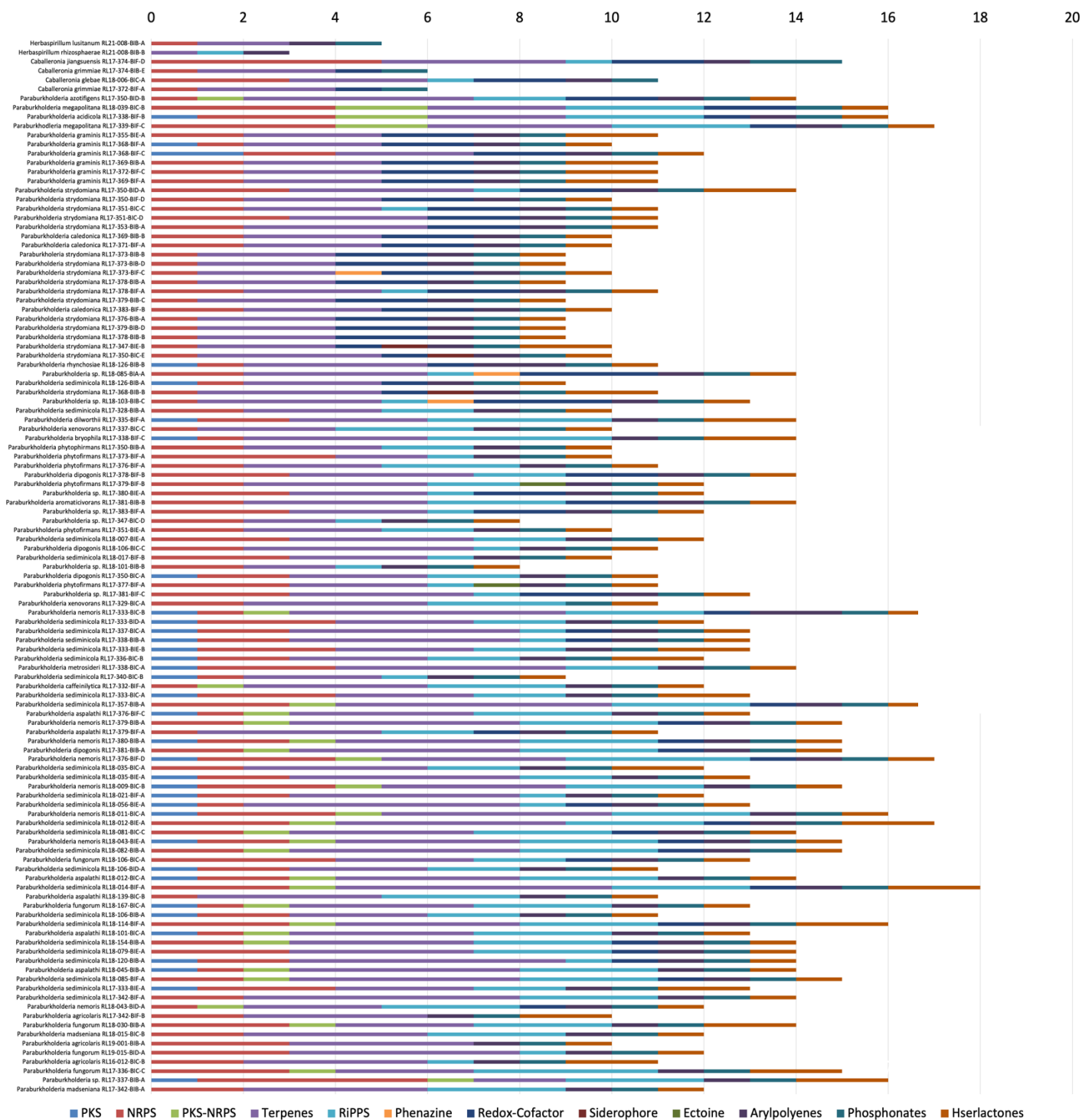


Figure S2. Biosynthetic Gene Cluster numbers and biosynthetic class by strain. 115 Burkholderiales strains (“y” axis) are depicted in terms of BGCs numbers (“x” axis) and biosynthetic class (12 in total, color coded) comprising PKS, NRPS, hybrid PKS-NRPS, terpenes, RiPPS, phenazines, redox-cofactor, siderophore, ectoines, arylpolyenes, phosphonates, homoserine lactones.

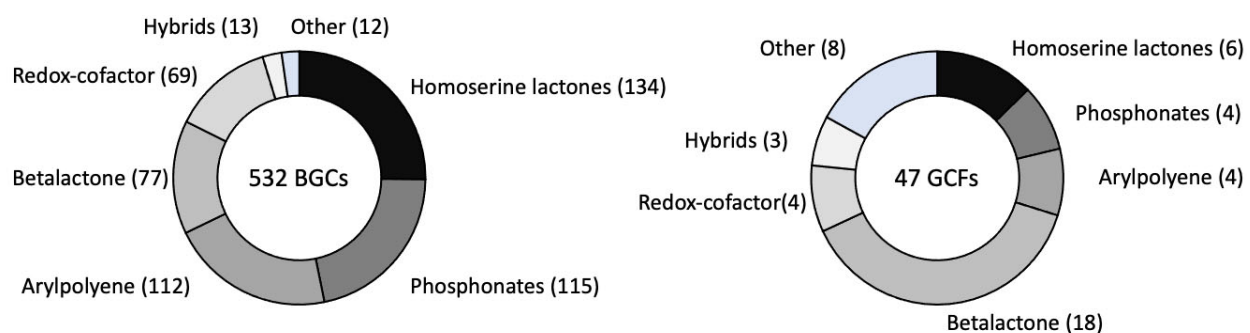


Figure S3. Pie charts showing subdivisions of ‘other’ biosynthetic gene clusters. The category ‘other’ from the main text is here subdivided in 7 major groups. The left donut chart represents BGCs and the right donut chart represents GCFs.

Tree scale: 0.1

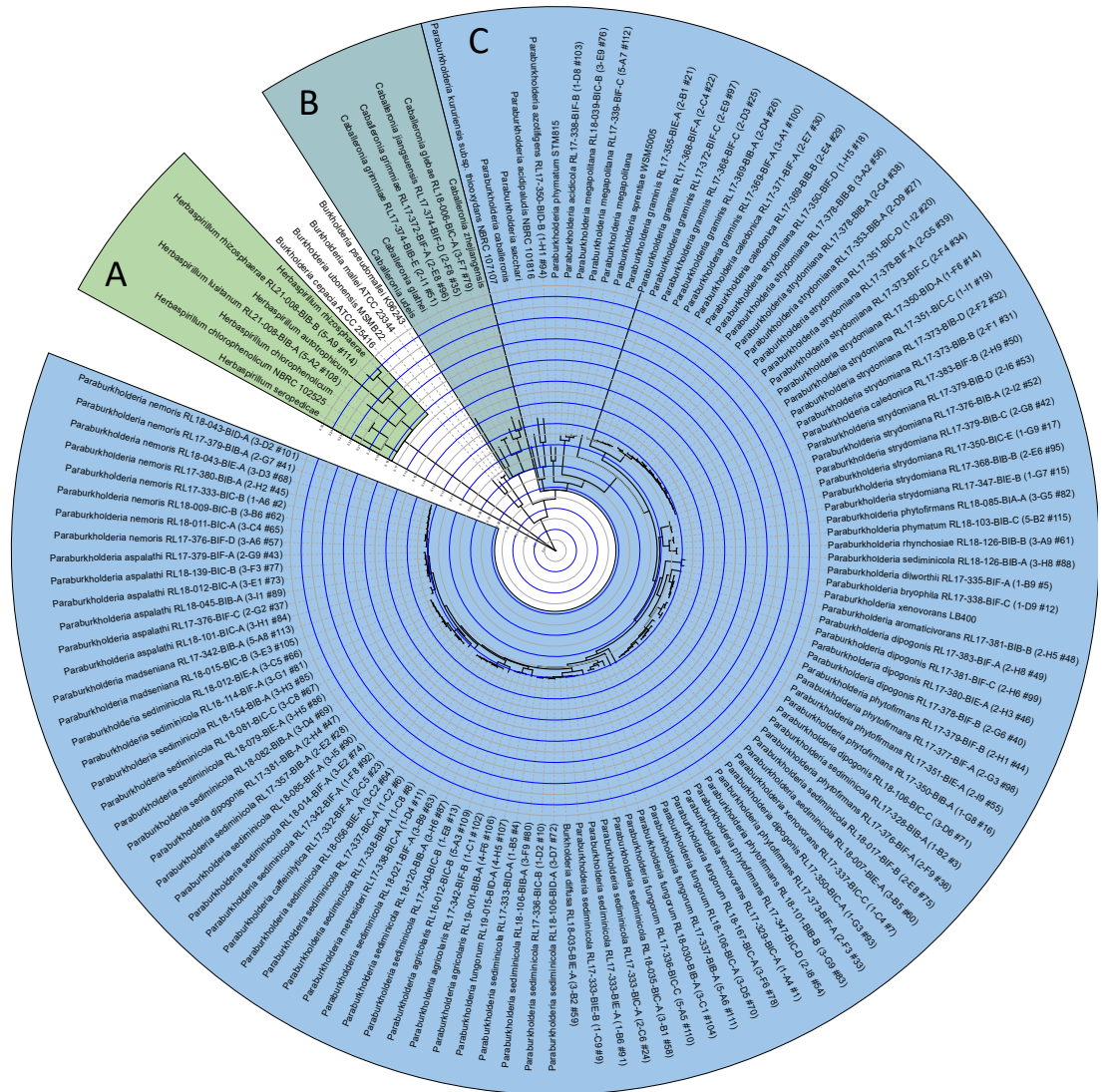


Figure S4. Phylogenomic tree of Burkholderiales library. The three genera present in the collection are highlighted. **(A)** *Herbaspirillum* spp. **(B)** *Caballeronia* spp. **(C)** *Paraburkholderia* spp. Select *Burkholderia*, *Paraburkholderia*, *Herbasparillum* and *Caballeronia* genomes available in public databases were included as well, scale bar represents the number of substitutions per site. The phylogenomic tree was constructed on KBase server by using the ‘Insert Genome into SpeciesTree – v2.2.0’ app¹⁹. KBase allows a user to build phylogenomic trees using a set of 49 core, universal genes (SI Table S6) defined by Cluster of Orthologous Genes (COG) families. SpeciesTree applies a heuristic variant of the neighbor-joining method.

Tree scale: 0.1

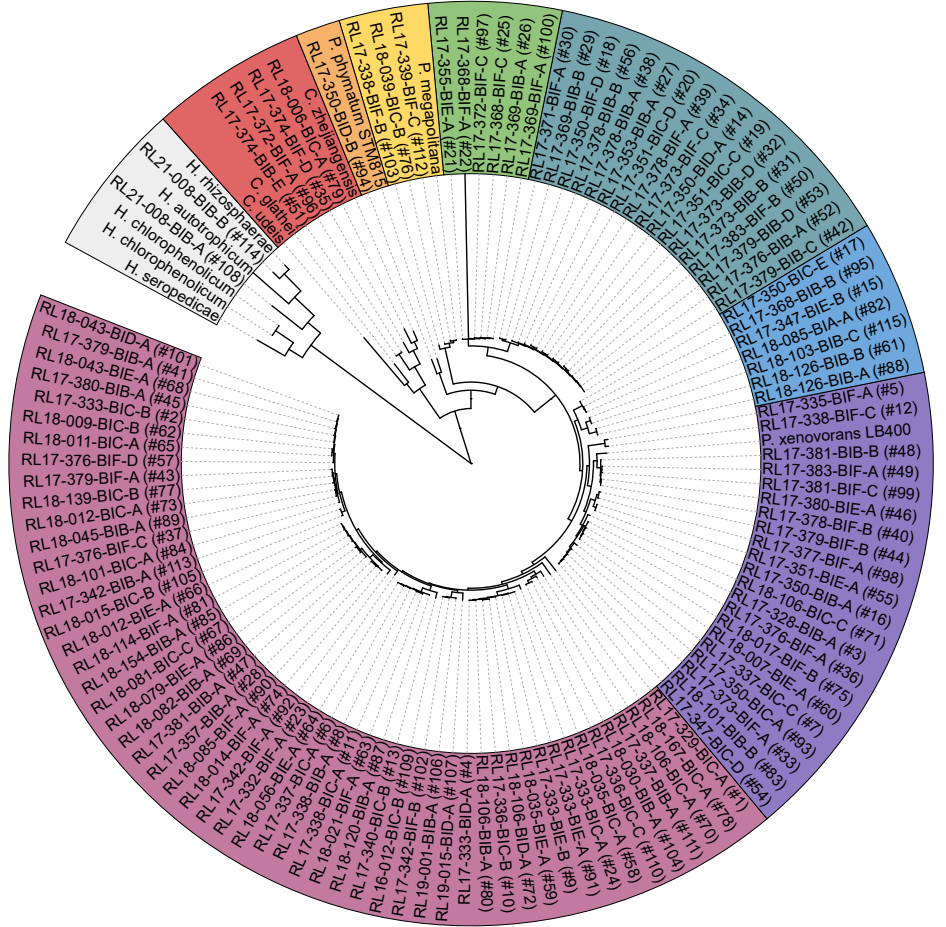
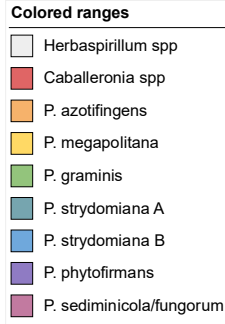


Figure S5. Phylogenomic tree of Burkholderiales library. Phylogenomic tree of Figure 3A. containing all *Burkholderiales* strains decorated with evolutionary distance.

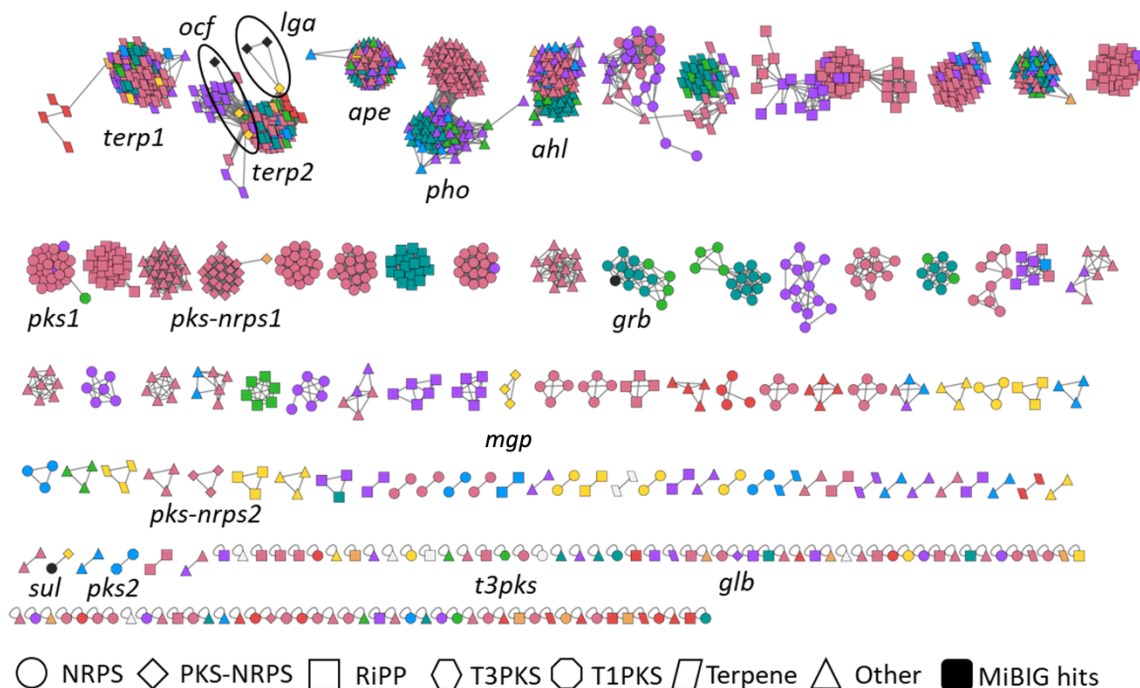


Figure S6. BiG-SCAPE biosynthetic gene cluster Sequence Similarity Network within the 115 Burkholderiales genomes. ($C = 0.4$). The direct antiSMASH output was used to generate the network. A total of 1,383 BGCs, that includes some superclusters, are displayed, color-coded according to the clades in Fig. S5. MiBiG BGCs are shown in black nodes. MiBiG BGCs that appeared as singletons were removed. Node shape indicates BGC class according to BiG-SCAPE classification. Known BGCs and orphan BGCs described in the text are highlighted. Superclusters containing PKS-NRPS BGCs were manually curated to split the clusters and generate **Figure 3B** in the main text. Examples of terpene and PKS-NRPS superclusters include *ocf* and *lga*, explaining why these two known PKS-NRPS clusters formed a network with terpenes (*terp2*).

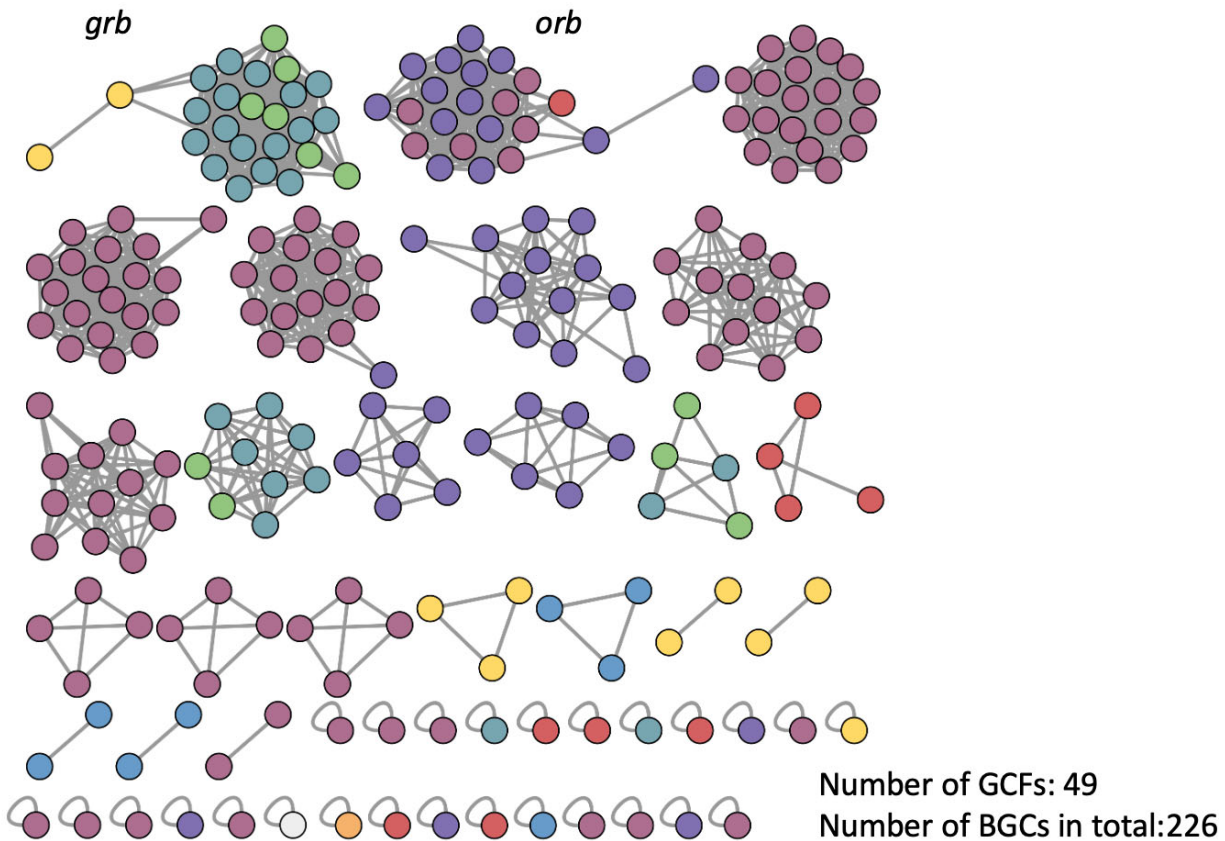


Figure S7. NRPS networks and singletons. All NRPS networks and singletons extracted from the BiG-SCAPE analysis shown in Fig. 3B. The gramibactin (*grb*) and ornibactin (*orb*) networks are highlighted.

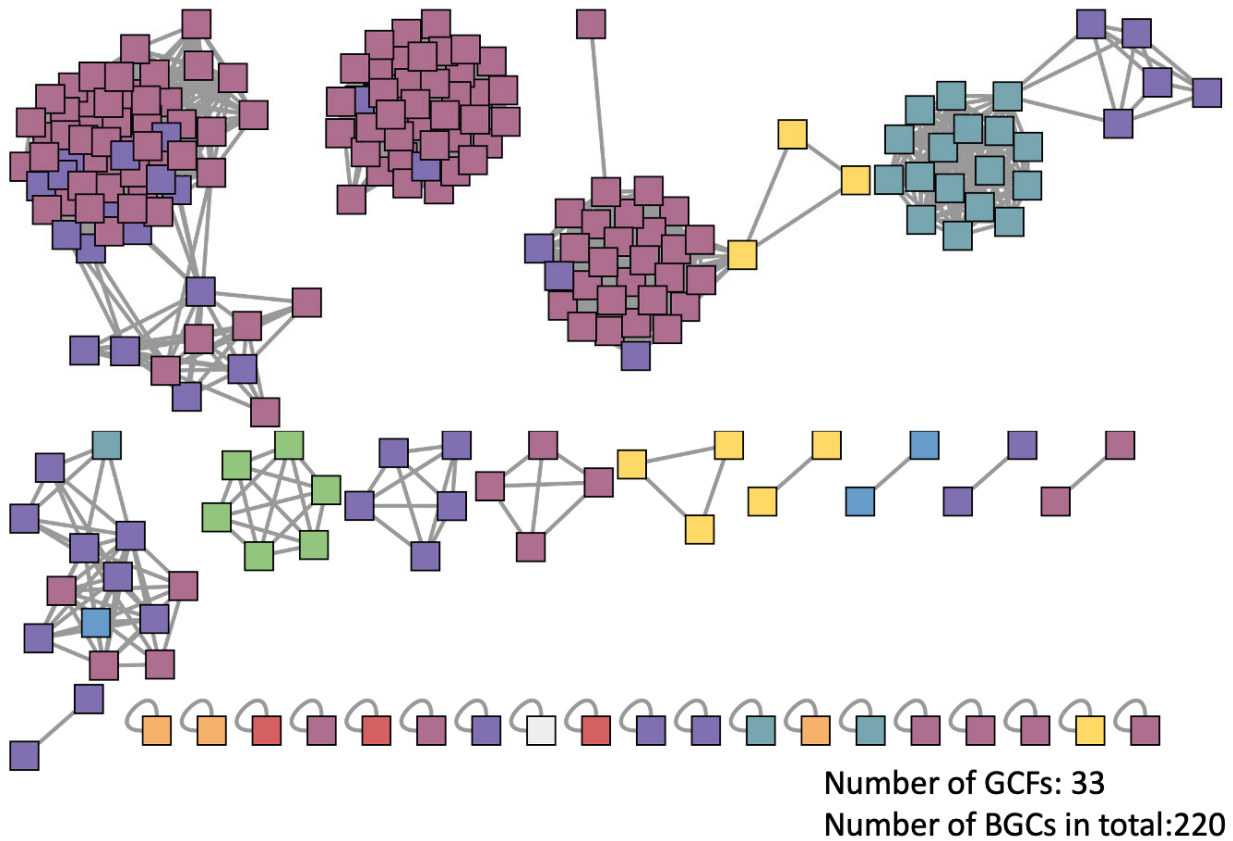


Figure S8. RiPP networks and singletons. All RiPP networks and singletons extracted from the BiG-SCAPE analysis shown in Fig. 3B.

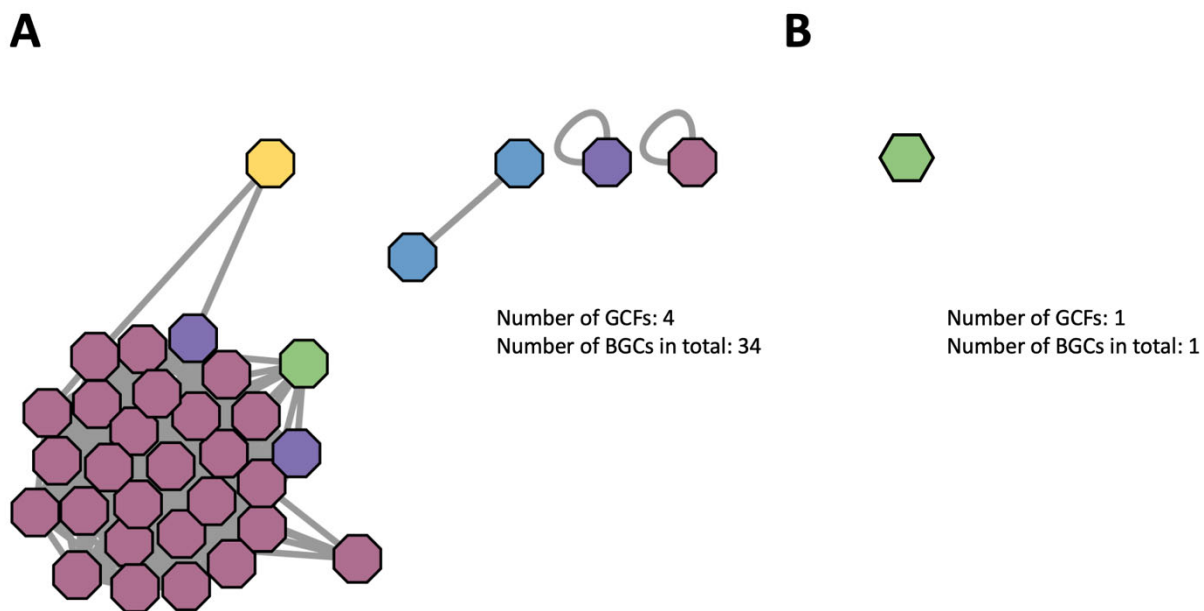


Figure S9. PKS networks and singletons. (A) Type I PKS, (B) type III PKS networks and singletons extracted from the BiG-SCAPE analysis shown in Fig. 3B.

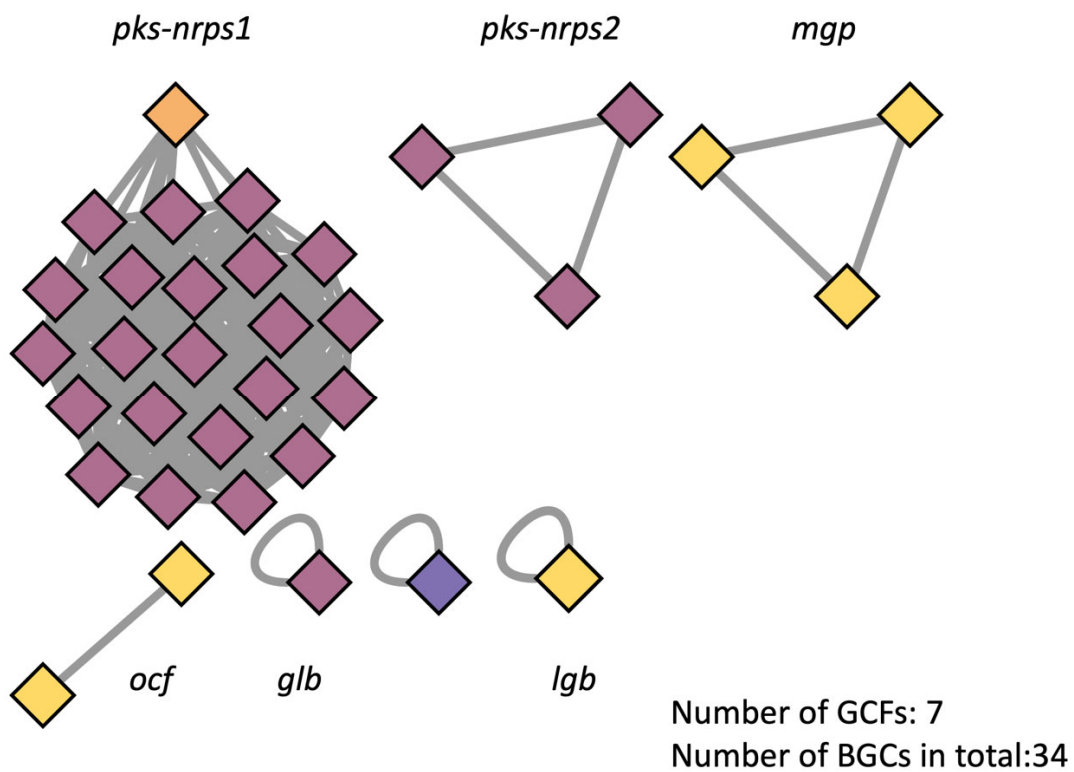


Figure S10. Hybrid PKS-NRPS networks and singletons. All PKS-NRPS networks and singletons extracted from the BiG-SCAPE analysis shown in Fig. 3B. The occidiofungin (*ocf*), glidobactin-like (*glb*), lagriamide B (*lgb*) and orphan networks are highlighted, including the *mgp* BGC studied here.

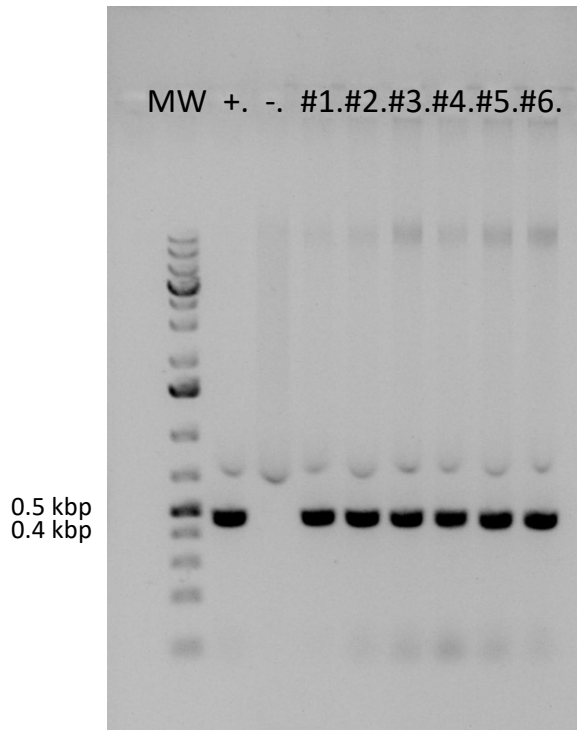


Figure S11. pBS001 screening in *Burkholderia* sp. FERM BP-3421. PCR analysis with primer pair (pBS001_scpT7_F/R). (+) positive control pBS001 plasmid; (-) negative control *Burkholderia* sp. FERM BP-3421 gDNA; (#1-6) tested exconjugant colonies of *Burkholderia* sp. FERM BP-3421 $\Delta fr9A$.

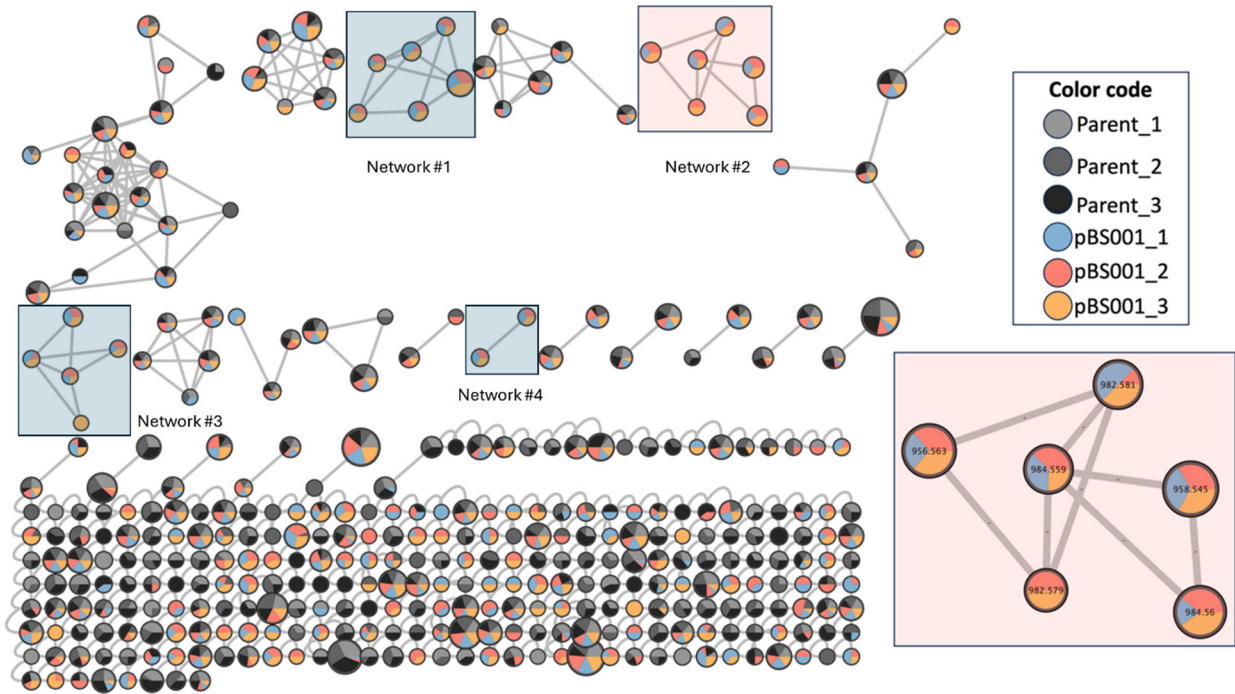


Figure S12. Molecular Network for *Burkholderia* sp. FERM BP-3421/pBS001. Nodes present in the parent strain containing the empty vector or in the strain containing the *mgp* BGC (pBS001) are color-coded. Four networks were detected only in strain carrying pBS001. The network #2 that we pursued is highlighted in a larger box. See Figures S13-S16 for details on all four networks.

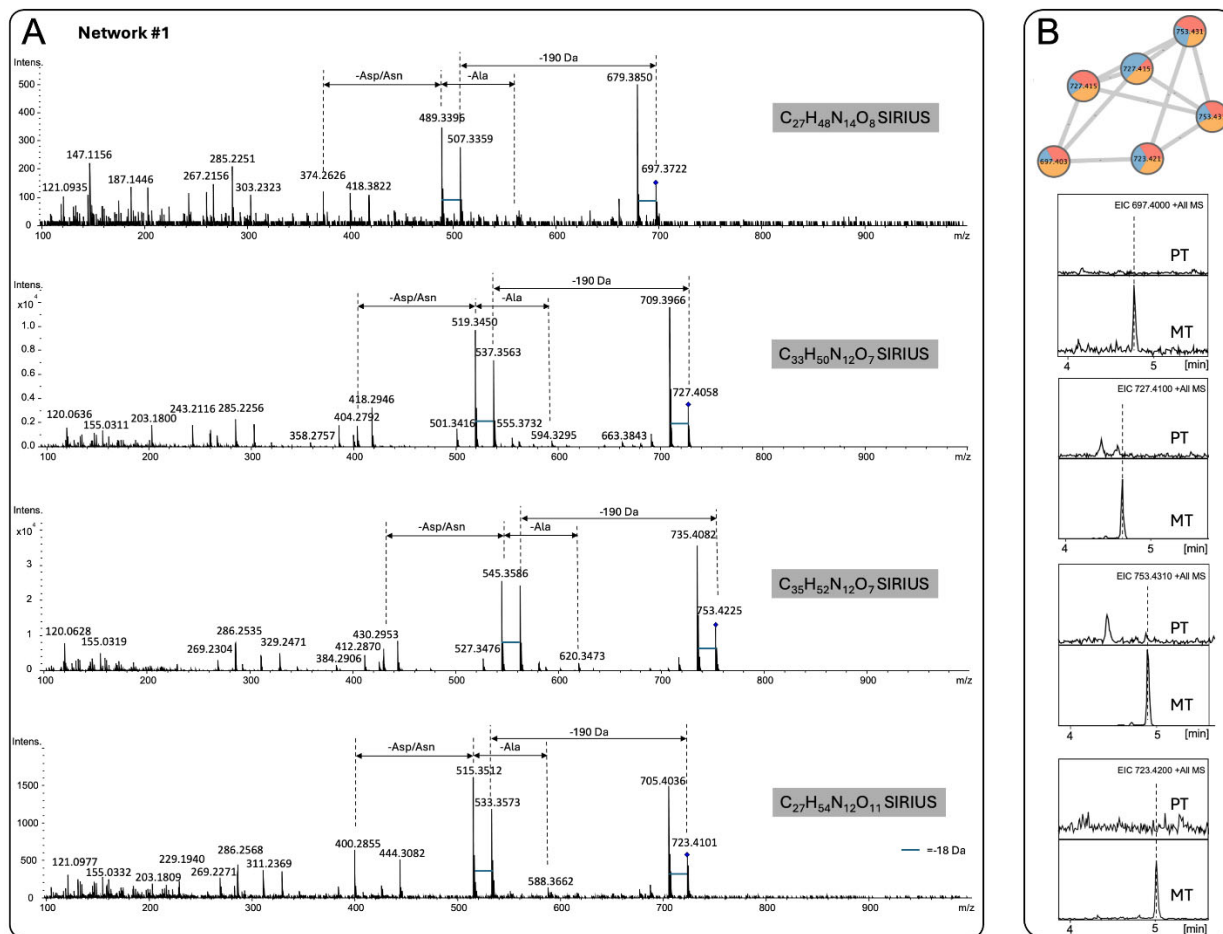


Figure S13. MS analysis of network #1. (A) MS2 spectra for nodes present in network #1 (Fig. S12). Neutral losses corresponding to Ala and Asp/Asn were observed. The molecular formulas predicted by SIRIUS v8.5.5 are indicated. No strong MS2 correlation with megapolipeptides MS2 were recognized suggesting a different compound. (B) Molecular network diagram (top) and extracted ion chromatograms (bottom) comparing parent type (PT) and mutant type (MT, carrying pBS001) strains showing detection of the m/z features exclusively in the MT extracts. Because the neutral losses for the amino acids were not the ones predicted from the *mgp* BGC, this network was deprioritized.

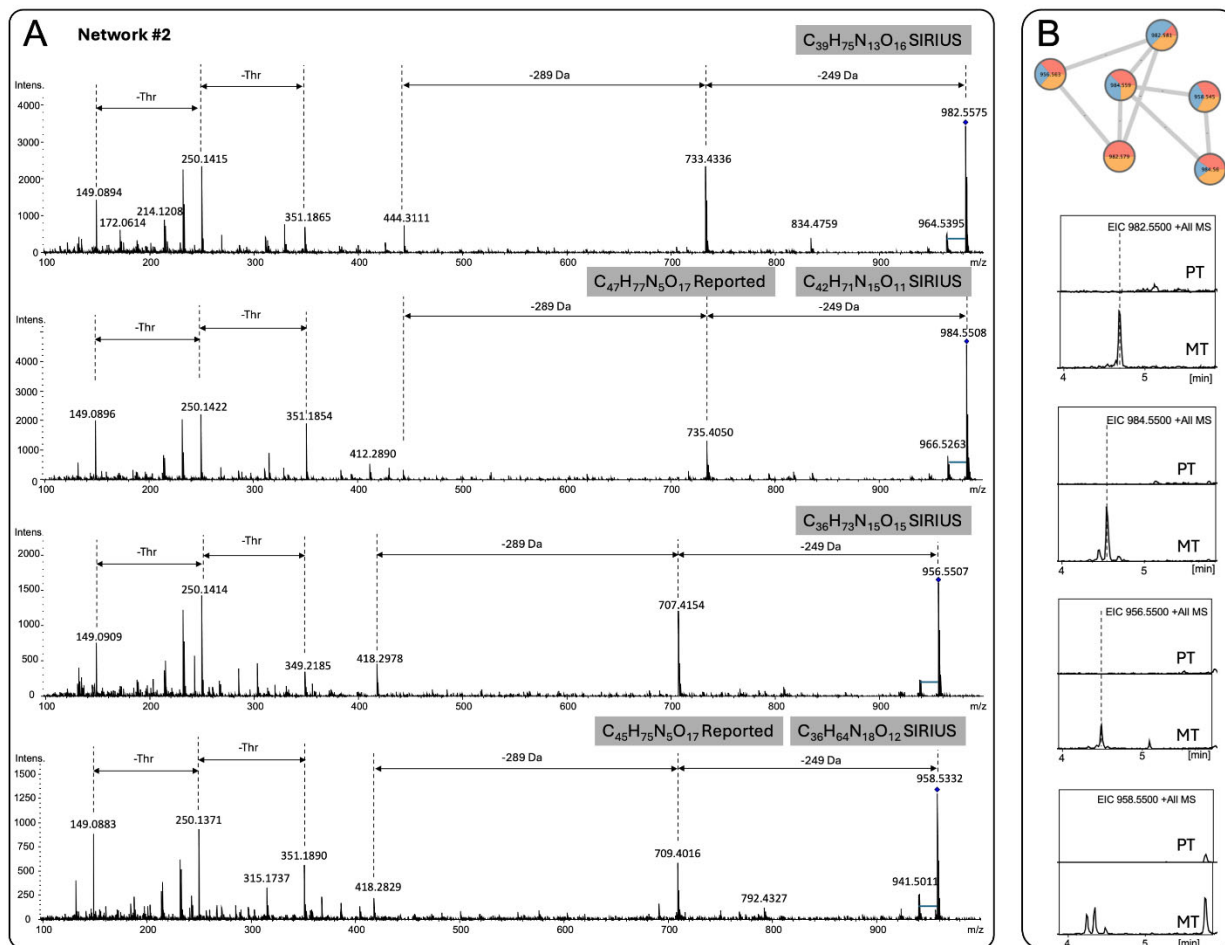


Figure S14. MS analysis of network #2 (megapolipeptins network). (A) MS2 spectra for nodes present in network #2 (Fig. S12). Neutral losses corresponding to 2 Thr residues (101 Da) were observed. The molecular formulas predicted by SIRIUS v8.5.5 and the ones we report here are indicated. (B) Molecular network diagram (top) and extracted ion chromatograms (bottom) comparing parent type (PT) and mutant type (MT, carrying pBS001) strains showing detection of the m/z features exclusively in the MT extracts. The same parent m/z features were observed by Zheng *et al.* (2020) after promoter replacement of a similar BGC (92% identity to *mgp*) from a different *P. megapolitana* strain²⁰.

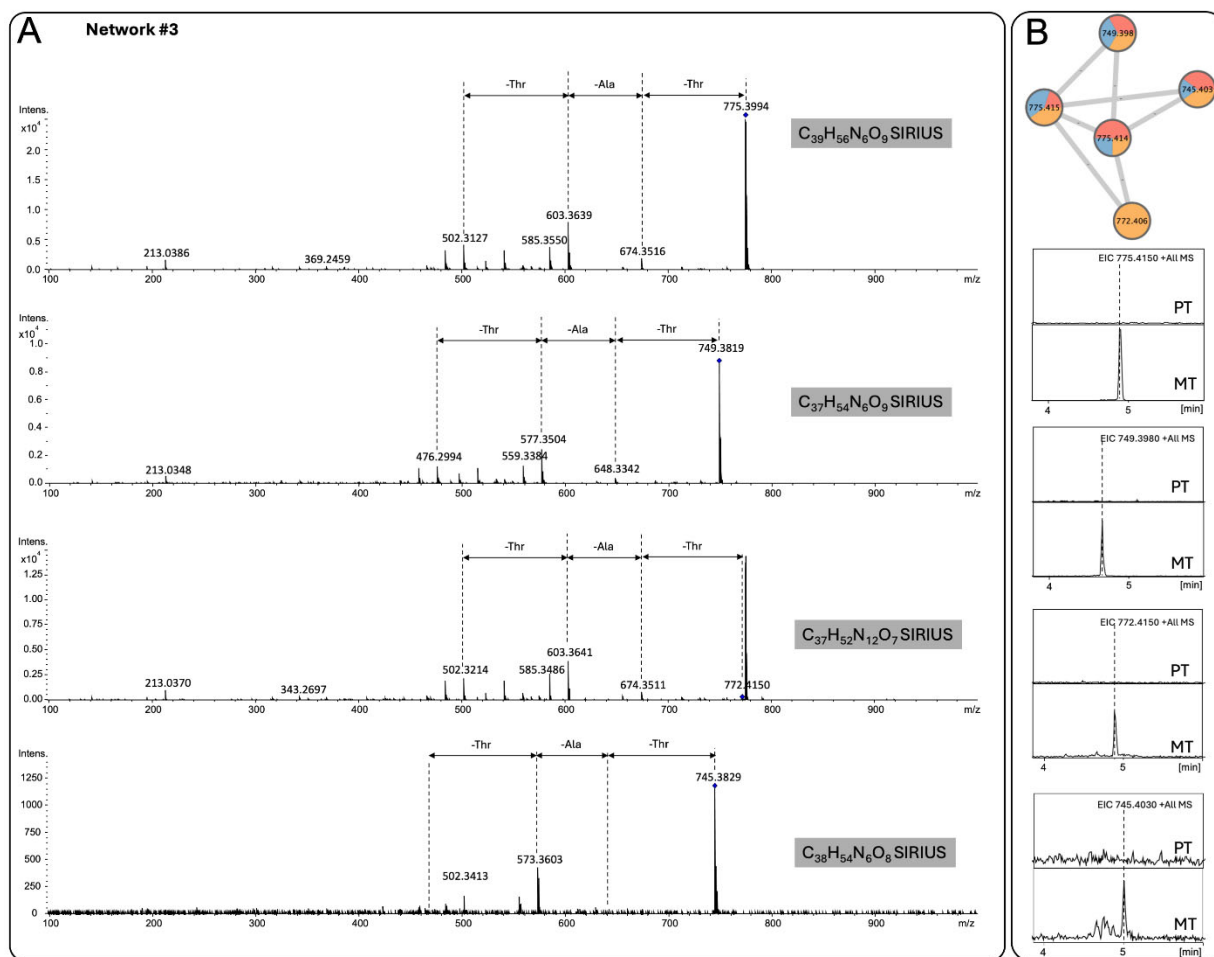


Figure S15. MS analysis of network #3. (A) MS2 spectra for nodes present in network #3 (Fig. S12). Neutral losses corresponding to 101 Da (Thr), 71 Da (Ala), followed by 101 Da (Thr) were observed. The molecular formulas predicted by SIRIUS v8.5.5 are indicated. (B) Molecular network diagram (top) and extracted ion chromatograms (bottom) comparing parent type (PT) and mutant type (MT, carrying pBS001) strains showing detection of the m/z features exclusively in the MT extracts. Although Thr neutral loss is also observed for the megapolipeptins they were not sequential for this compound family so that network 3 is likely unrelated to megapolipeptins.

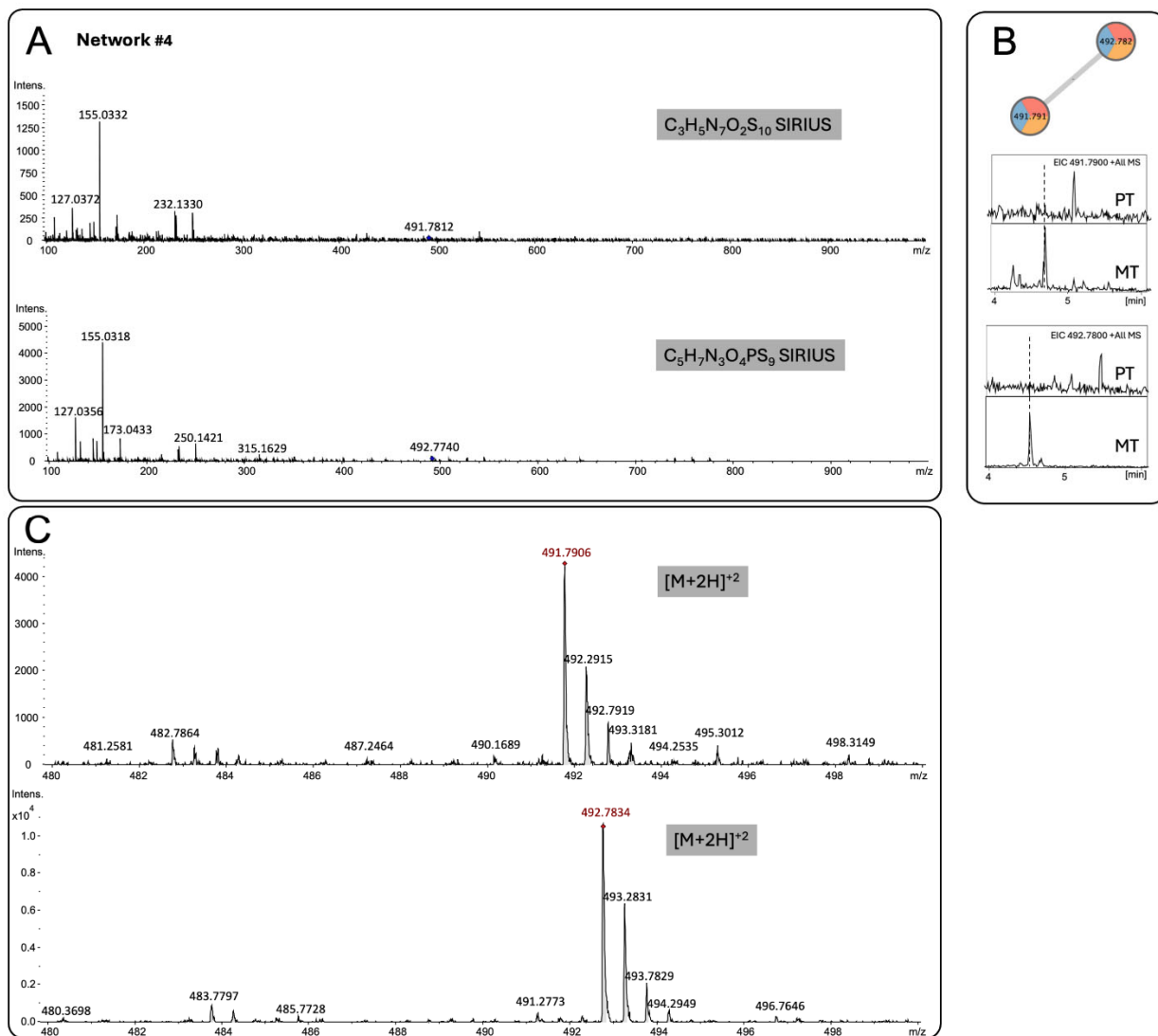


Figure S16. MS analysis of network #4. (A) MS2 spectra for nodes present in network #4 (Fig. S12). The molecular formulas predicted by SIRIUS v8.5.5 are indicated. (B) Molecular network diagram (top) and extracted ion chromatograms (bottom) comparing parent type (PT) and mutant type (MT, carrying pBS001) strains showing detection of the m/z features exclusively in the MT extracts. (C) Isotope pattern of the observed features indicating that they are doubly charged species. Note that SIRIUS only works with singly charged precursors, giving inaccurate predictions for doubly charged features. This network likely represents doubly charged megapolypeptins.

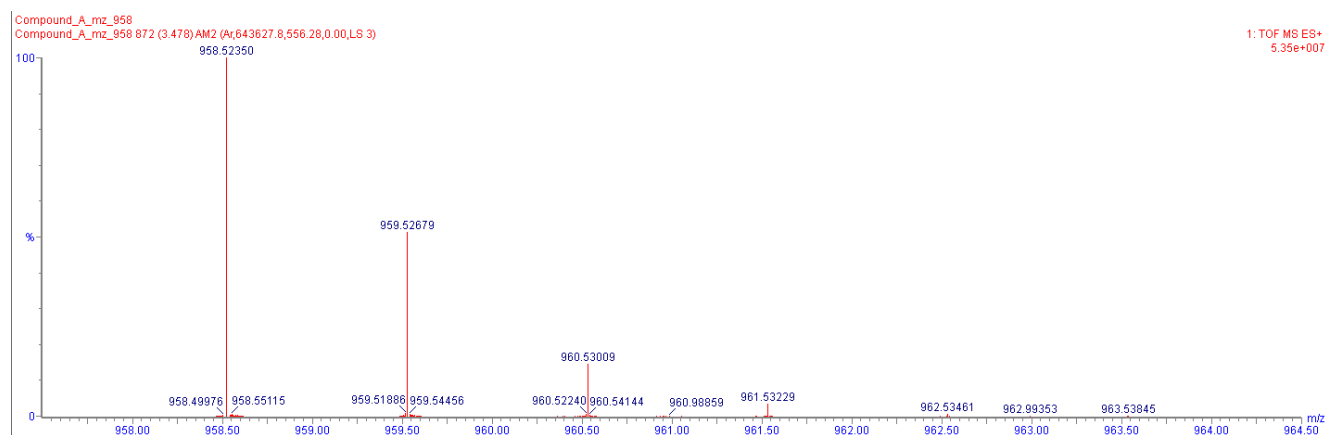


Figure S17. HR-ESI-MS data for megapolipeptin A (1).

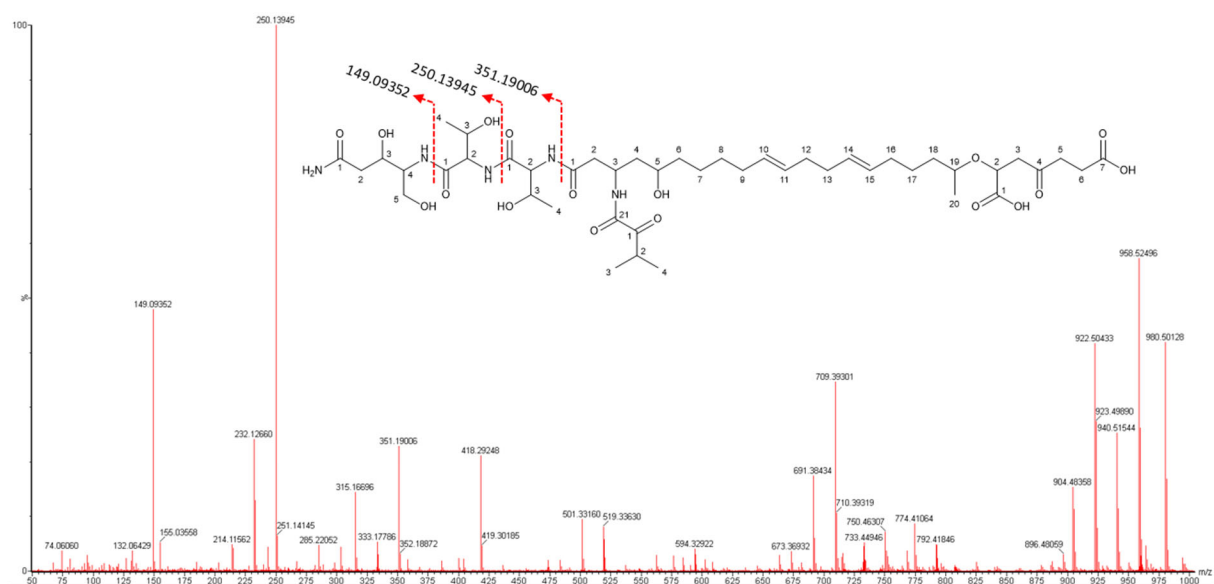


Figure S18. MS/MS data for megapolipeptin A (1).

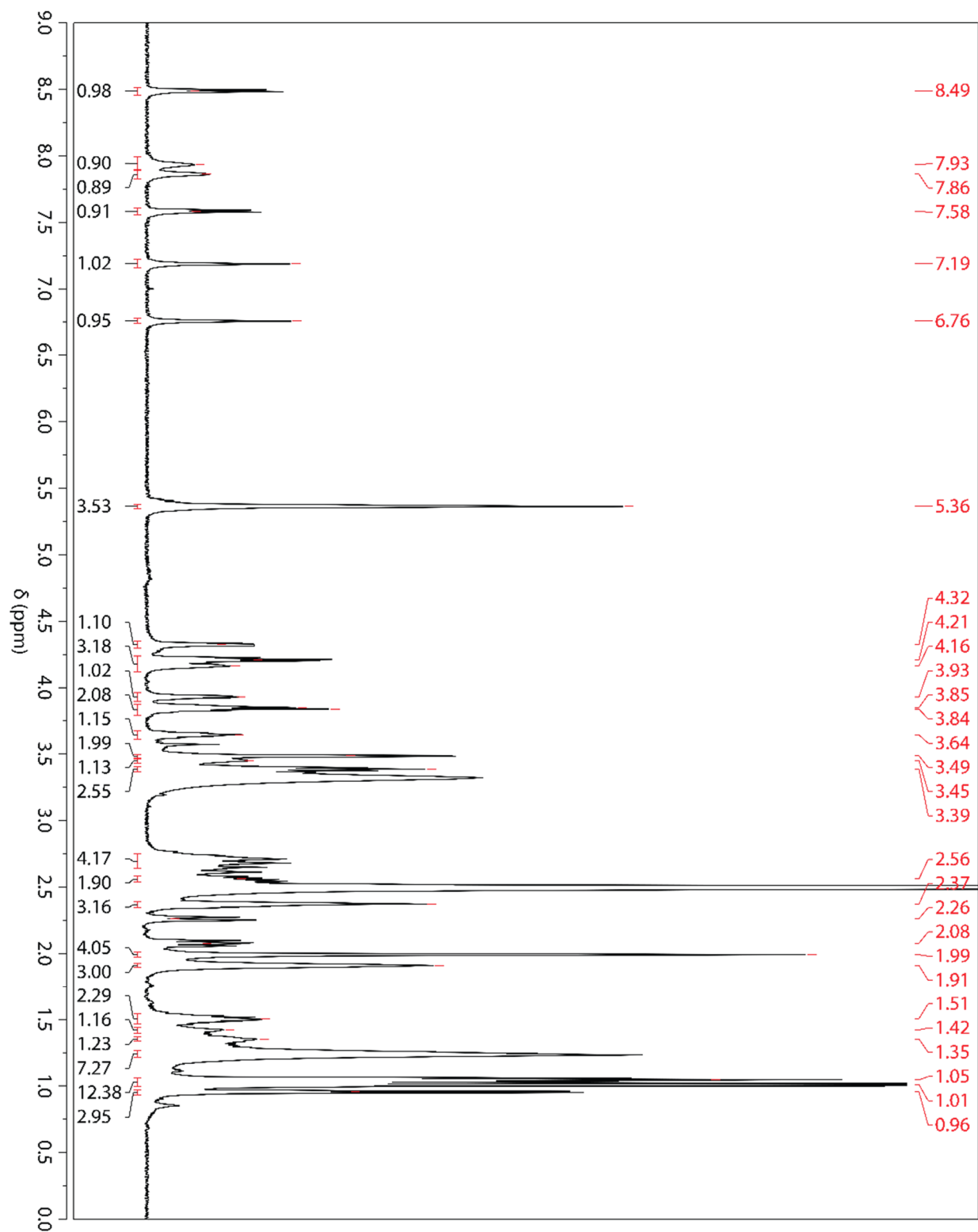


Figure S19. ¹H NMR spectrum of megapolipeptin A (1) acquired in DMSO-*d*₆ at 600 MHz.

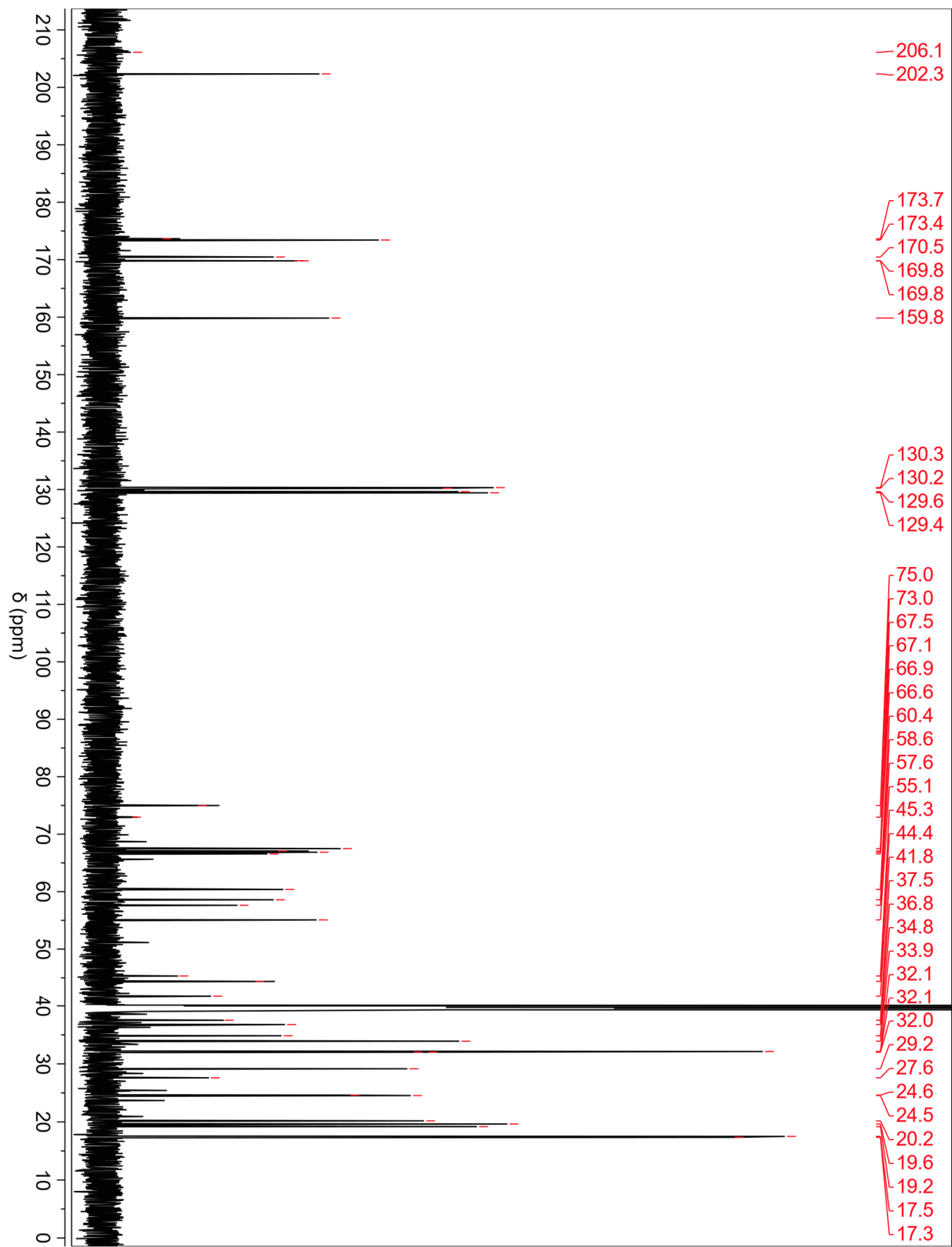


Figure S20. ^{13}C NMR spectrum of megapolipeptin A (1) acquired in $\text{DMSO-}d_6$ at 150 MHz.

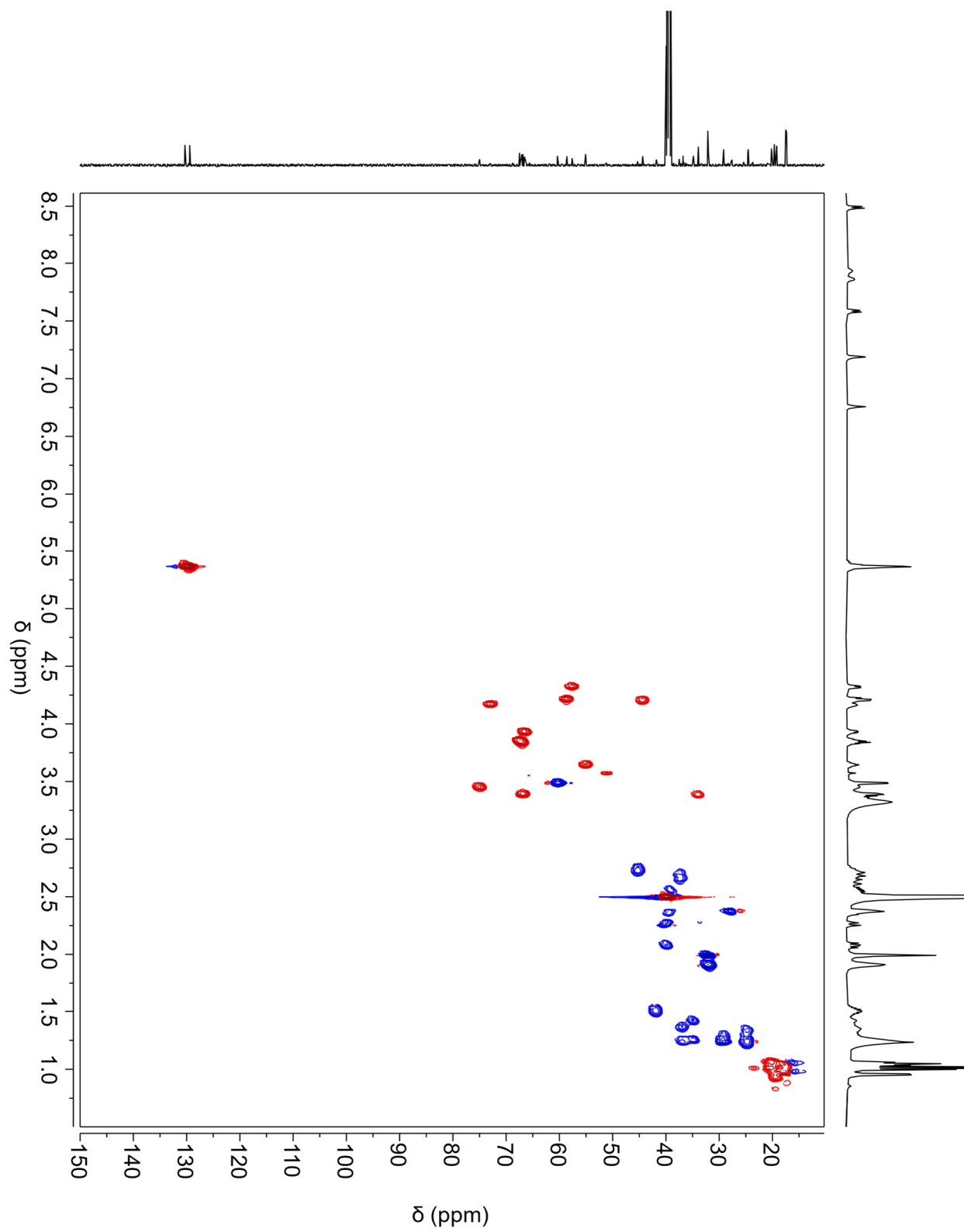


Figure S21. HSQC spectrum of megapolipeptin A (1) acquired in $\text{DMSO-}d_6$ at 600 MHz.

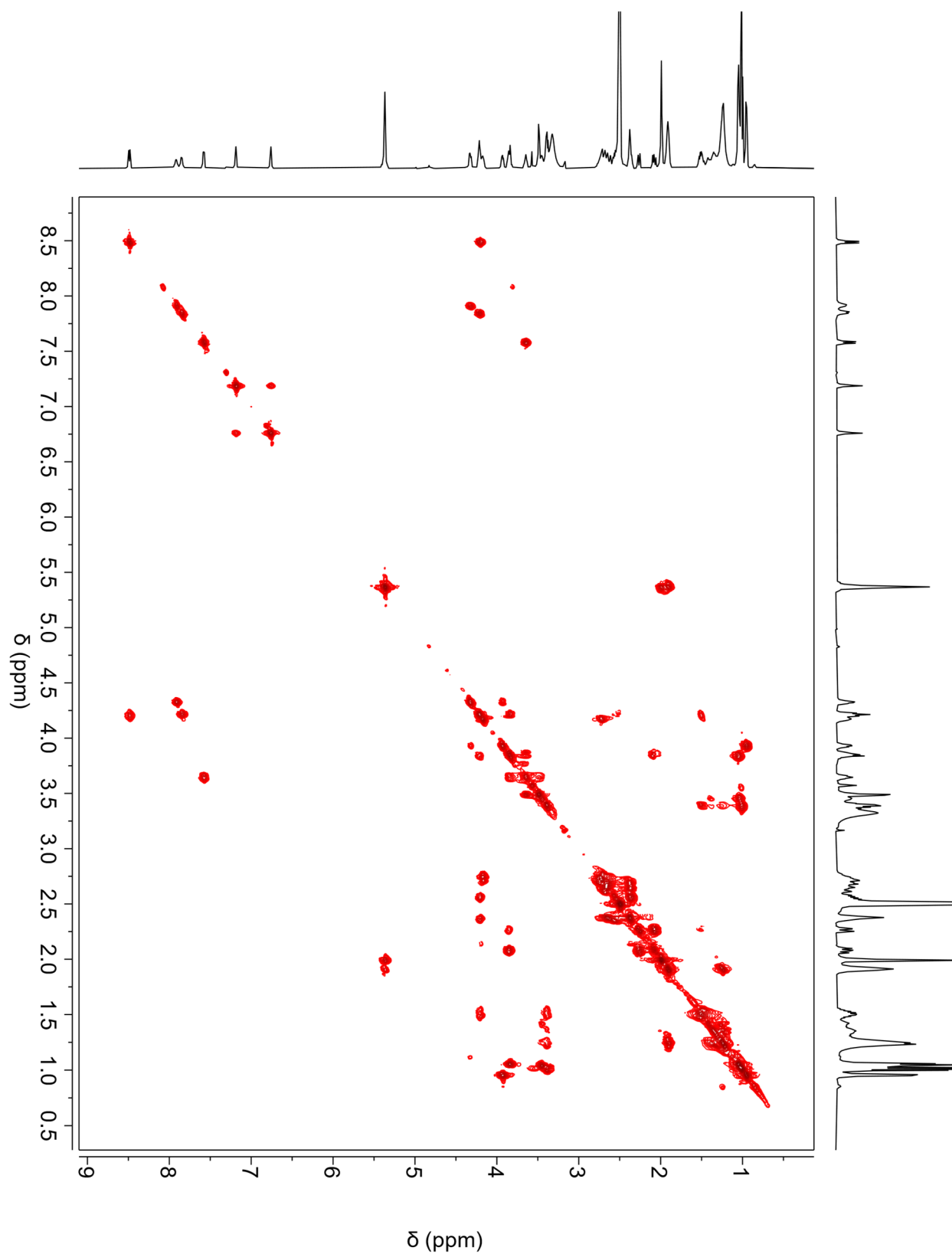


Figure S22. ^1H - ^1H COSY spectrum of megapolipeptin A (1) acquired in $\text{DMSO-}d_6$ at 600 MHz.

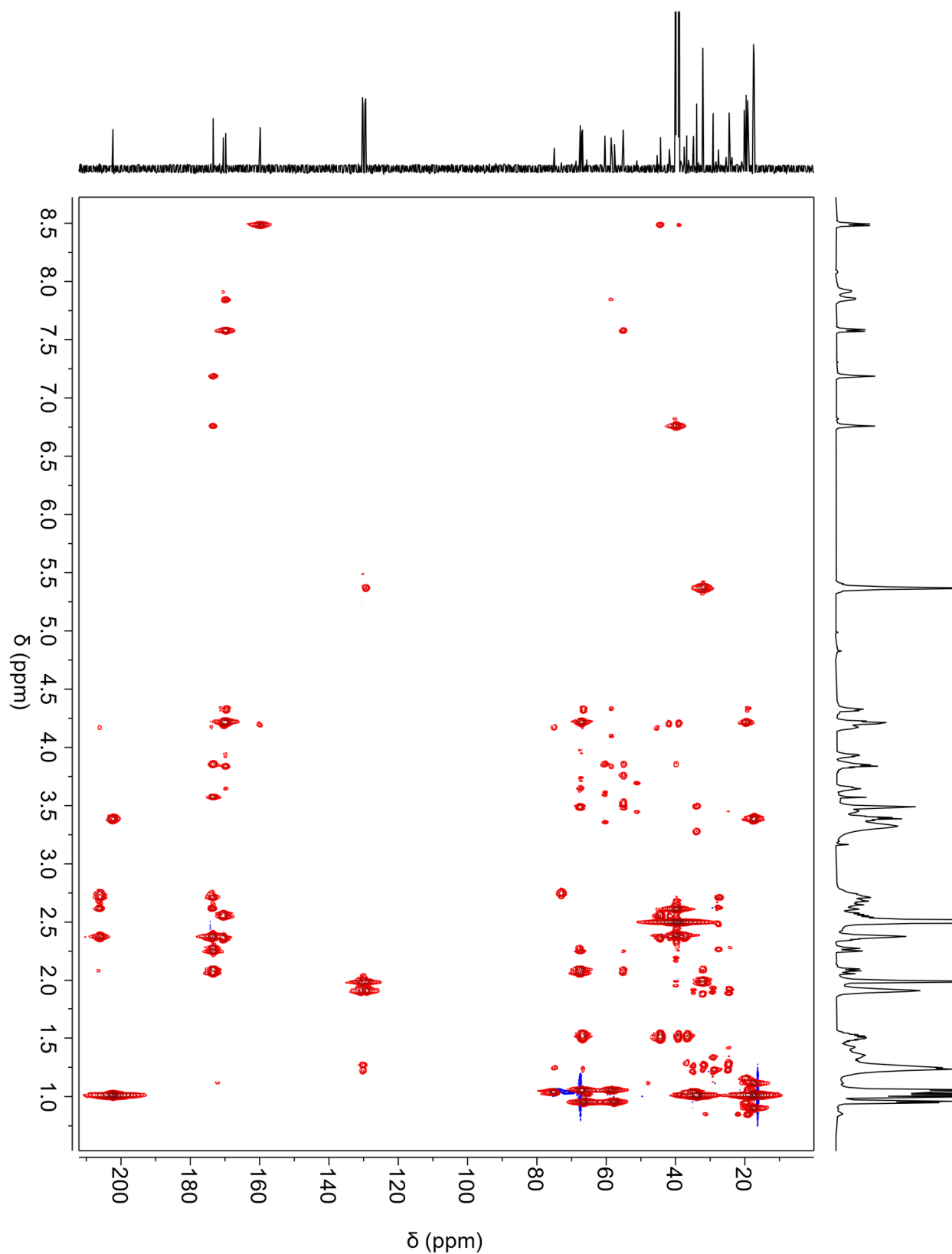


Figure S23. HMBC spectrum of megapolipeptin A (1) acquired in $\text{DMSO-}d_6$ at 600 MHz.

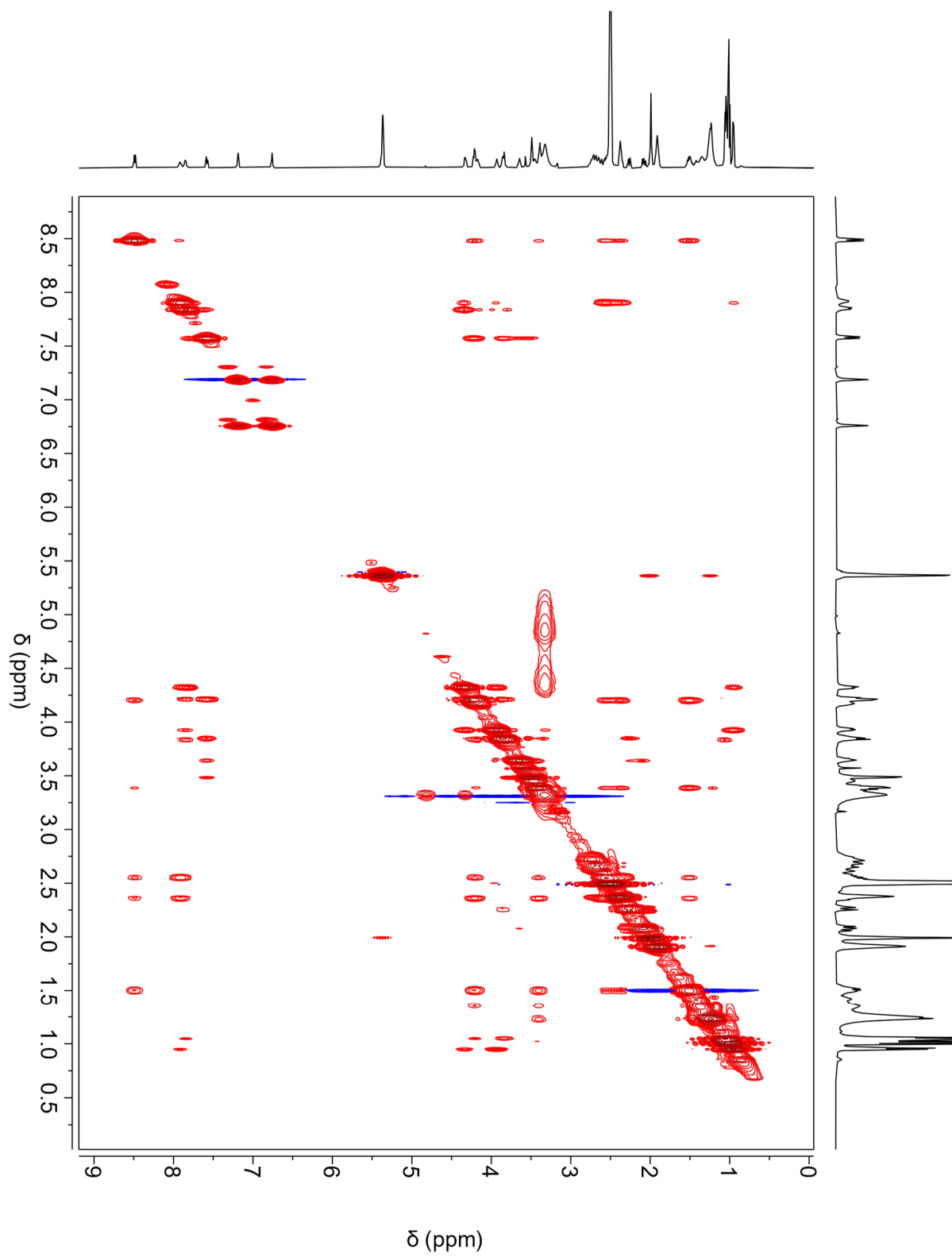


Figure S24. NOESY spectrum of megapolipeptin A (1) acquired in DMSO- d_6 at 600 MHz.

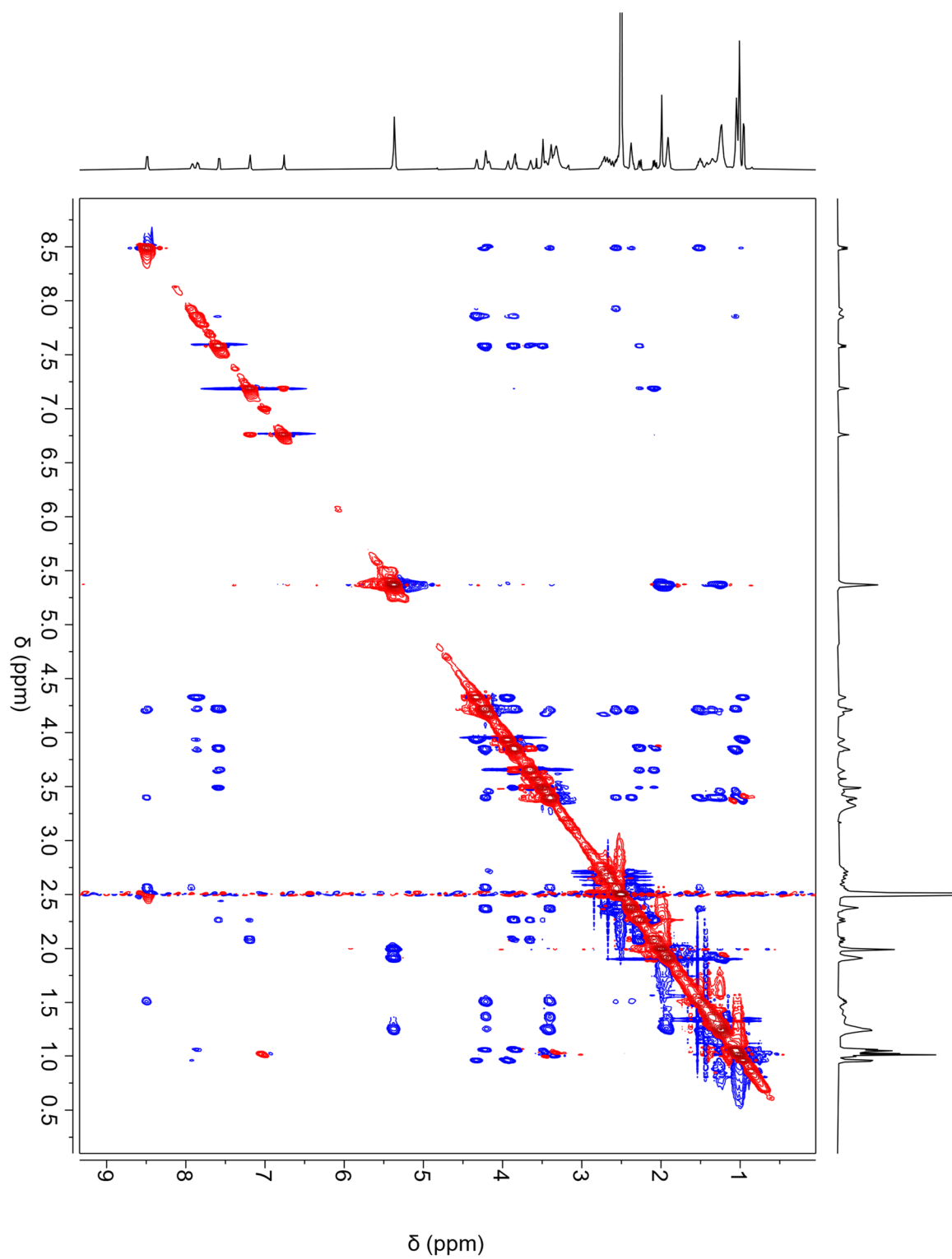


Figure S25. ROESY spectrum of megapolipectin A (1) acquired in DMSO-*d*₆ at 600 MHz.

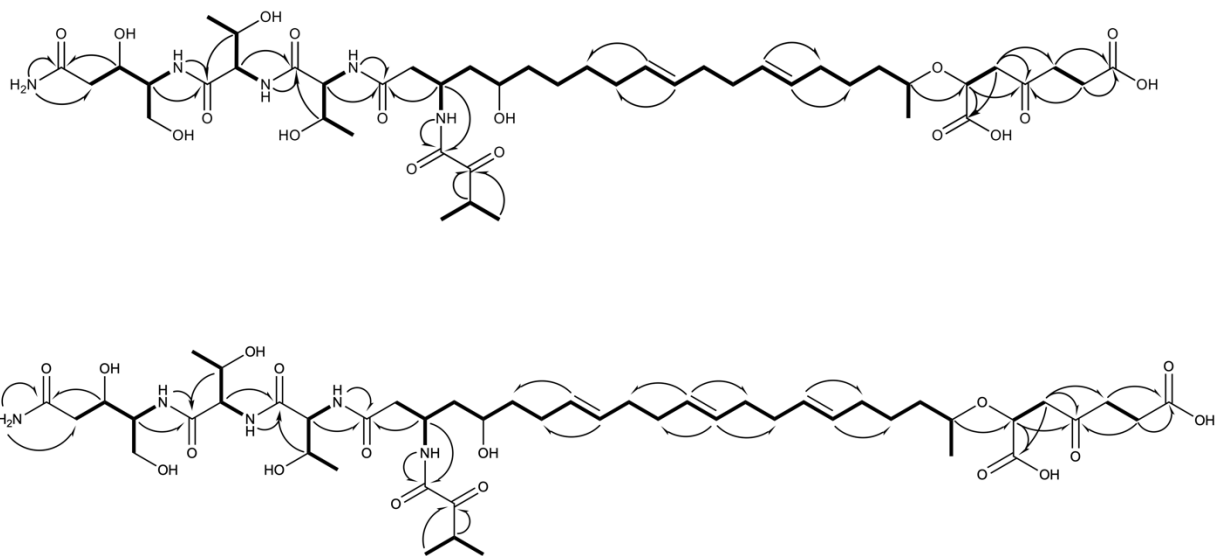


Figure S26. Key COSY (bold lines) and HMBC (arrows) correlations for the planar structures of megapolipeptin A (1) and megapolipeptin B (2).

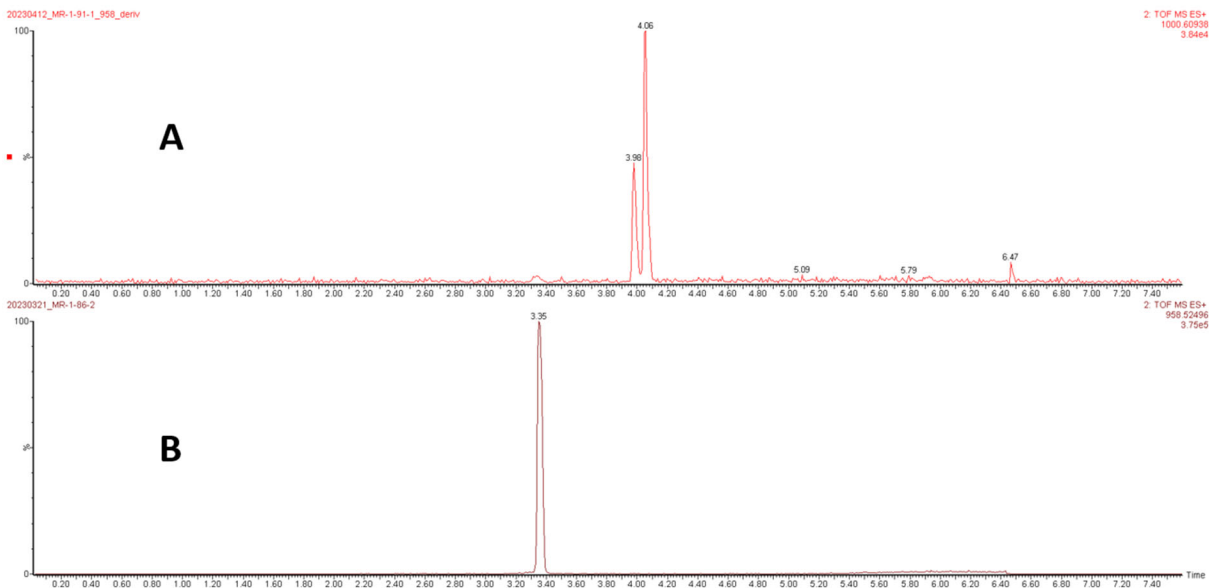


Figure S27. Comparative Extracted Ion Chromatograms of megapolipectin A (1) and methyl ester derivatives. (A) EIC of the megapolipectin A (1) methyl ester derivatives. Two products were observed and isolated by HPLC. (B) EIC of purified megapolipectin A (1).

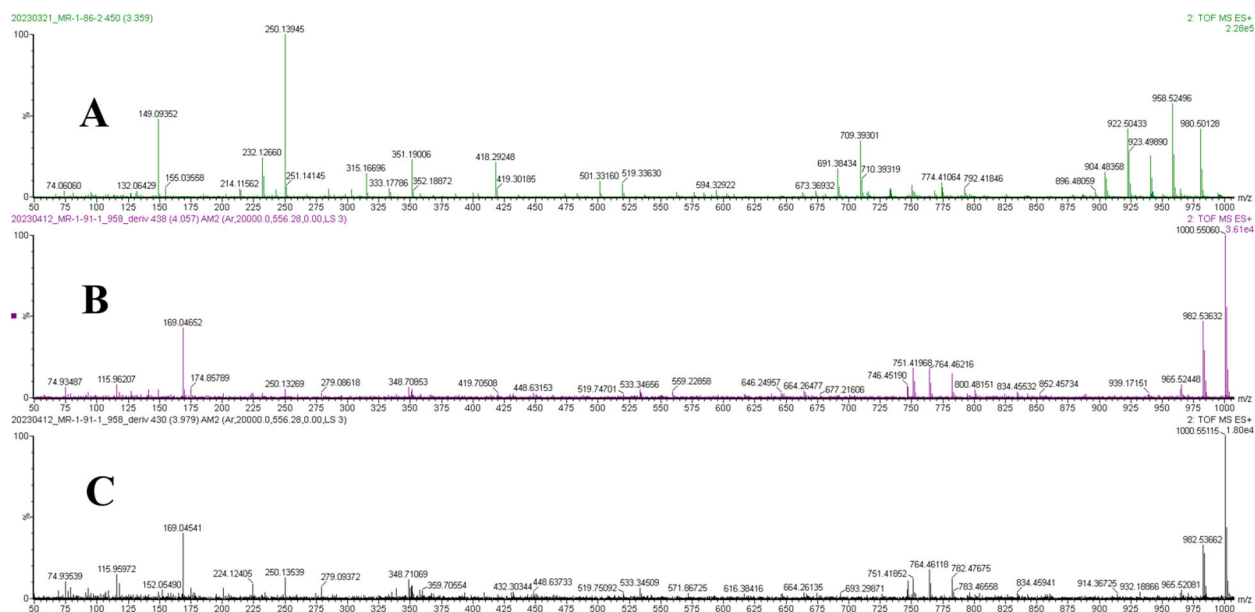


Figure S28. Comparative MS spectra of megapolipectin A (1) and methyl ester derivatives. (A) megapolipectin A (1). (B) and (C) The two megapolipectin A (1) methyl ester derivatives (B: t_R 4.06 min; C: t_R 3.98 min).

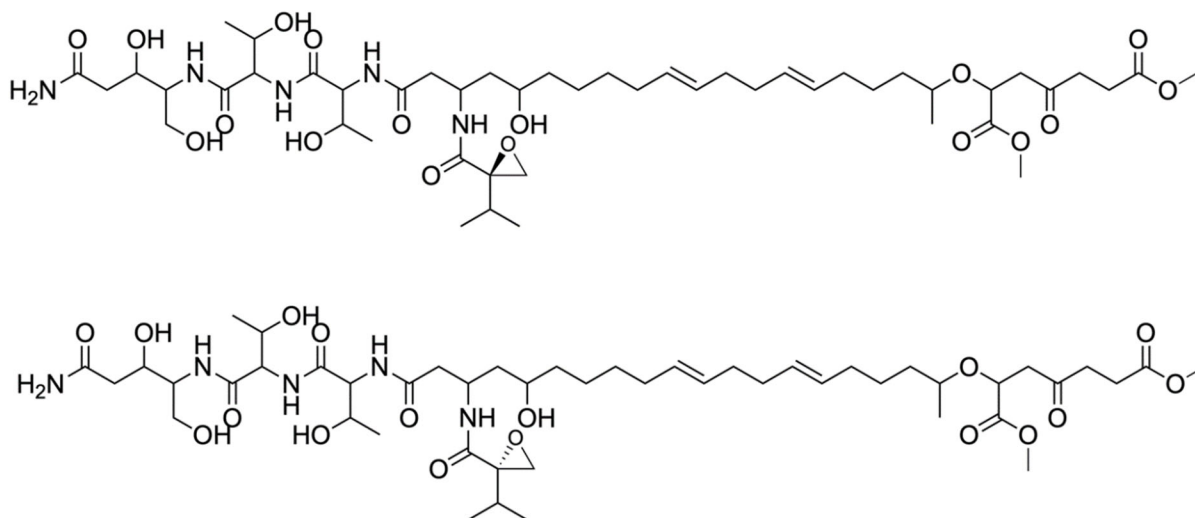


Figure S29. Planar structures of the megapolipeptin A (1) methyl ester derivatives (3 and 4).

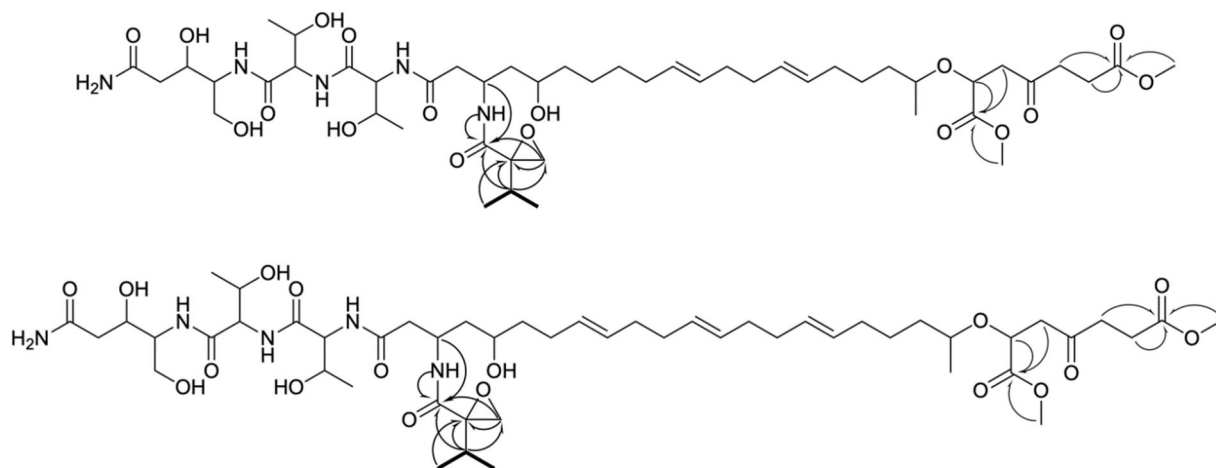


Figure S30. Key COSY and HMBC correlations of the methylated planar structures of megapolipeptin A (1) methyl ester (3) and B methyl ester (4).

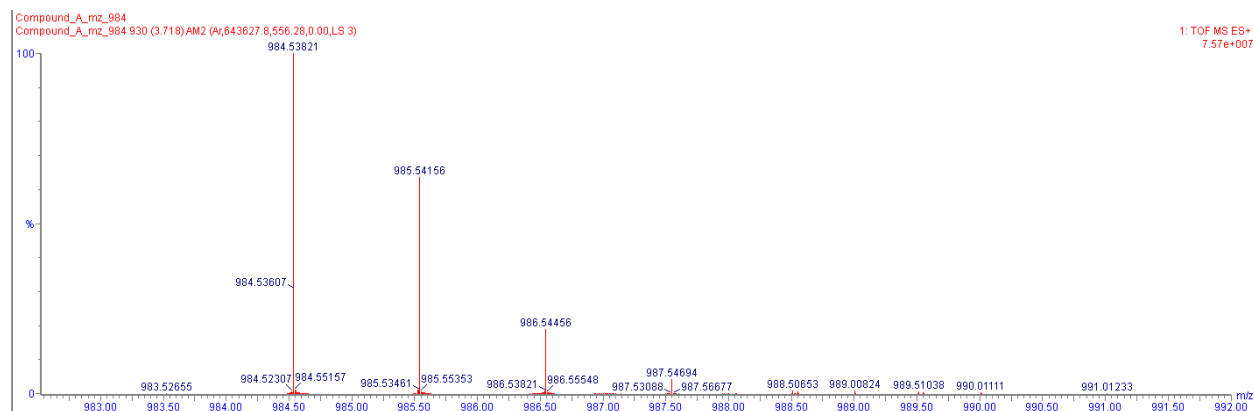


Figure S31. HR-ESI-MS data for megapolipeptin B (2).

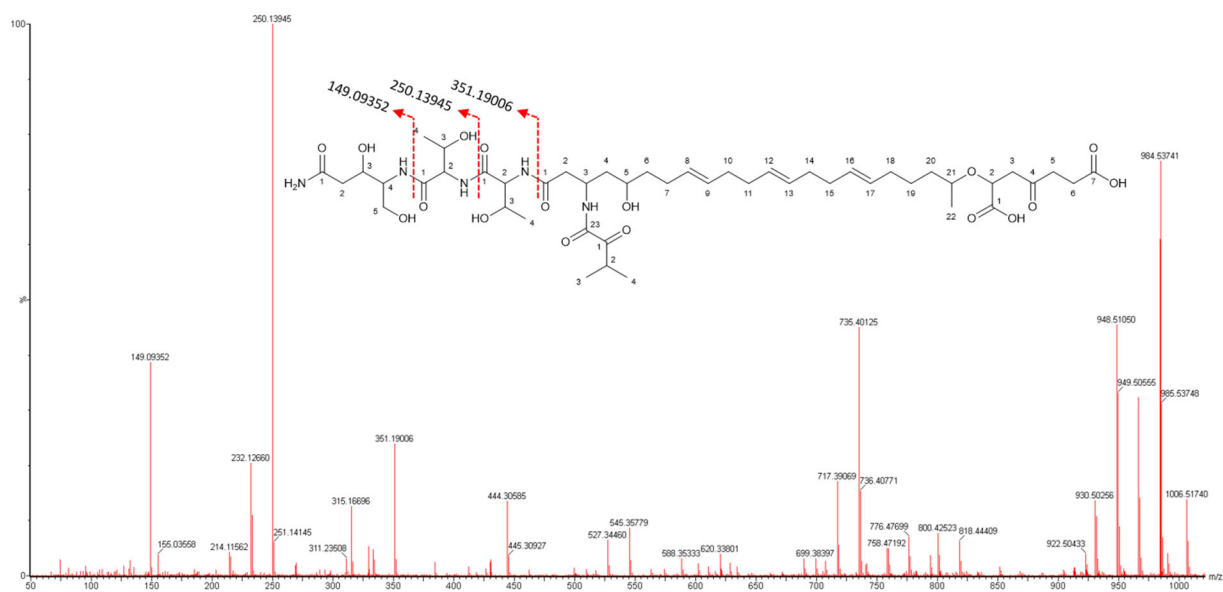


Figure S32. MS/MS data for megapolipeptin B (2).

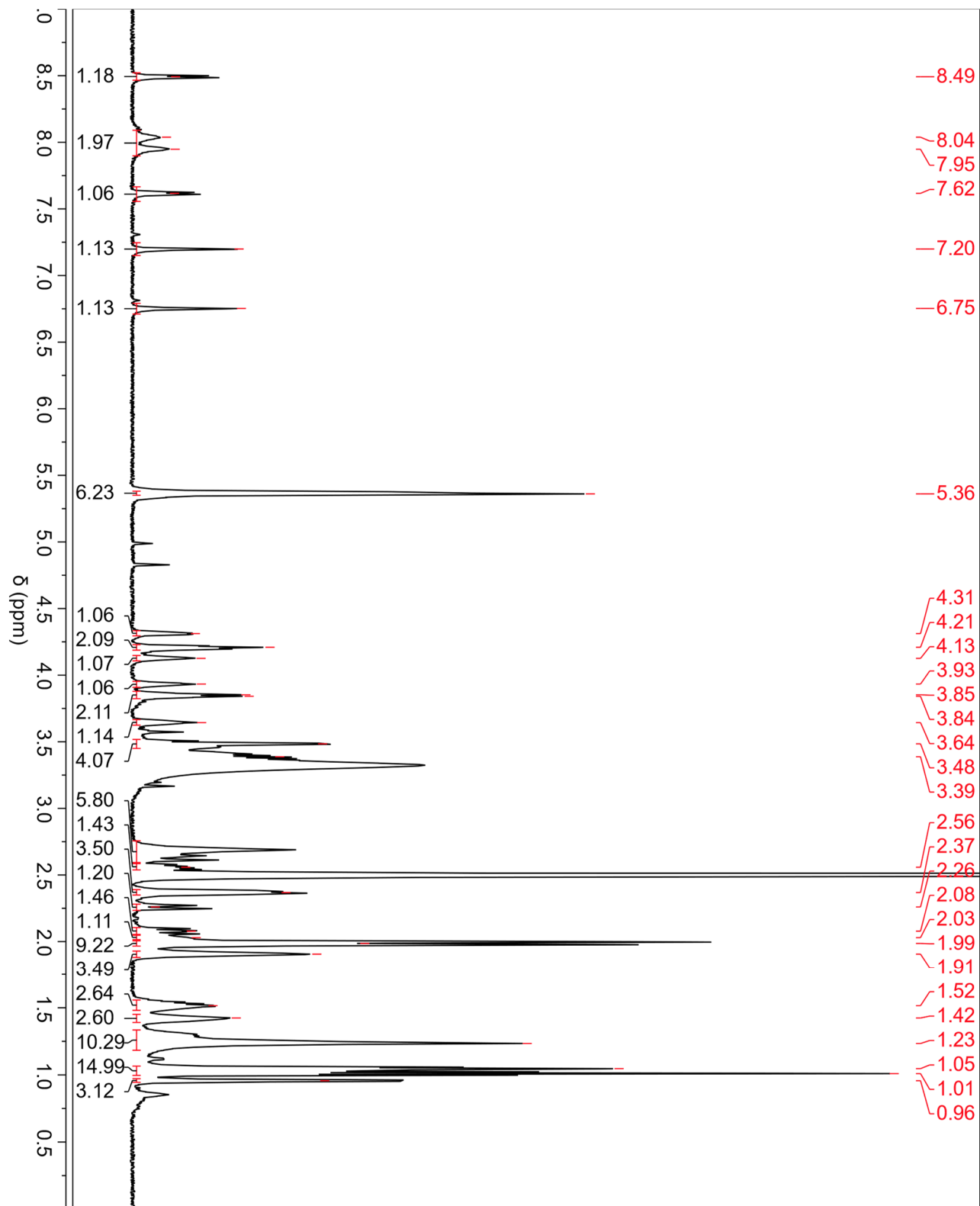


Figure S33. ^1H NMR spectrum of megapolipeptin B (2) acquired in $\text{DMSO-}d_6$ at 600 MHz.

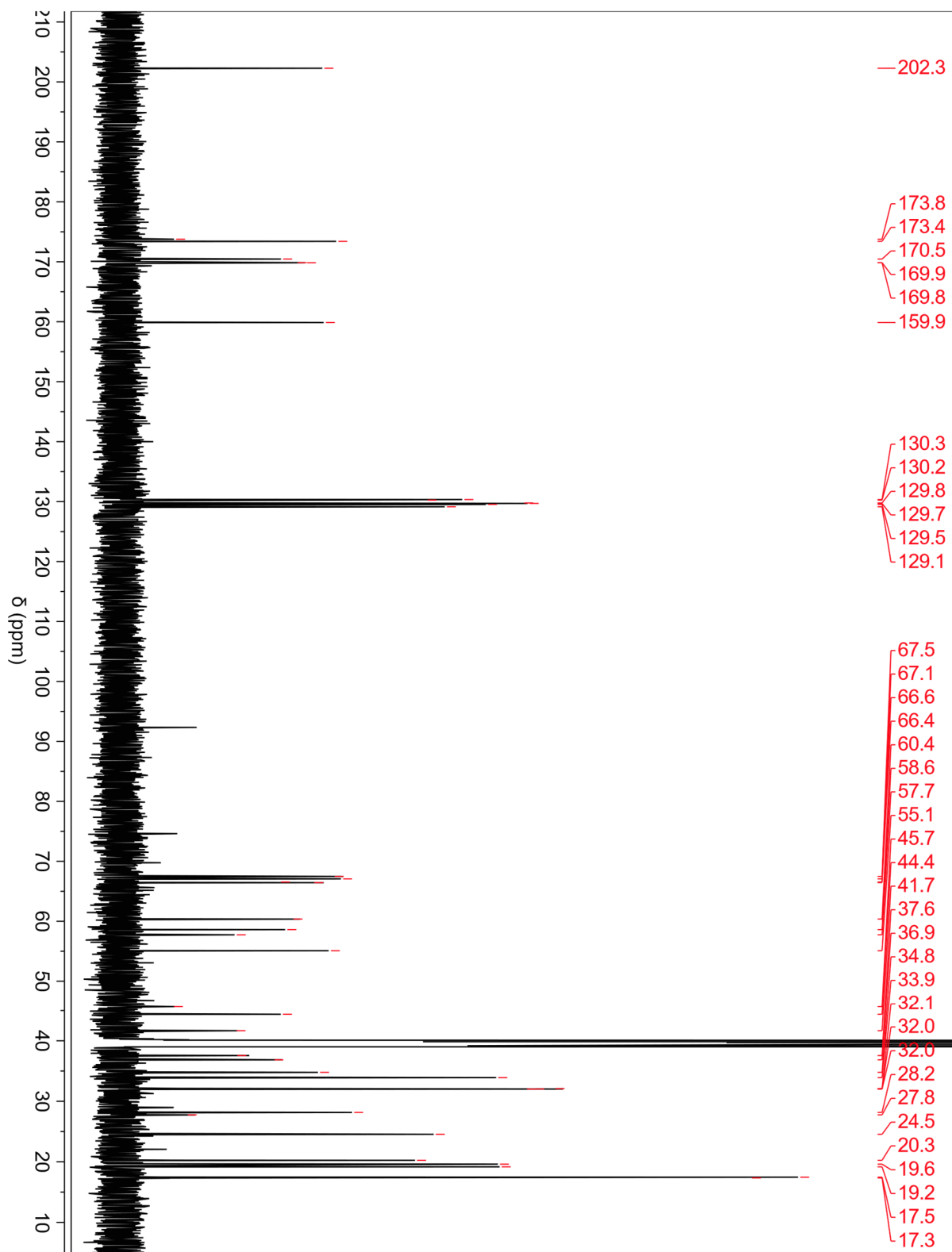


Figure S34. ^{13}C NMR spectrum of megapolipeptin B (2) acquired in $\text{DMSO-}d_6$ at 150 MHz.

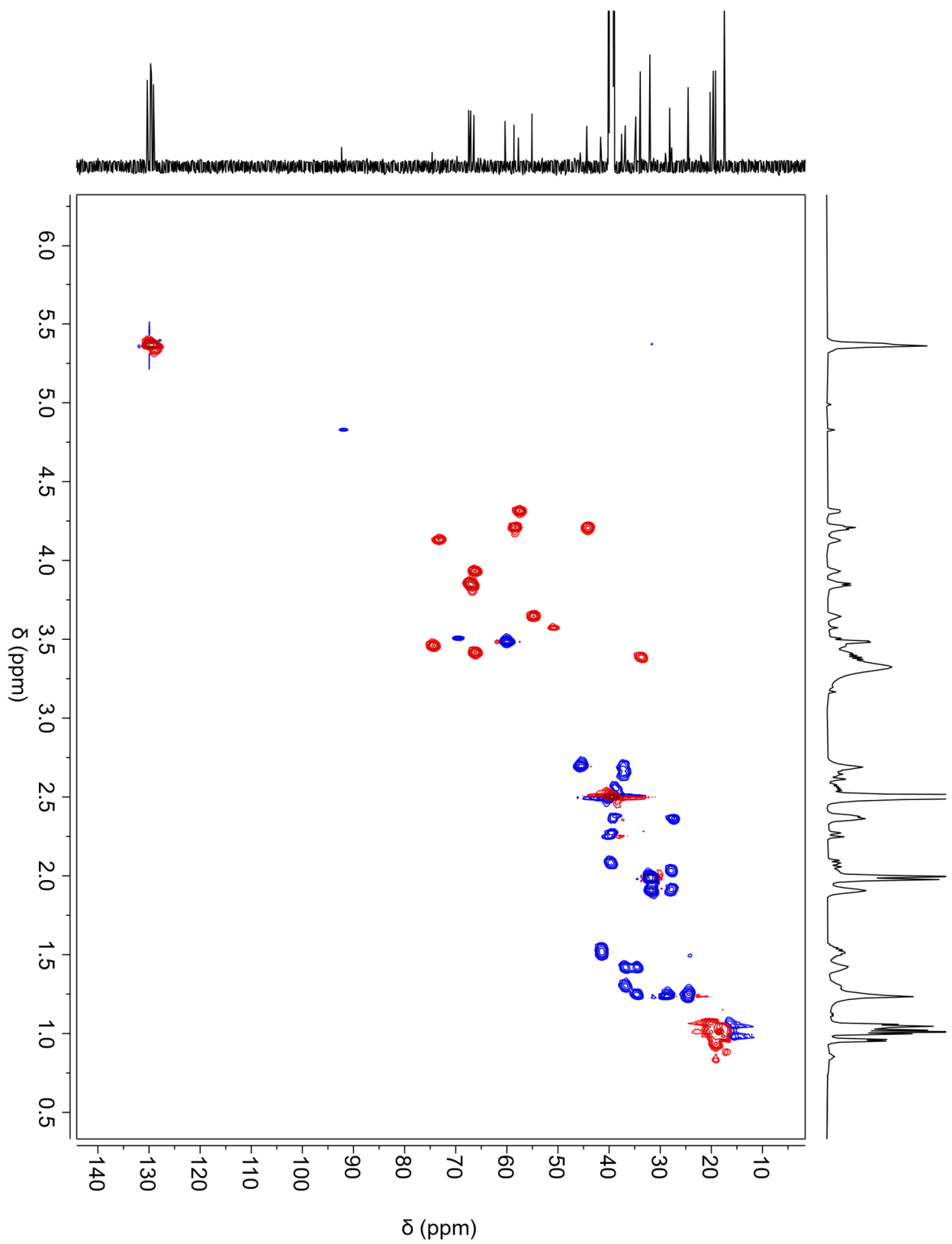


Figure S35. HSQC spectrum of megapolipeptin B (2) acquired in $\text{DMSO-}d_6$ at 600 MHz.

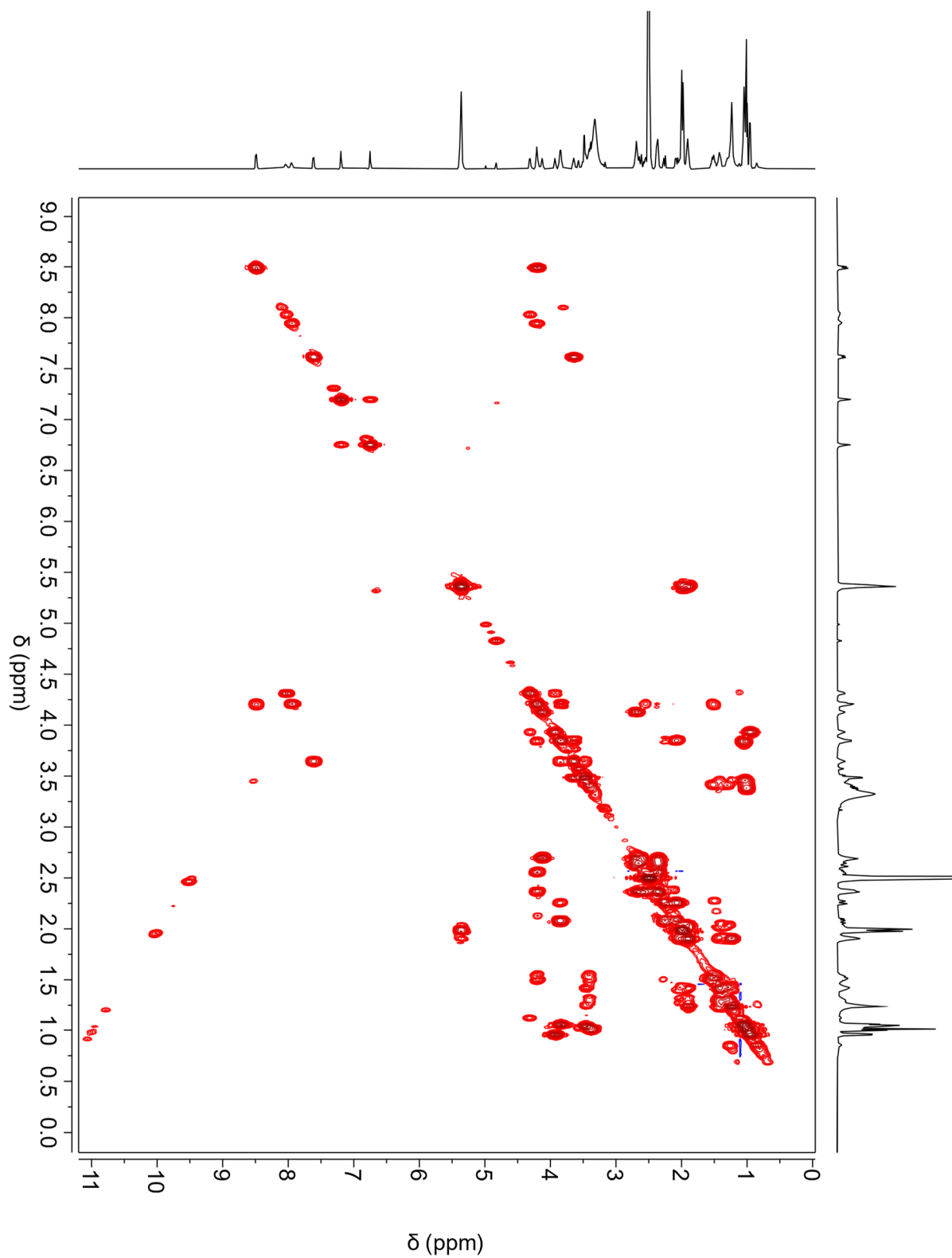


Figure S36. ^1H - ^1H COSY spectrum of megapolipeptide B (2) acquired in $\text{DMSO-}d_6$ at 600 MHz.

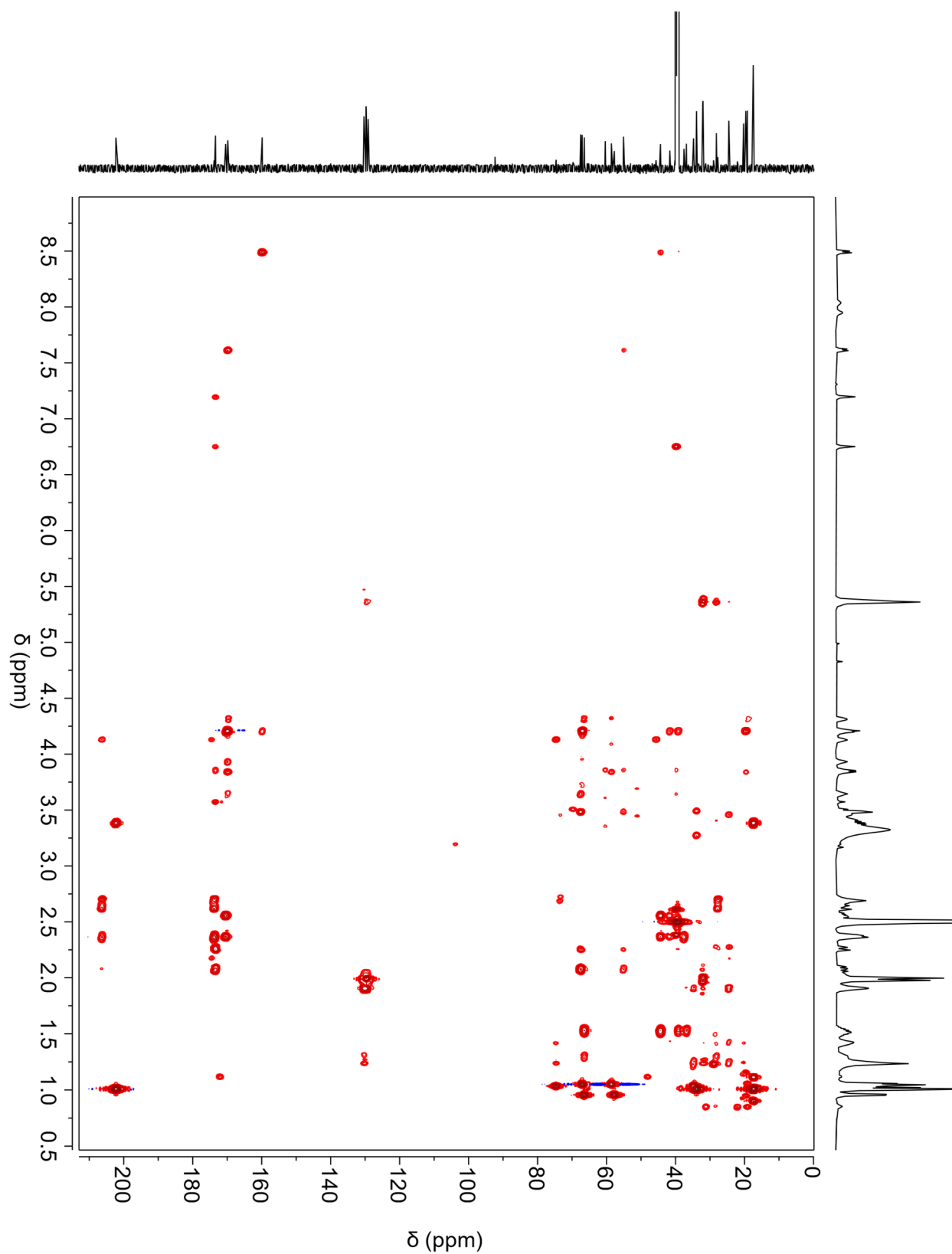


Figure S37. HMBC spectrum of megapolipeptin B (2) acquired in DMSO-*d*₆ at 600 MHz.

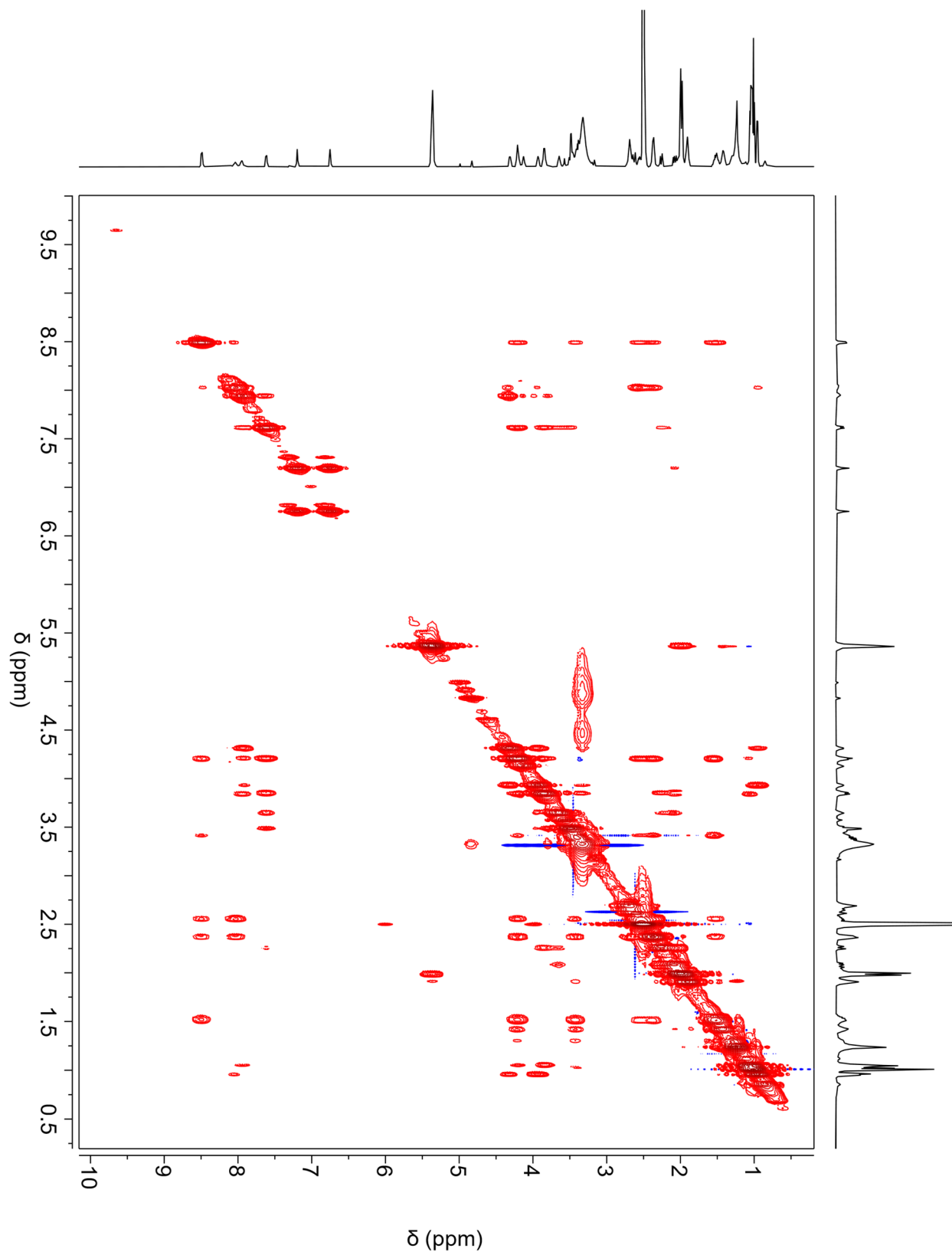


Figure S38. NOESY spectrum of megapolipeptin B (2) acquired in DMSO-*d*₆ at 600 MHz.

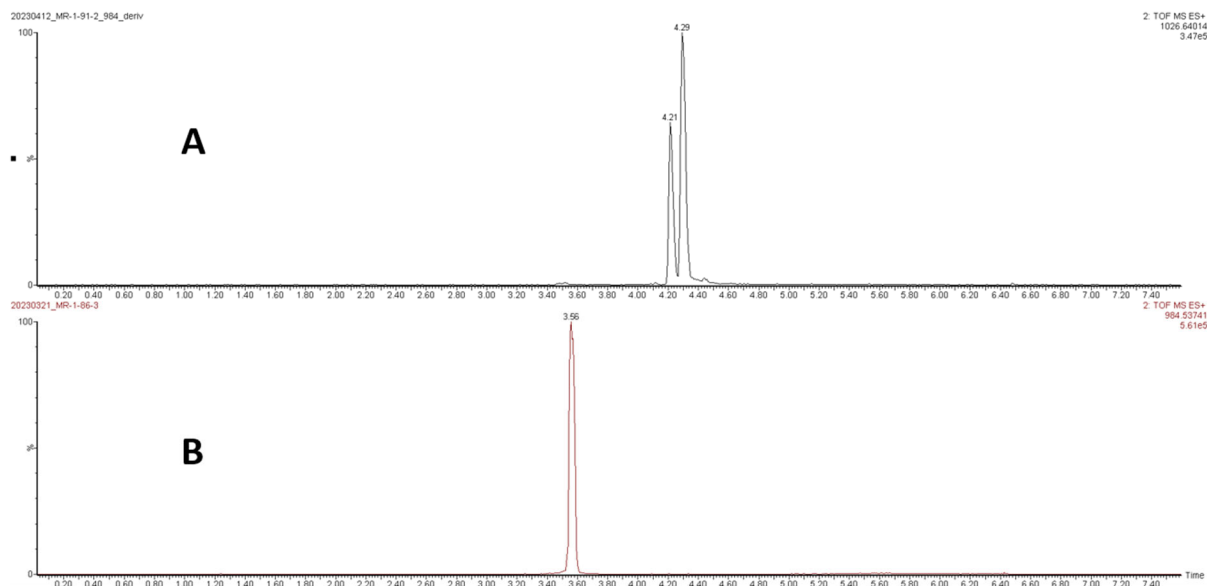


Figure S39. Extracted ion chromatograms of megapolipeptin B (2) and methyl ester derivatives. (A) EIC of the megapolipeptin B (2) methyl ester derivatives. Two products were observed and isolated by HPLC. (B) EIC of purified megapolipeptin B (2).

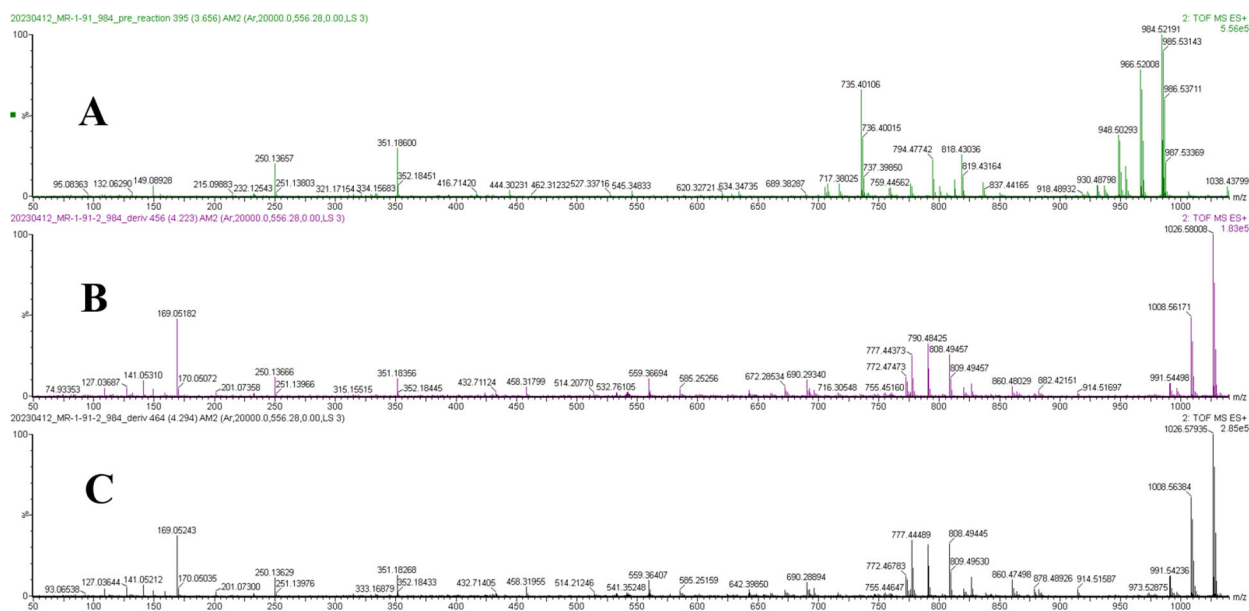


Figure S40. Comparative MS spectra of megapolipeptin B (2) and methyl ester derivatives. (A) megapolipeptin B (2) and (B) and (C) the two megapolipeptin B (2) methyl ester derivatives (B: 5, t_R 4.21 min; C: 6, t_R 4.29 min).

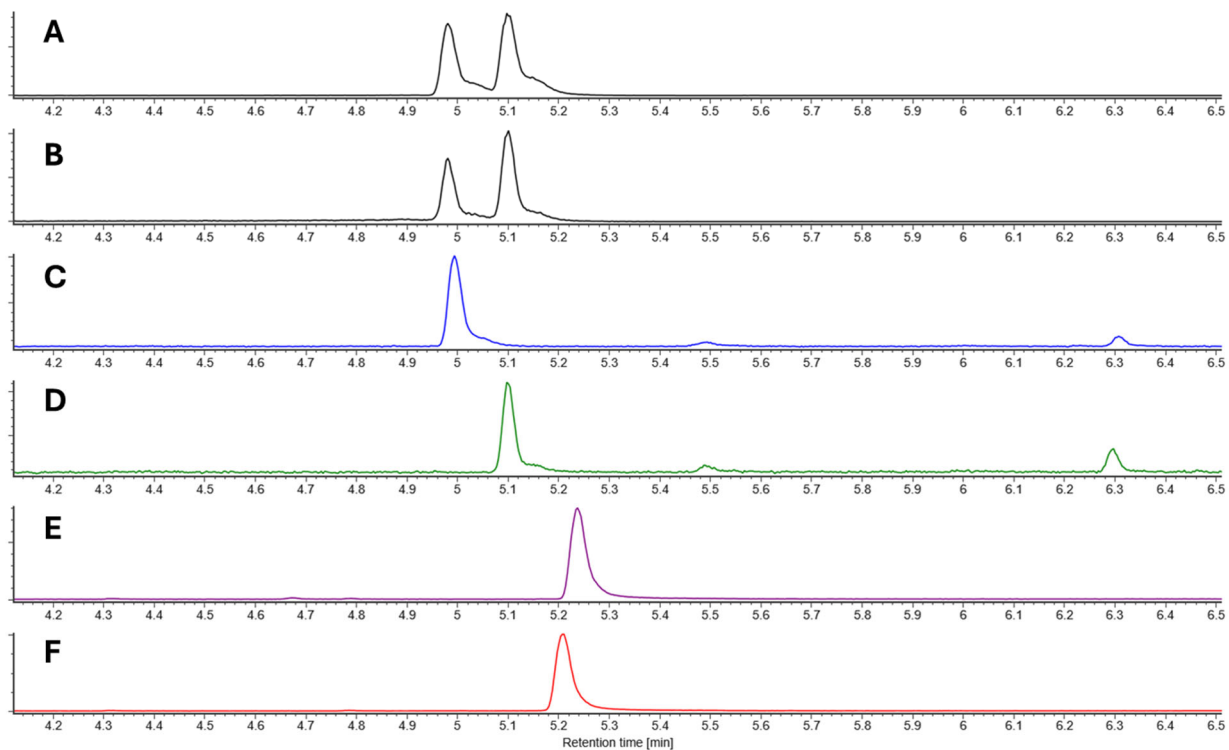


Figure S41. Marfey's analysis of megapolipeptin A (1) and megapolipeptin B (2). (A) EIC $[M+H]^+$ m/z 400.15 of megapolipeptin A (1) hydrolysate. (B) EIC $[M+H]^+$ m/z 400.15 of megapolipeptin B (2) hydrolysate. (C) FDVA-L-threonine standard. (D) FDVA-L-*allo*-threonine standard. (E) FDVA-D-*allo*-threonine standard. (F) FDVA-D-threonine standard.

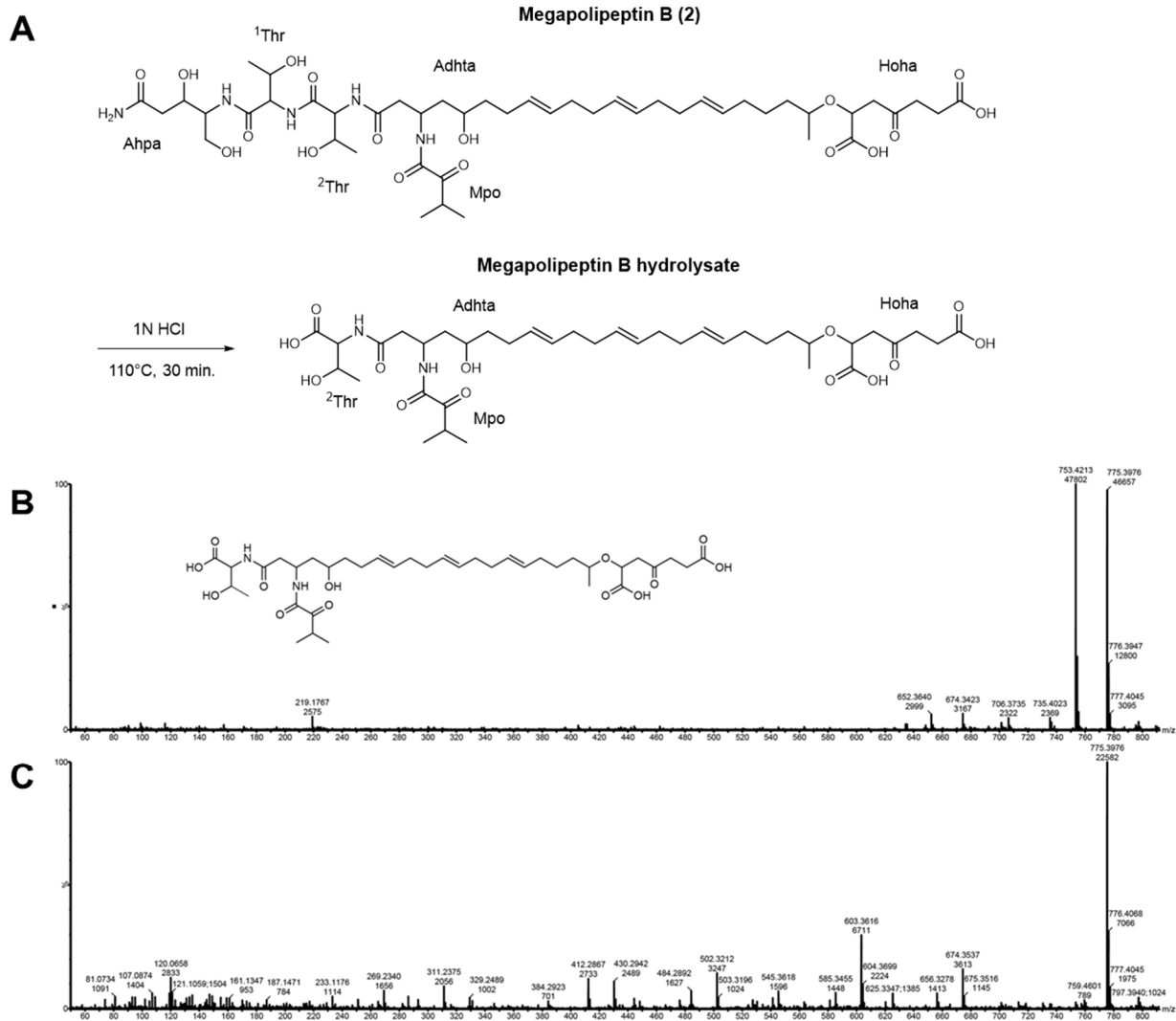


Figure S42. Partial hydrolysis of megapolipeptin B (2). (A) Reaction scheme. (B) MS¹ and (C) MS² spectra obtained for the hydrolysate product following partial hydrolysis of megapolipeptin B (2). The observed product peak (m/z 753.4213) corresponds to the removal of the Ahpa and ¹Thr moieties, leaving a single threonine residue in the isolated fragment.

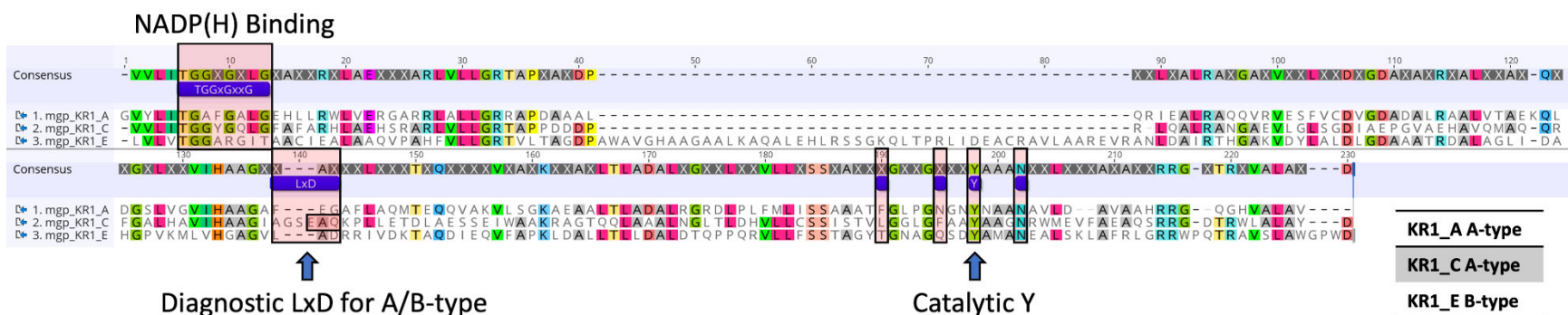


Figure S43. Multiple sequence alignment of KR domains from the megapolipeptin BGC. The NADP(H) binding motif GGxGxxG is highlighted in the first box from the top left. An analysis of the diagnostic Asp (D) presence within an LxD signature motif represented in the second box allows the classification of KR types in A-type or B-type. The presence of the catalytic Tyr (Y) indicates functionality for all KR domains²¹.

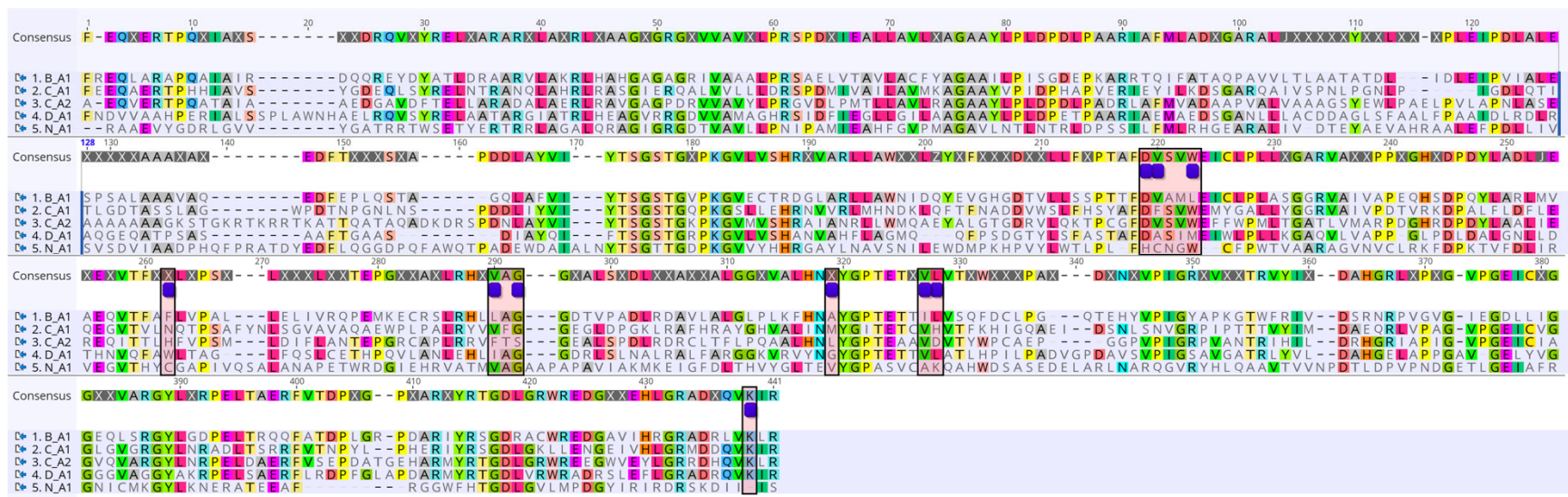


Figure S44. Multiple sequence alignment of A domains from the megapolipeptin BGC. The residues at positions 235, 236, 239, 278, 299, 301, 322, 330, 331, and 517 (highlighted in boxes) are responsible for amino acid selectivity¹⁷. See also **Table S13**.



Figure S45. Multiple sequence alignment of C domains from the megapolipeptin BGC. The conserved motif **HHxxxDG** that includes the active site histidine is highlighted in a box²².

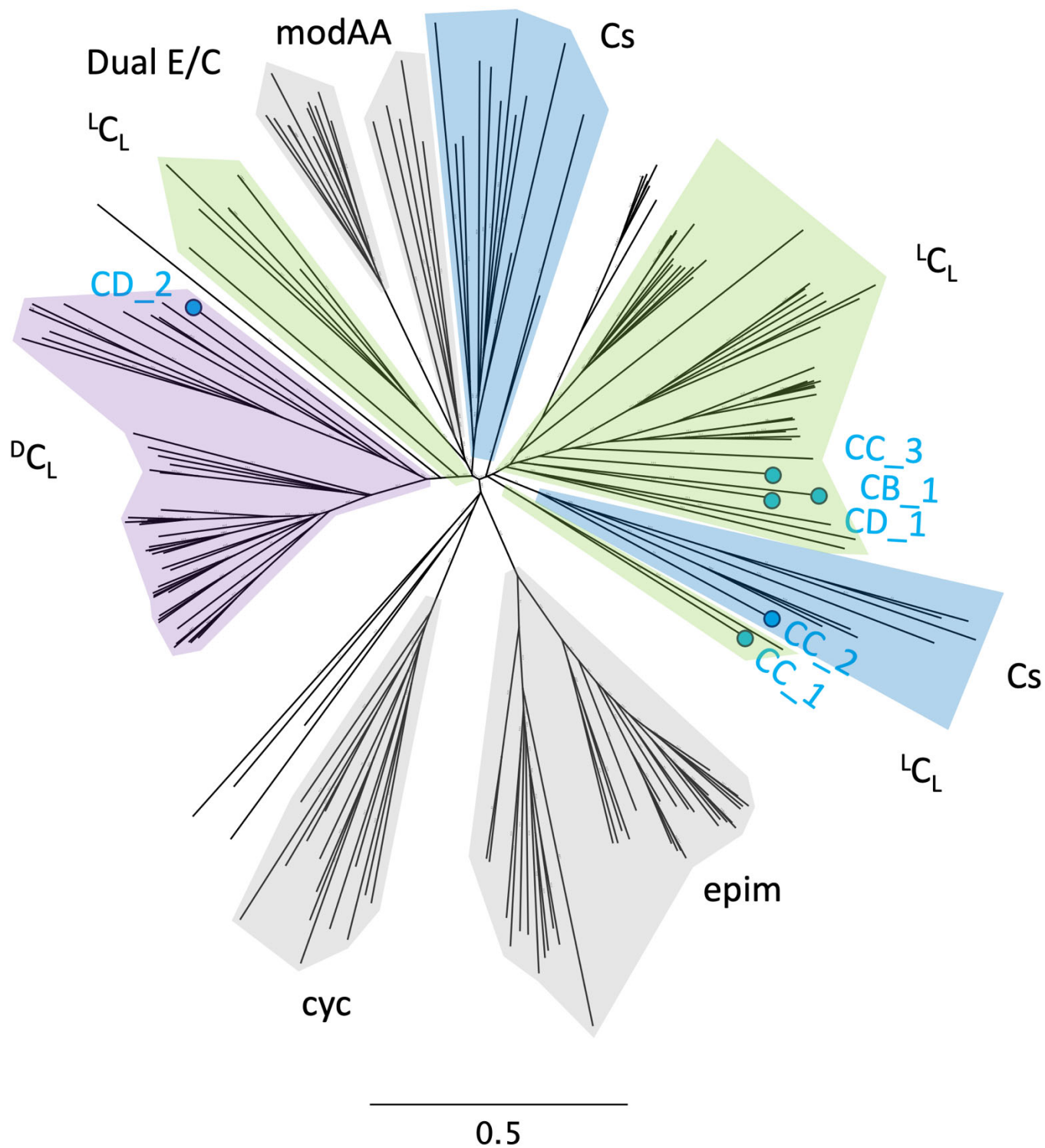


Figure S46. Neighbor-Joining phylogenetic tree of 189 NRPS C domains. Blue dots represent the six Mgp domains: MgpB1 (CB_1), MgpC1 (CC_1), MgpC2 (CC_2), MgpC3 (CC_3), and

MgpD1 (CD_1). The phylogenetic tree was generated using Geneious Prime (2023.2.1) software with the JTT model of amino acid substitution. The scale bar represents the average number of amino acid substitutions. Cs, starter C domain; ^LCL, domains that catalyze formation of a peptide bond between two L-amino acids; ^DCL, C domain that condenses a D-amino acid donor with an L-amino acid acceptor; Cyc, cyclization domains that catalyze both peptide bond formation and subsequent cyclization of cysteine, serine or threonine residues; epim, epimerization domain; dual E/C, catalyzes epimerization and condensation; modAA, modified amino acid domains are involved in any modification of the incorporated amino acid, for example the dehydration of serine to dehydroalanine.



Figure S47. Multiple sequence alignment of DH domains from the megapolipeptin BGC and lagriamide B BGC. The catalytic D (DxxxQ/H, third box from the left) and H residues (HxxxGxxxxP, first box from the left) are not present in the DH domain from MgpC (sequence highlighted in grey), and neither is the conserved motif GxxYGP (second box) where the Y residue may aid in β -hydroxyl group binding. The alignment was generated using sequences of DH domains encoded in the lagriamide B biosynthetic gene cluster from *P. acidicola* RL17-338-BIF-B²³ to show the expected motifs.

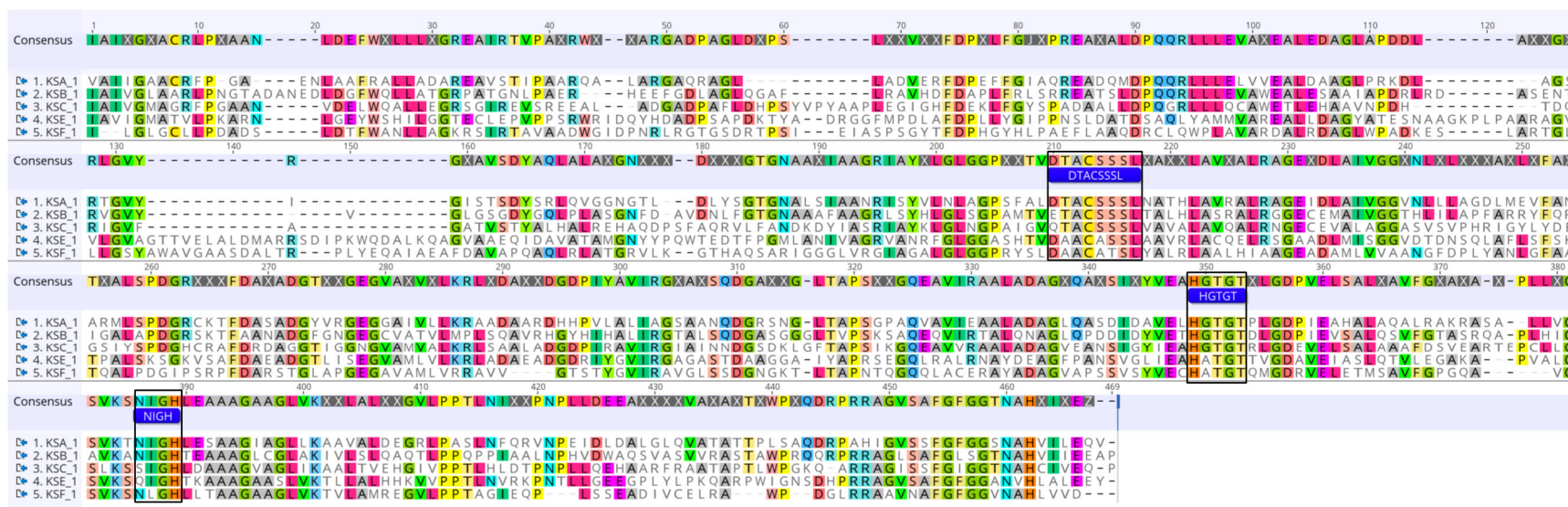


Figure S48. Multiple sequence alignment of KS domains from the megapolipeptin BGC. The conserved motifs that include the Cys-His-His catalytic triad (DTACSSSLV, HGTGT, NIGH) essential for decarboxylative condensation are highlighted in boxes²¹.

REFERENCES

1. Wang, Z., Xiong, G. & Lutz, F. Site-specific integration of the phage Φ CTX genome into the *Pseudomonas aeruginosa* chromosome: Characterization of the functional integrase gene located close to and upstream of *attP*. *Mol. Gen. Genet.* **246**, 72–79 (1995).
2. Wang, J. W. *et al.* CRISPR/Cas9 nuclease cleavage combined with Gibson assembly for seamless cloning. *Biotechniques* **58**, 161–170 (2015).
3. Gibson, Daniel. G. *et al.* Enzymatic assembly of DNA molecules up to several hundred kilobases. *Nat Methods* **6**, 343–345 (2009).
4. Montaser, R. & Kelleher, N. L. Discovery of the biosynthetic machinery for stravidins, biotin antimetabolites. *ACS Chem Biol* **15**, 1134–1140 (2020).
5. Wang, M. *et al.* Sharing and community curation of mass spectrometry data with global natural products social molecular networking. *Nat Biotechnol* **34**, 828–837 (2016).
6. Shannon, P. *et al.* Cytoscape: A software environment for integrated models of biomolecular interaction networks. *Gen Res* **13**, 2498–2504 (2003).
7. Hawkins, P. M. E., Liu, D. Y., Linington, R. G. & Payne, R. J. Solid-phase synthesis of coralmycin A/*epi*-coralmycin A and desmethoxycoralmycin A. *Org Biomol Chem* **19**, 6291–6300 (2021).
8. Tran, W. *et al.* Synthetic sansanmycin analogues as potent *Mycobacterium tuberculosis* translocase I inhibitors. *J Med Chem* **64**, 17326–17345 (2021).
9. Lee, S. *et al.* NP Analyst: An open online platform for compound activity mapping. *ACS Cent Sci* **8**, 223–234 (2022).
10. Hawkins, P. M. E. *et al.* Potent bactericidal antimycobacterials targeting the chaperone ClpC1 based on the depsipeptide natural products ecumicin and ohmyungsamycin A. *J Med Chem* **65**, 4893–4908 (2022).
11. Morehouse, N. J. *et al.* Tolypocaibols: Antibacterial lipopeptaibols from a *Tolypocladium* sp. endophyte of the marine macroalga *Spongomorpha arcta*. *J Nat Prod* **86**, 1529–1535 (2023).
12. Recchia, M. J. J., Baumeister, T. U. H., Liu, D. Y. & Linington, R. G. MultiplexMS: A mass spectrometry-based multiplexing strategy for ultra-high-throughput analysis of complex mixtures. *Anal Chem* **95**, 11908–11917 (2023).
13. Romanowski, S. B. *et al.* Identification of the lipodepsipeptide selethramide encoded in a giant nonribosomal peptide synthetase from a *Burkholderia* bacterium. *Proc Natl Acad Sci* **120**,

e2304668120 (2023).

14. Wilson, D. M. *et al.* Targeted sampling of natural product space to identify bioactive natural product-like polyketide macrolides. *Nat Commun* **15**, (2024).
15. McCulloch, M. W. B., Berrue, F., Haltli, B. & Kerr, R. G. One-pot syntheses of pseudopteroxazoles from pseudopterosins: A rapid route to non-natural congeners with improved antimicrobial activity. *J Nat Prod* **74**, 2250–2256 (2011).
16. Collins, L. A. & Franzblau, S. G. Microplate alamar blue assay versus BACTEC 460 system for high-throughput screening of compounds against *Mycobacterium tuberculosis* and *Mycobacterium avium*. *Antimicrob Agents Chemother* **41**, 1004–1009 (1997).
17. Stachelhaus, T., Mootz, H. D. & Marahiel, M. A. The specificity-conferring code of adenylation domains in nonribosomal peptide synthetases. *Chem Biol* **6**, 493–505 (1999).
18. Alonzo, D. A., Chiche-Lapierre, C., Tarry, M. J., Wang, J. & Schmeing, T. M. Structural basis of keto acid utilization in nonribosomal depsipeptide synthesis. *Nat Chem Biol* **16**, 493–496 (2020).
19. Arkin, A. P. *et al.* KBase: The United States department of energy systems biology knowledgebase. *Nat Biotechnol* **36**, 566–569 (2018).
20. Zheng, W. *et al.* Establishment of recombineering genome editing system in *Paraburkholderia megapolitana* empowers activation of silent biosynthetic gene clusters. *Microb Biotechnol* **13**, 397–405 (2020).
21. Keatinge-Clay, A. T. The structures of type I polyketide synthases. *Nat Prod Rep* **29**, 1050–1073 (2012).
22. Stachelhaus, T., Mootz, H. D., Bergendah, V. & Marahiel, M. A. Peptide bond formation in nonribosomal peptide biosynthesis: Catalytic role of the condensation domain. *J Biol Chem* **273**, 22773–22781 (1998).
23. Fergusson, C. H. *et al.* Discovery of a lagriamide polyketide by integrated genome mining, isotopic labeling, and untargeted metabolomics. *Chem Sci* **15**, 8089–8096 (2024).